

## Supportive Information

### **Endophytic *Akanthomyces* sp. LN303 from Edelweiss produces emestrin and two new 2-hydroxy-4 pyridone alkaloids**

Martina Oberhofer<sup>1\*</sup>, Judith Wackerlig<sup>2</sup>, Martin Zehl<sup>3</sup>, Havva Büyükk<sup>2</sup>, Jia Jian Cao<sup>2</sup>, Alexander Prado-Roller<sup>4</sup>, Ernst Urban<sup>2</sup>, Sergey B. Zotchev<sup>1</sup>

<sup>1</sup>Department of Pharmacognosy, University of Vienna, Austria

<sup>2</sup>Department of Pharmaceutical Chemistry, University of Vienna, Austria

<sup>3</sup>Department of Analytical Chemistry, Faculty of Chemistry, University of Vienna, Austria

<sup>4</sup>Department of Inorganic Chemistry, Faculty of Chemistry, University of Vienna, Austria

Corresponding author: E-mail, [martina.oberhofer@univie.ac.at](mailto:martina.oberhofer@univie.ac.at). Tel. and Fax: +43-14277-55294, +43-14277-85294

## Table of Contents

### Supplementary Information

Phylogenetic analysis of endophytic <i>Akanthomyces</i> isolates (Figure S1)	S4, 5
BPC of purified compounds <b>1</b> and <b>2</b> (Figure S2-3)	S6, 7
HRESIMS spectrum of compound <b>1</b> (Figure S4)	S8
HRESIMS/MS spectra of different ions of compound <b>1</b> (Figure S5)	S9
Proposed fragmentation pathway of compound <b>1</b> [M+Na] <sup>+</sup> ion (Scheme S1)	S10
Proposed fragmentation pathway of compound <b>1</b> [M+H] <sup>+</sup> ion (Scheme S2)	S11
HRESIMS spectrum of compound <b>2</b> (Figure S6)	S12
HRESIMS/MS spectra of different ions of compound <b>2</b> (Figure S7)	S13
Proposed fragmentation pathway of compound <b>2</b> [M+Na] <sup>+</sup> ion (Scheme S3)	S14
Proposed fragmentation pathway of compound <b>2</b> [M+H] <sup>+</sup> ion (Scheme S4)	S15
HRESIMS and HRESIMS/MS of the [M-CO <sub>2</sub> -H] <sup>-</sup> ion of compound <b>2</b> (Figure S8)	S16
Proposed fragmentation pathway of compound <b>2</b> [M-H] <sup>-</sup> ion (Scheme S5)	S17
HRESIMS spectrum of compound <b>3</b> (Figure S9)	S18
BPC of compound <b>3</b> in all total extracts (Figure S10)	S19, 20
EIC of compound <b>3</b> in all total extracts (Figure S11, S12)	S21-24
HRESIMS/MS spectrum of the emestrin isomer and emestrin (Figure S13)	S25
Proposed fragmentation pathway of compound <b>3</b> [M-H] <sup>-</sup> ion (Scheme S6)	S26
BPC of the total extract from LN303 in negative and positive ion mode by LC-MS (Figure S14)	S27
Experimental crystallographic parameters and CCDC code of emestrin (Table S1)	S28
Crystallographic data on emestrin (Table S2)	S28
Crystallographic data collection on emestrin (Table S3)	S28
Asymmetric unit of the emestrin crystal (Figure S15)	S29

<sup>1</sup> H NMR spectrum of <b>1</b> in CDCl <sub>3</sub> ( $\delta$ in ppm) (Figure S16)	S30-S33
<sup>13</sup> C NMR spectrum of <b>1</b> in CDCl <sub>3</sub> ( $\delta$ in ppm)	S34-S37
COSY spectrum of <b>1</b> in CDCl <sub>3</sub> ( $\delta$ in ppm)	S38-S41
HSQC spectrum of <b>1</b> in CDCl <sub>3</sub> ( $\delta$ in ppm)	S42-S45
HMBC spectrum of <b>1</b> in CDCl <sub>3</sub> ( $\delta$ in ppm)	S46-S59
<sup>1</sup> H NMR spectrum of <b>2</b> in CDCl <sub>3</sub> ( $\delta$ in ppm) (Figure S17)	S60-S63
COSY spectrum of <b>2</b> in CDCl <sub>3</sub> ( $\delta$ in ppm)	S64-S67
HSQC spectrum of <b>2</b> in CDCl <sub>3</sub> ( $\delta$ in ppm)	S68-S71
HMBC spectrum of <b>2</b> in CDCl <sub>3</sub> ( $\delta$ in ppm)	S72-S82
<sup>1</sup> H NMR spectrum of <b>3</b> in CDCl <sub>3</sub> ( $\delta$ in ppm) (Figure S18)	S83-S87
<sup>13</sup> C NMR spectrum of <b>3</b> in CDCl <sub>3</sub> ( $\delta$ in ppm)	S88-S91
COSY spectrum of <b>3</b> in CDCl <sub>3</sub> ( $\delta$ in ppm)	S92-S94
HSQC spectrum of <b>3</b> in CDCl <sub>3</sub> ( $\delta$ in ppm)	S95-S101
HMBC spectrum of <b>3</b> in CDCl <sub>3</sub> ( $\delta$ in ppm)	S102-S112

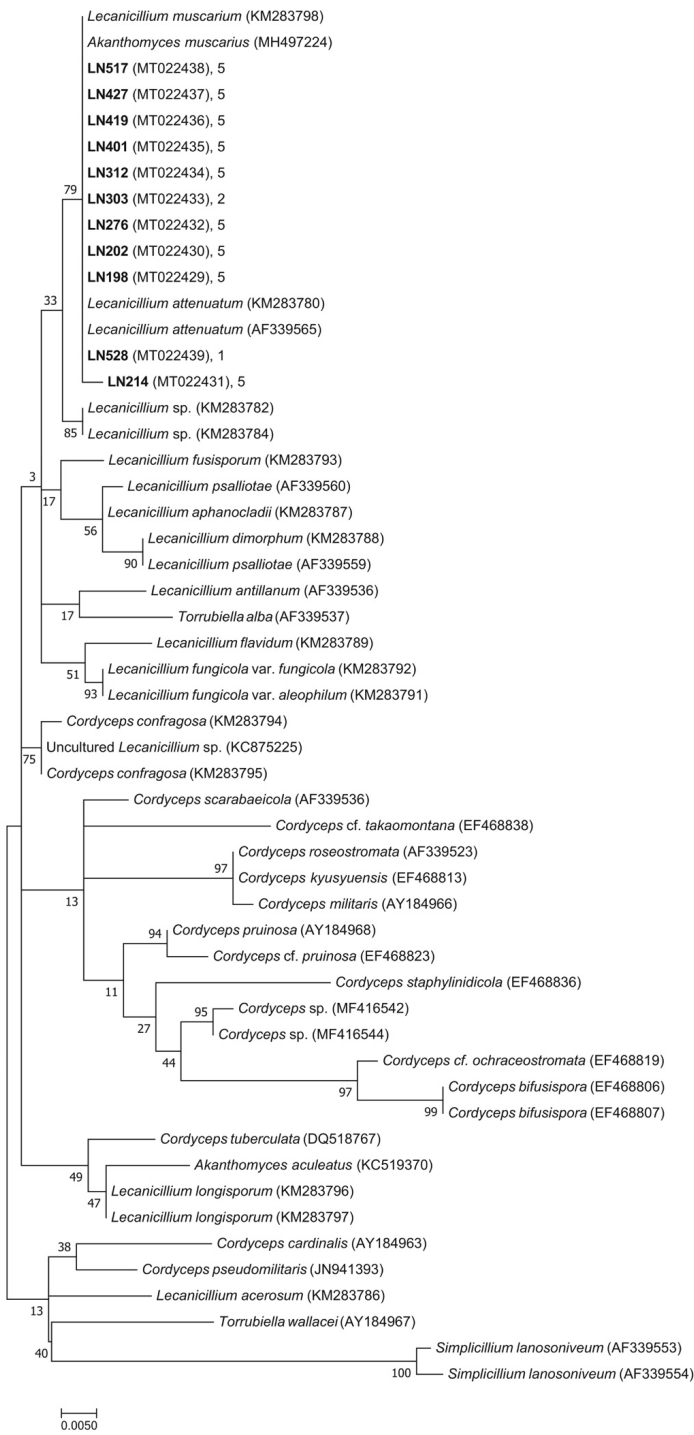


**Figure S1.** Phylogenetic relationship of endophytic *Akanthomyces* isolates from *Leontopodium nivale* subsp. *alpinum* with closely related members of Cordycipitaceae. Maximum likelihood analysis of the LSU region of endophytic *Akanthomyces* sp. strains with Genbank accession numbers in brackets and the plant number, from which they were isolated, referenced to closely related fungi from Cordycipitaceae [9]. Best fitting model was K2+G+I and bootstrap support was estimated with 1000 replicates. The tree is drawn to scale, with branch lengths measured in the number of substitutions per site. The analysis involved 53 nucleotide sequences. Codon positions included were 1st+2nd+3rd+Noncoding. All positions containing gaps and missing data were eliminated. A total of 392 positions were in the final dataset. Evolutionary analyses were conducted in MEGA7 [31].

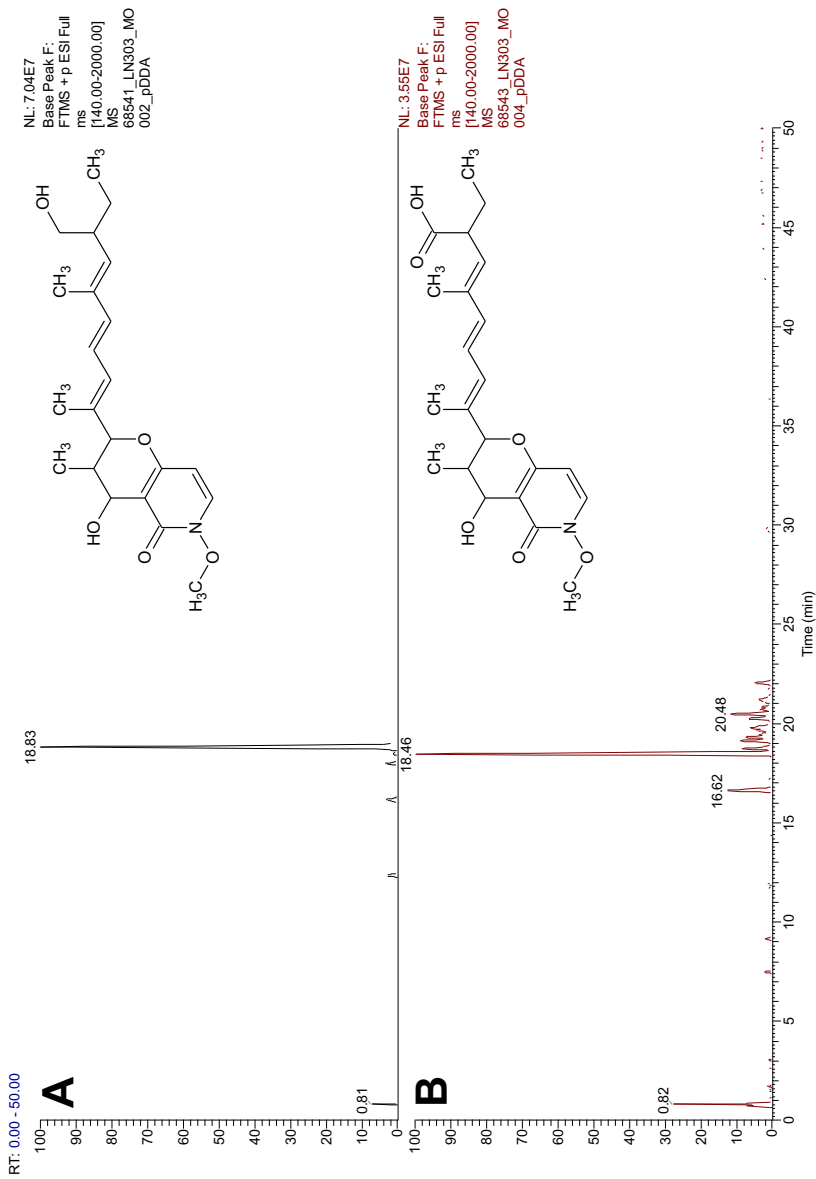


**Figure S2.** LC-MS data of purified compounds **1** (A) and **2** (B) shown as base peak chromatogram in the range  $m/z$  140-2000.

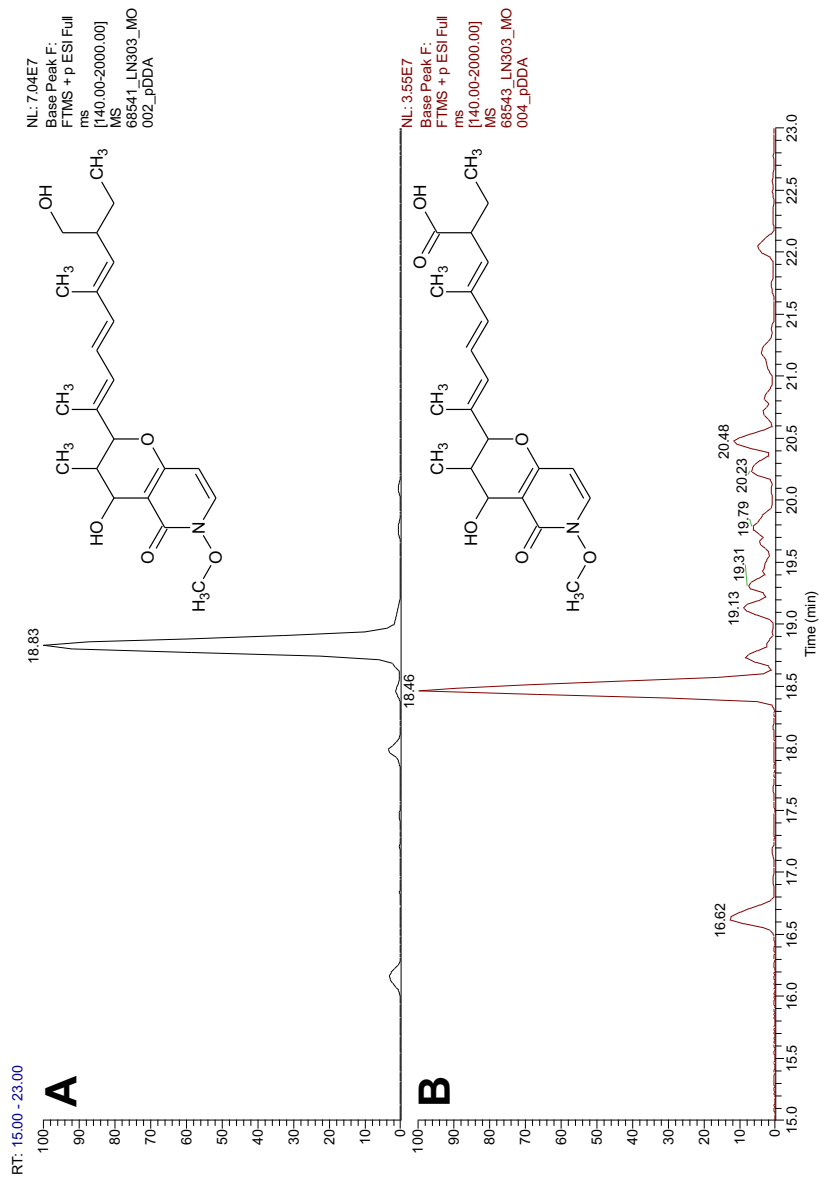


**Figure S3.** LC-MS data (zoom) of purified compounds **1** (**A**) and **2** (**B**) shown as base peak chromatogram in the range  $m/z$  140-2000.

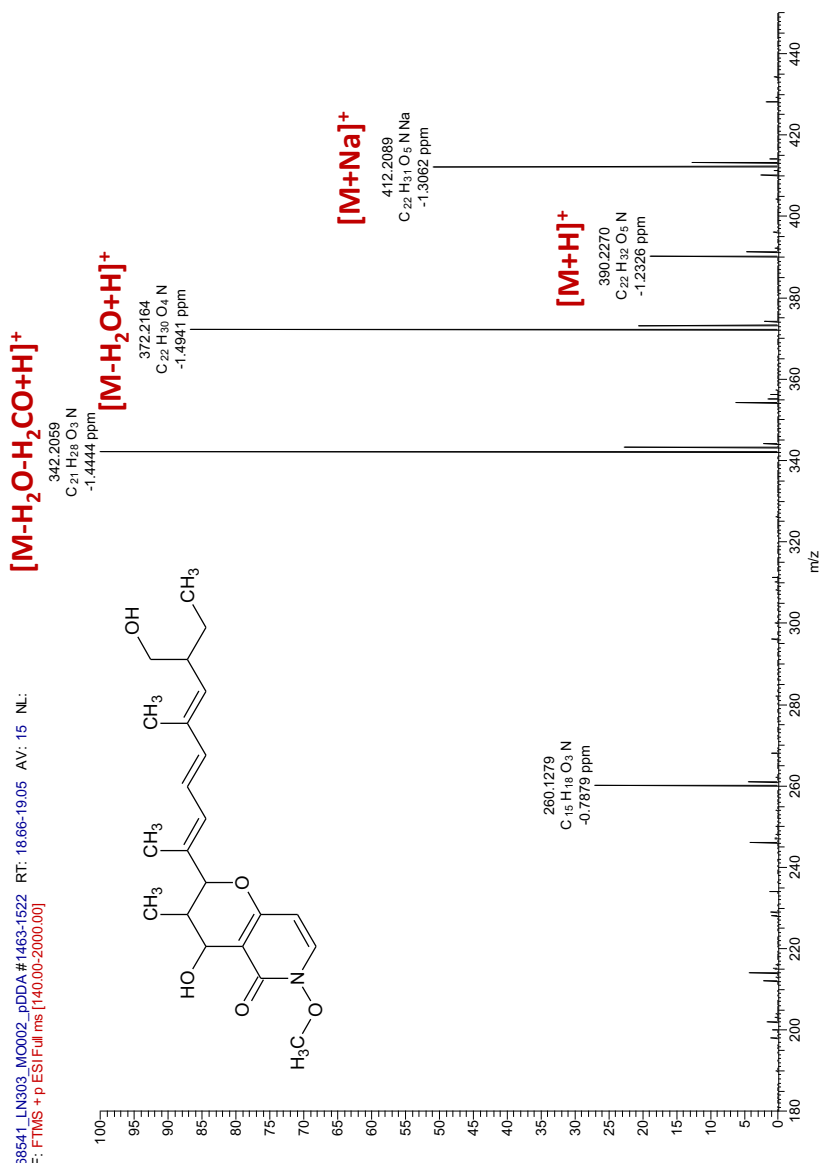
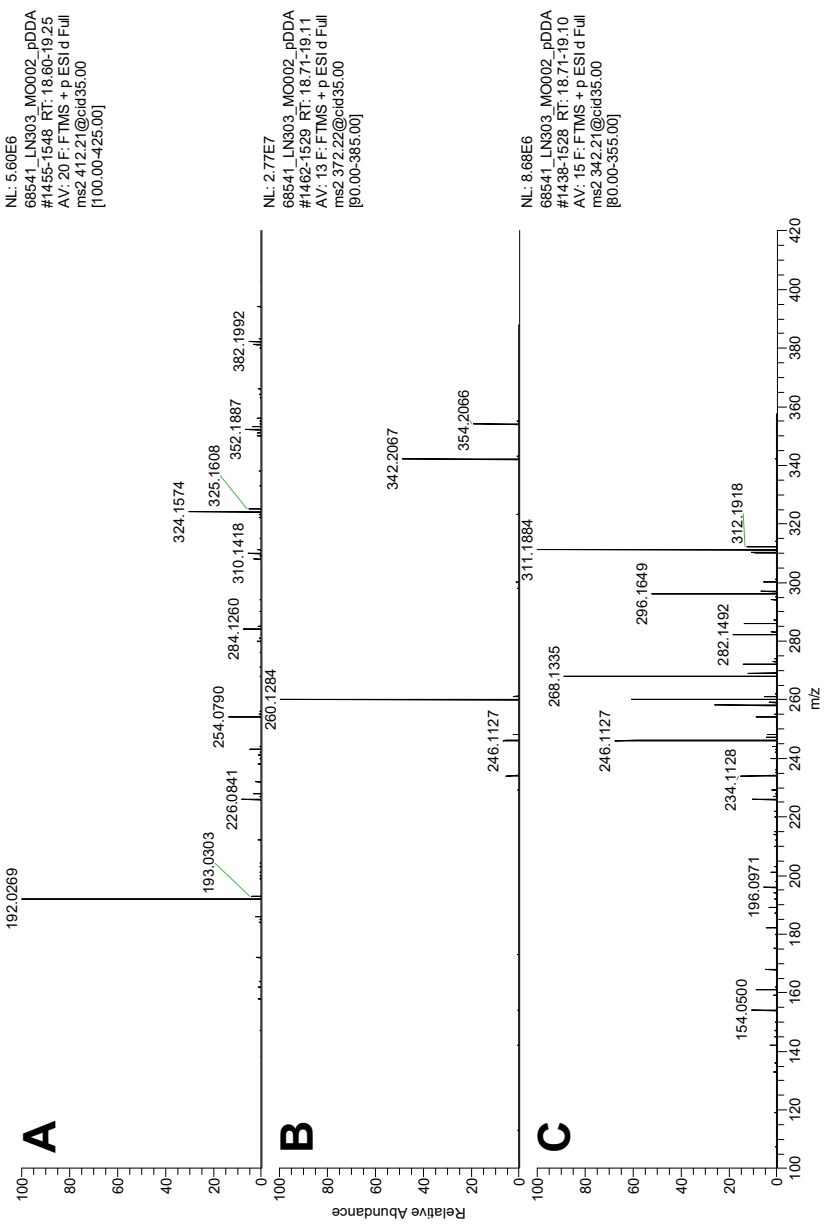
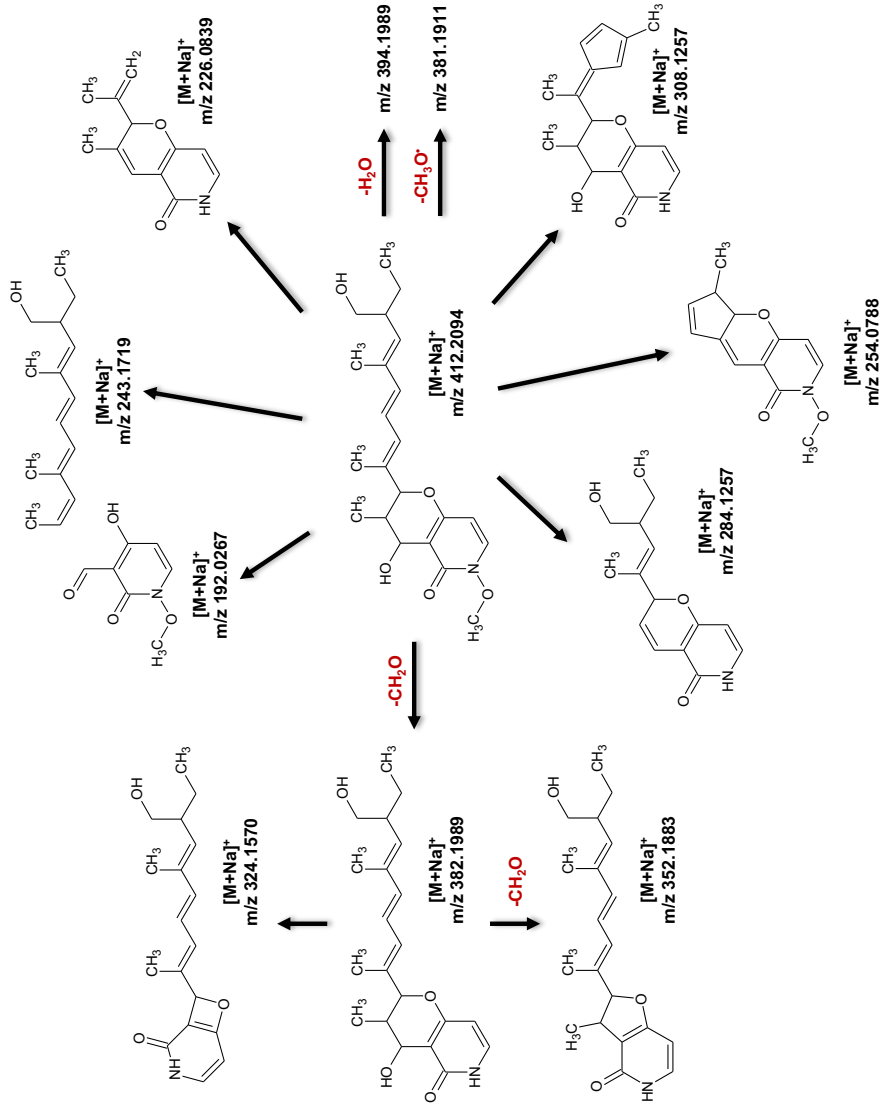


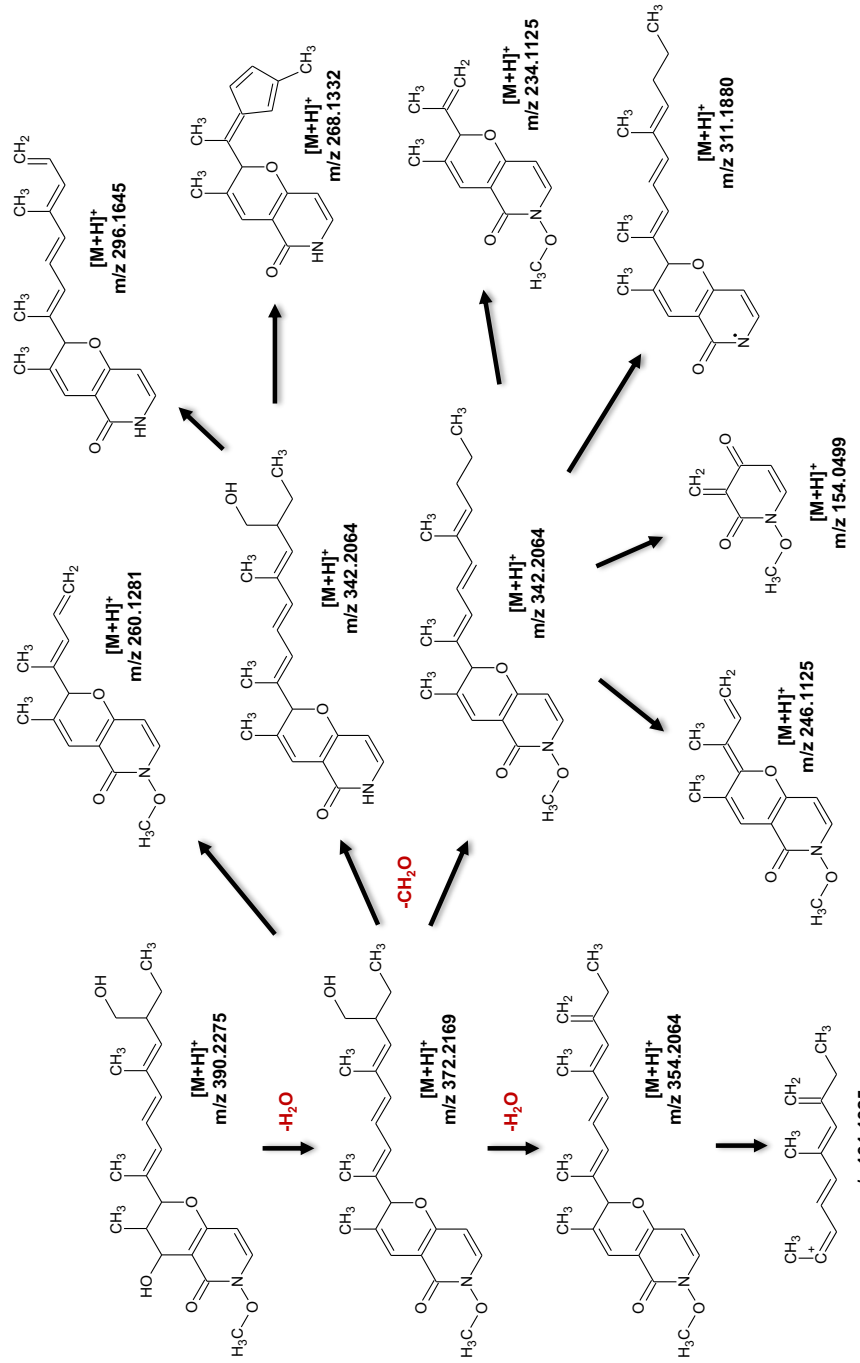
Figure S4. HREIMS spectrum of the purified compound 1 obtained by LC-MS in positive ion mode.



**Figure S5.** HREIMS/MS spectra of the  $[M+Na]^+$  ion (A), the  $[M-H_2O+H]^+$  ion (B), and the  $[M-H_2O-H_2CO+H]^+$  ion (C) of the purified compound **1** obtained by LC-MS in positive ion mode.



**Scheme S1.** Proposed fragmentation pathway of the  $[M+Na]^+$  ion of the purified compound 1 showing selected key fragment ions.



**Scheme S2.** Proposed fragmentation pathway of the  $[M+H]^+$  ion of the purified compound I showing selected key fragment ions.

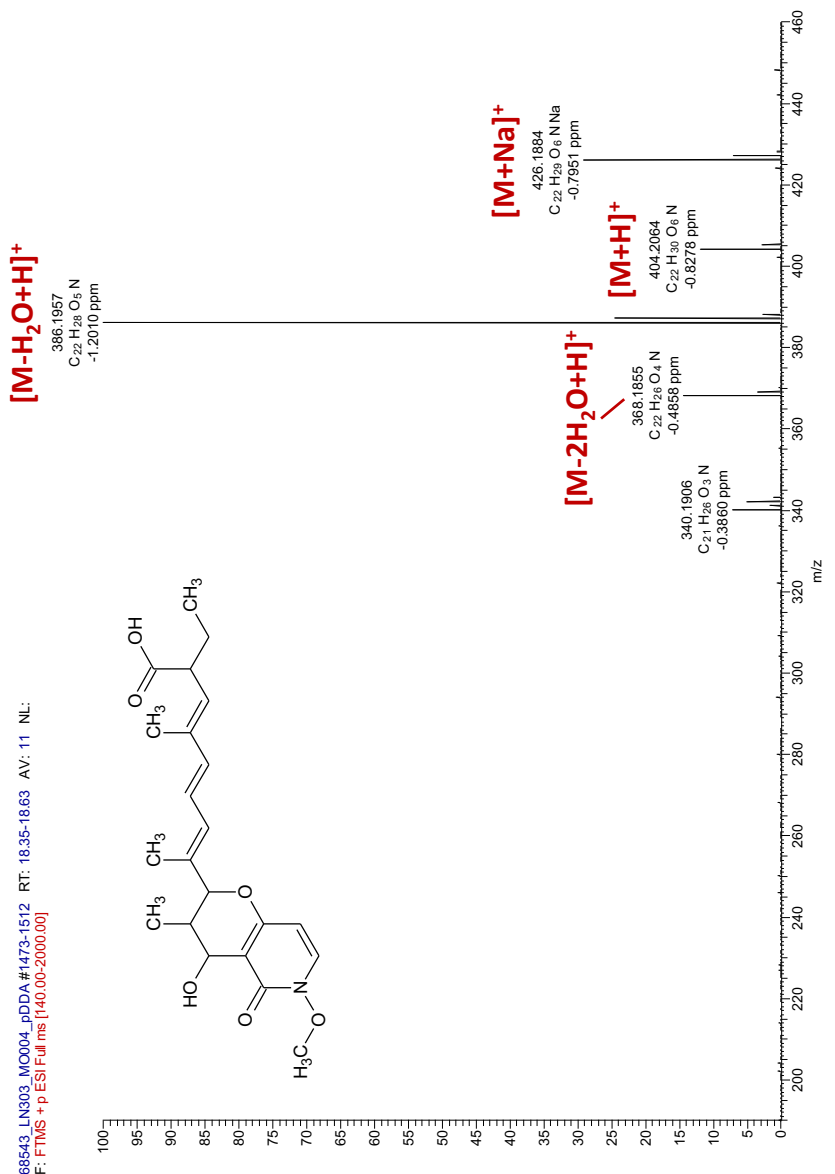
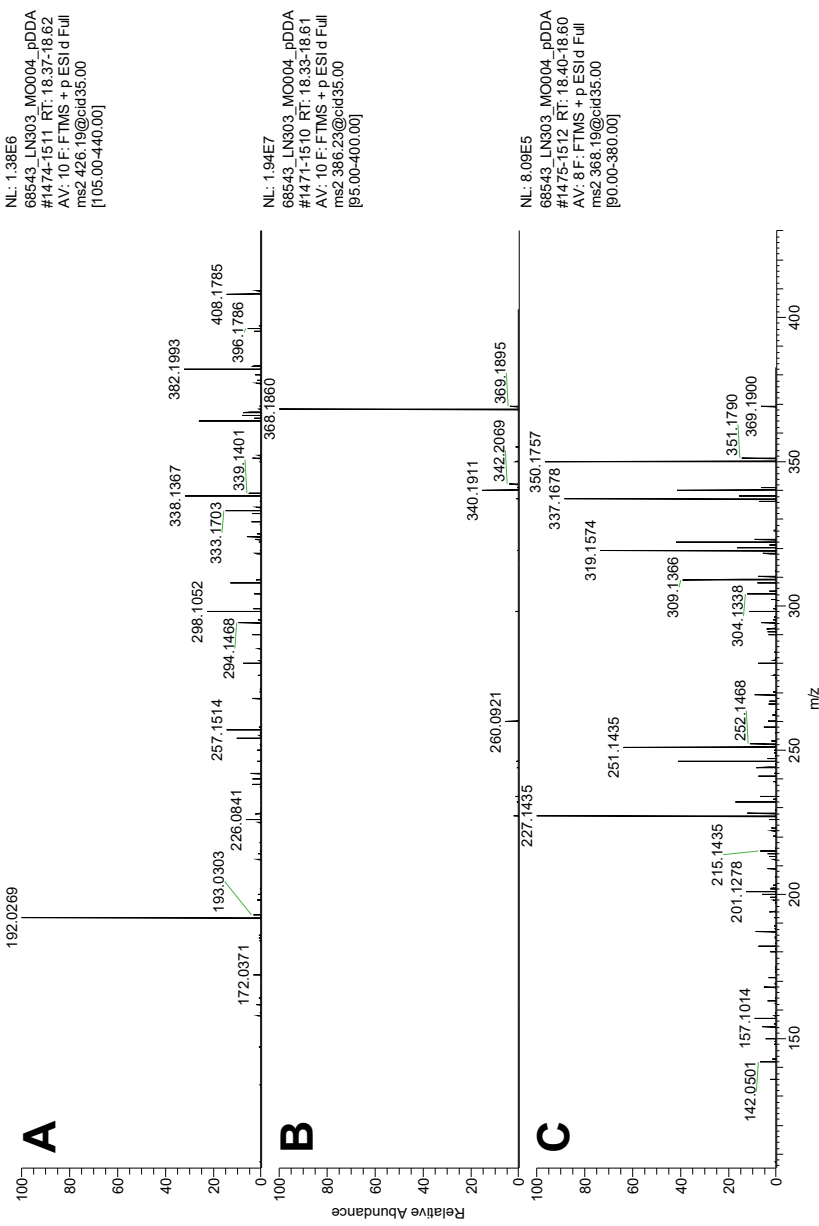
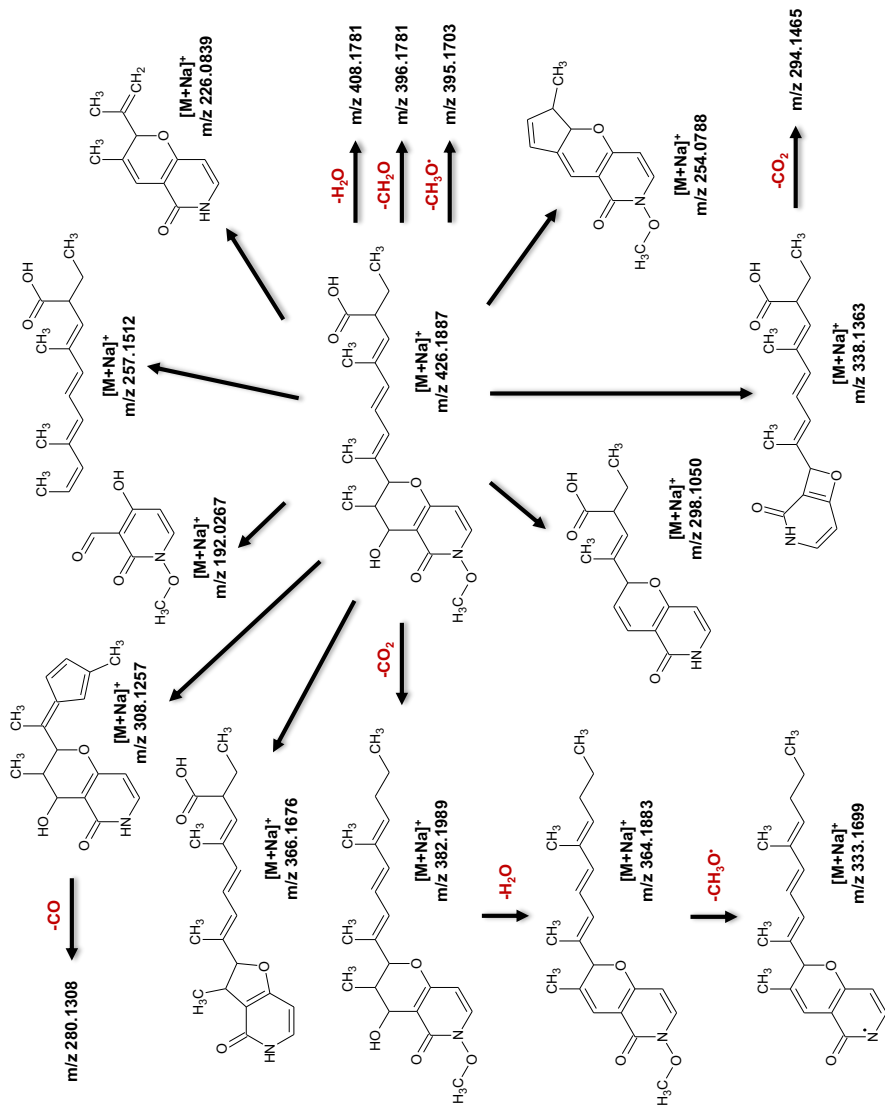


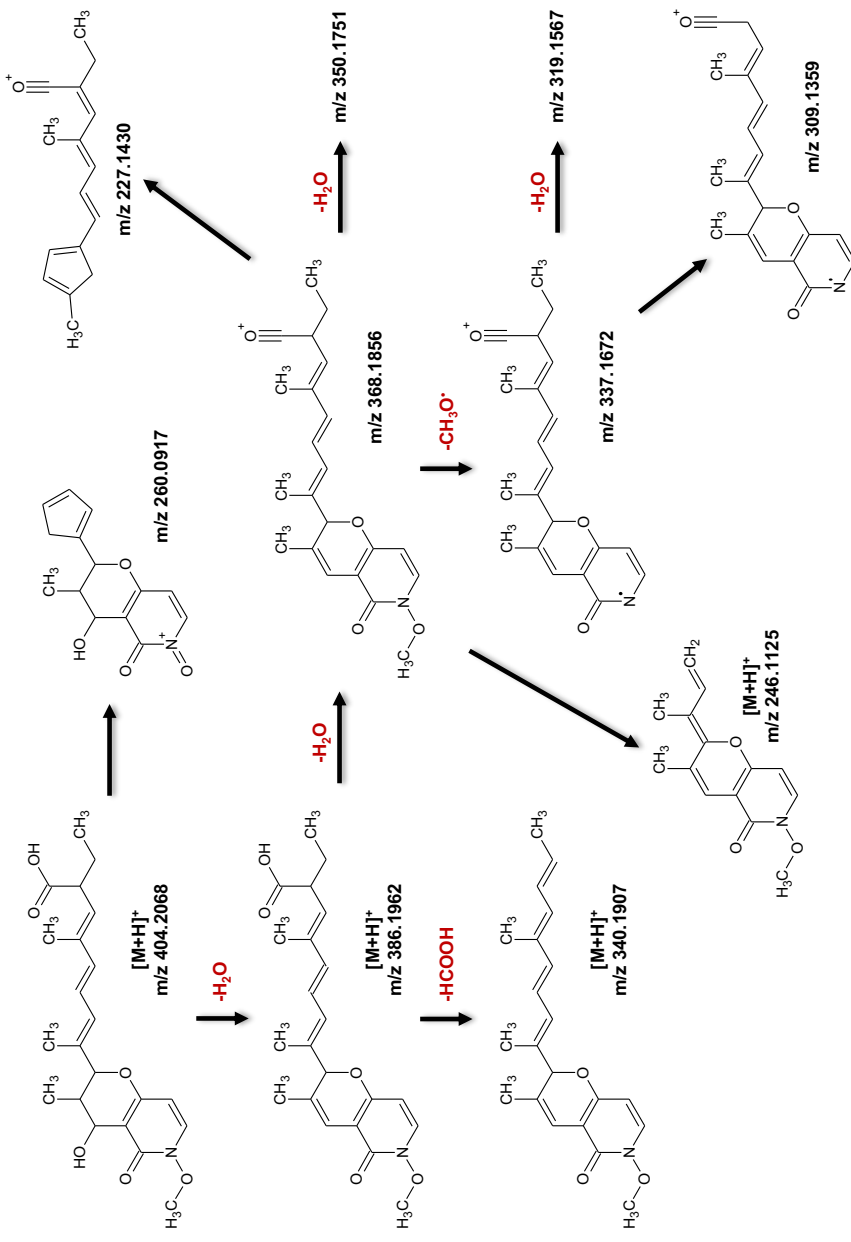
Figure S6. HREIMS spectrum of the purified compound **2** obtained by LC-MS in positive ion mode.



**Figure S7.** HRESIMS/MS spectra of the  $[M+Na]^+$  ion (A), the  $[M-H_2O+H]^+$  ion (B), and the  $[M-2H_2O+H]^+$  ion (C) of the purified compound 2 obtained by LC-MS in positive ion mode.



**Scheme S3.** Proposed fragmentation pathway of the  $[M+Na]^+$  ion of the purified compound 2 showing selected key fragment ions.



**Scheme S4.** Proposed fragmentation pathway of the  $[M+H]^+$  ion of the purified compound 2 showing selected key fragment ions.

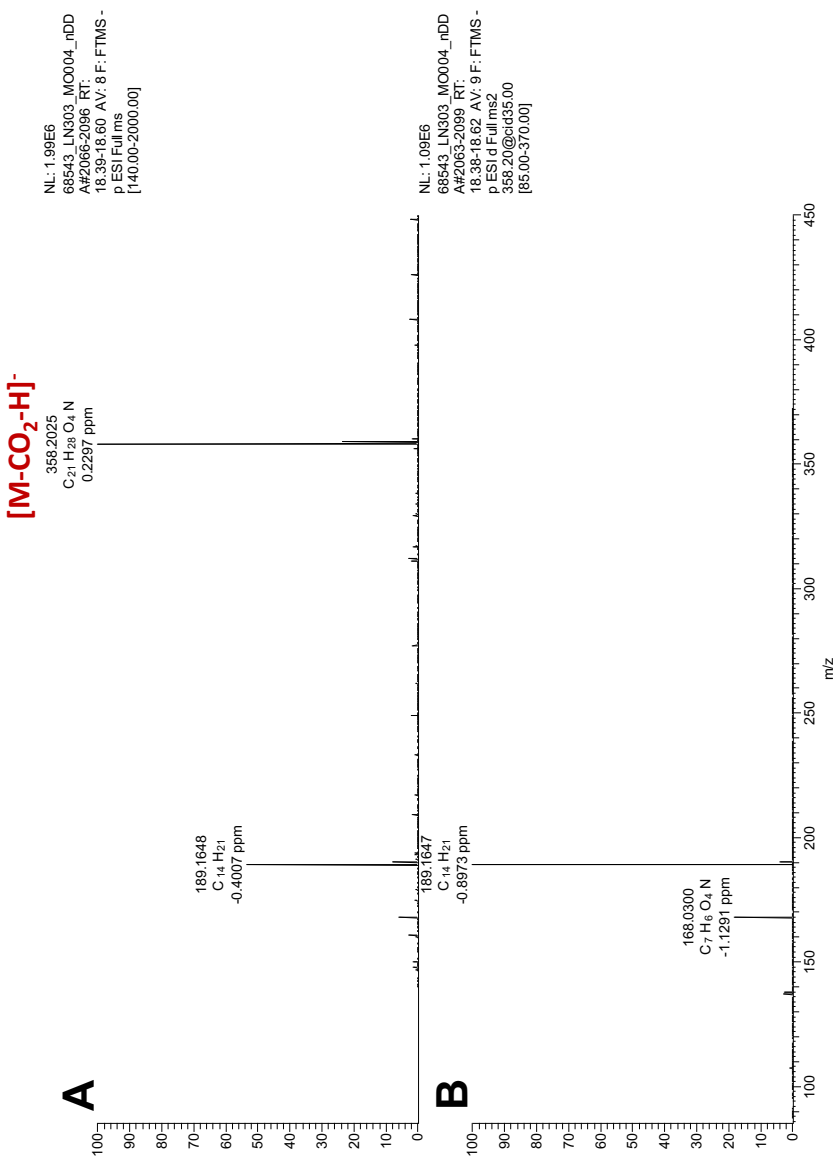
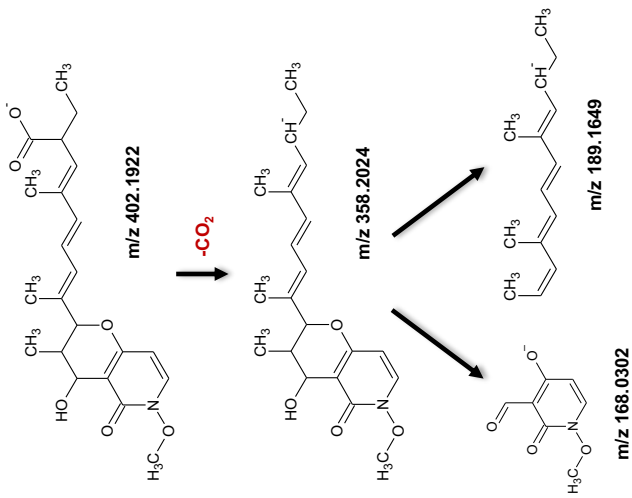


**Figure S8.** HRESIMS spectrum (A) and HRESIMS/MS spectrum of the [M-CO<sub>2</sub>-H]<sup>-</sup> ion (B) of the purified compound **2** obtained by LC-MS in negative ion mode.



**Scheme S5.** Proposed fragmentation pathway of the  $[M-H]^-$  ion of the purified compound 2 showing selected key fragment ions.

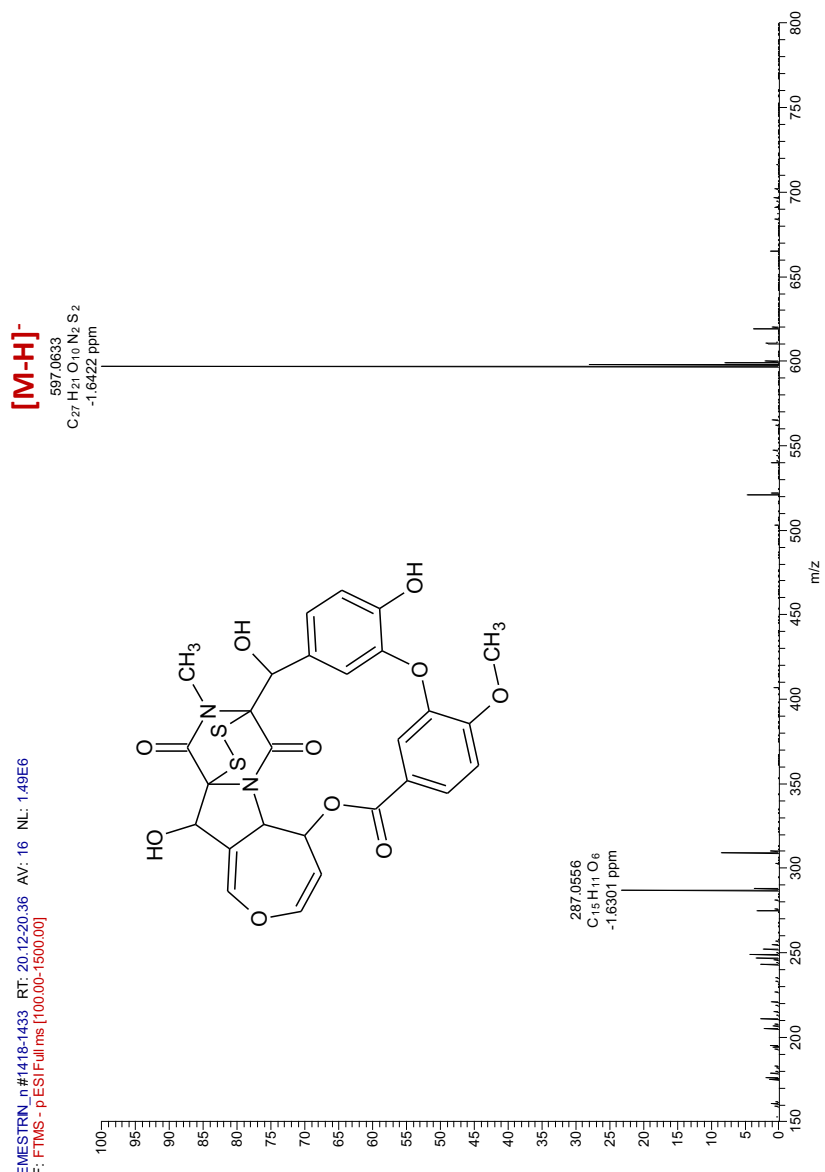
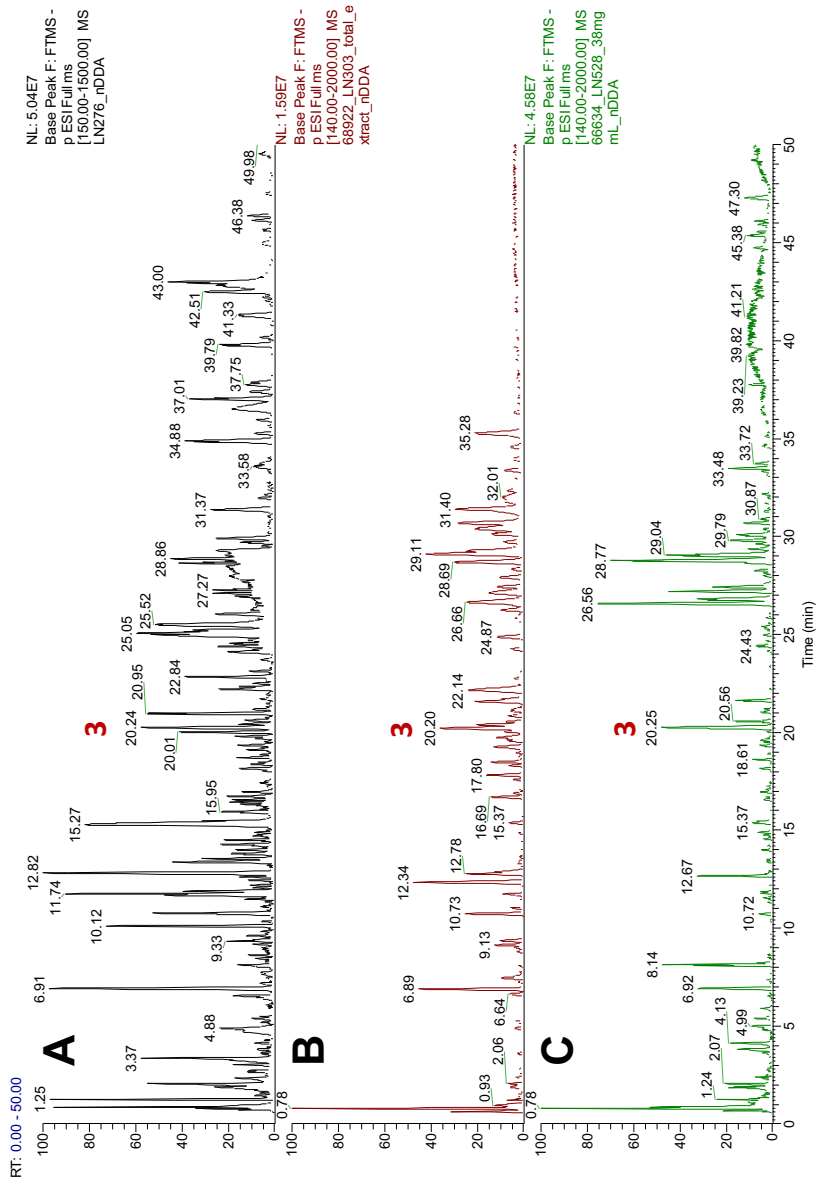
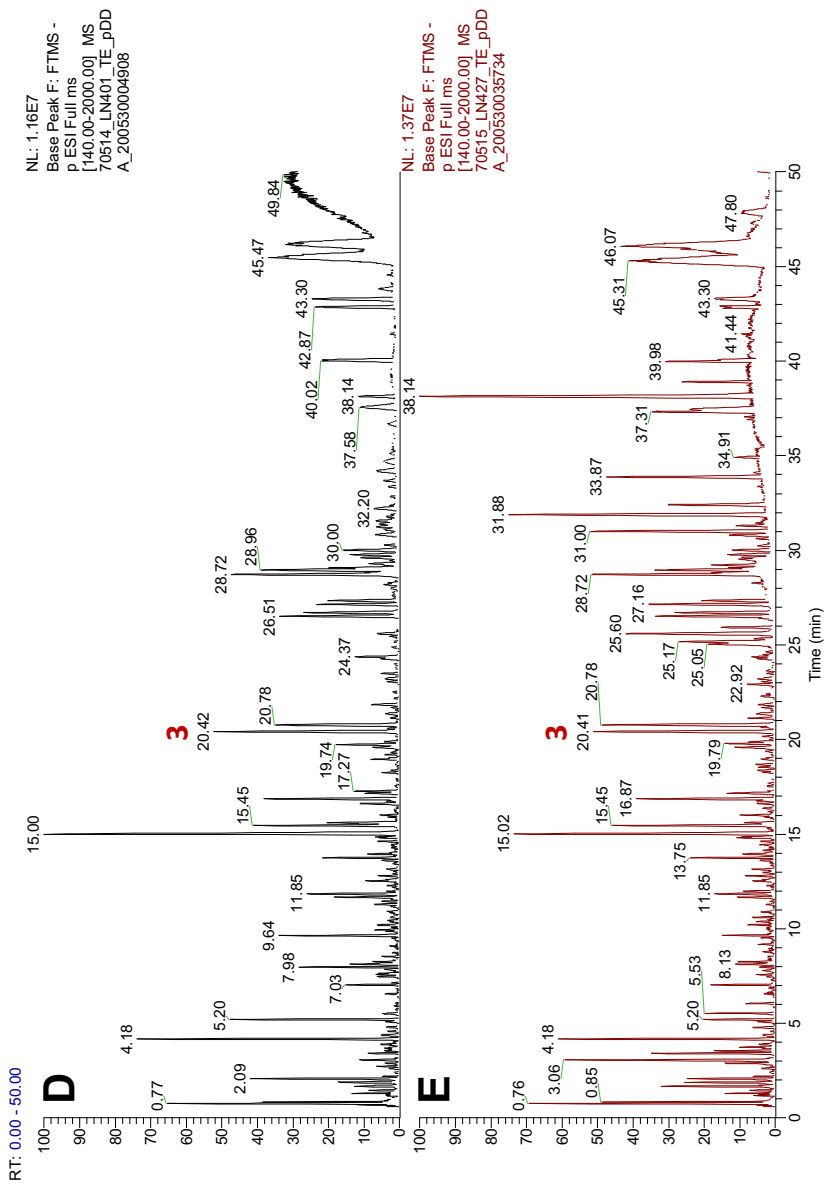


Figure S9. HRESIMS spectrum of the purified compound 3 obtained by LC-MS in negative ion mode.



**Figure S10.** Base peak chromatograms obtained by LC-MS in negative ion mode of the extracts from isolates LN276 (A), LN303 (B), and LN528 (C). The peak corresponding to emestrin is marked with **3**.



**Figure S10 (cont.).** Base peak chromatograms obtained by LC-MS in negative ion mode of the extracts from isolates LN401 (D) and LN427 (E). The peak corresponding to emestrin is marked with **3**.

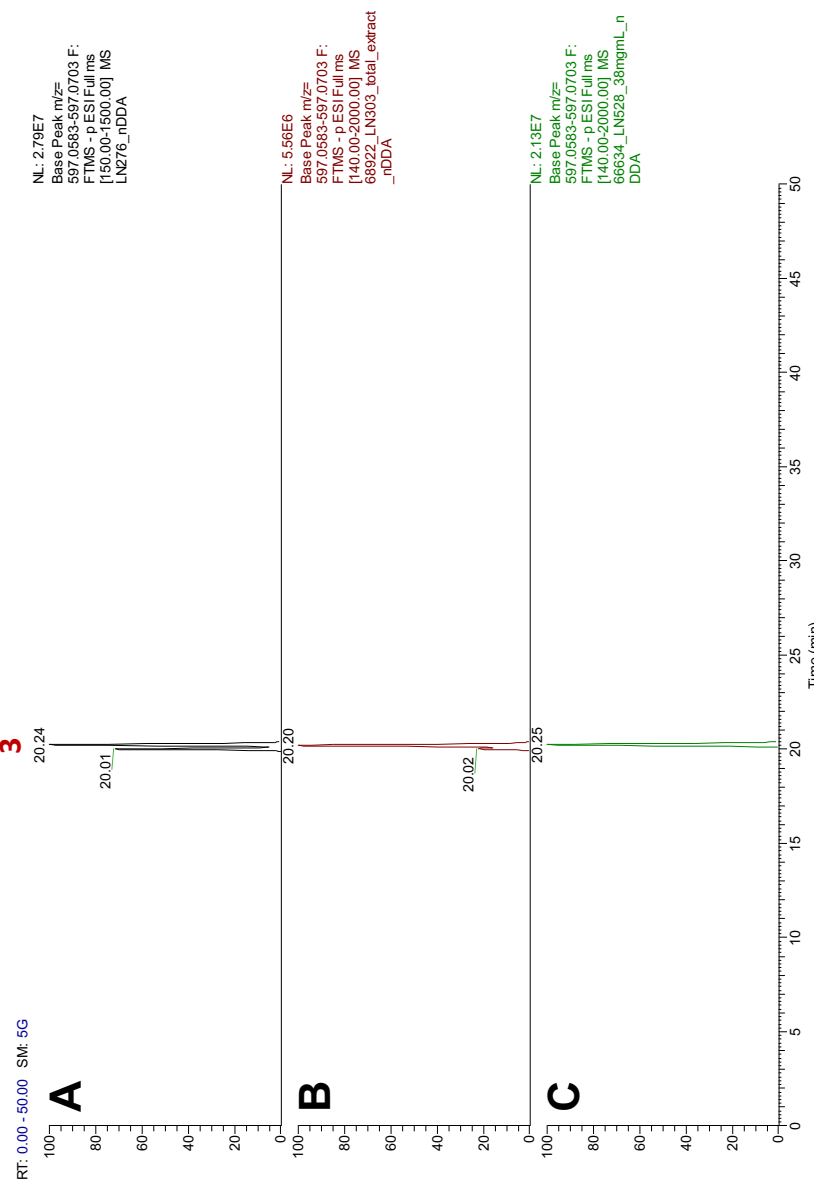


**Figure S11.** Extracted ion chromatograms ( $m/z$  597.0643 $\pm$ 0.0060) obtained by LC-MS in negative ion mode of the extracts from isolates LN276 (A), LN303 (B), and LN528 (C). The peak corresponding to emestrin is marked with 3.

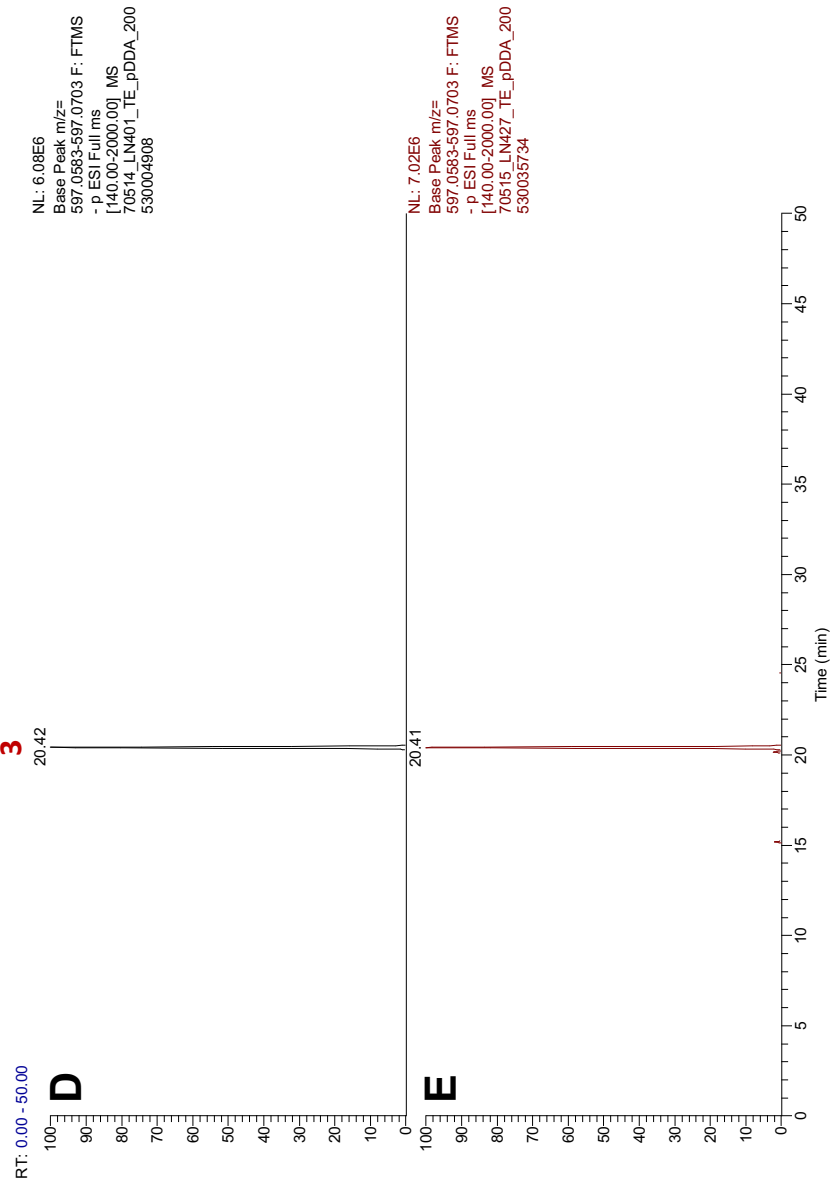


**Figure S11 (cont.).** Extracted ion chromatograms ( $m/z$  597.0643 $\pm$ 0.0060) obtained by LC-MS in negative ion mode of the extracts from isolates LN401 (D) and LN427 (E). The peak corresponding to emestrin is marked with **3**.

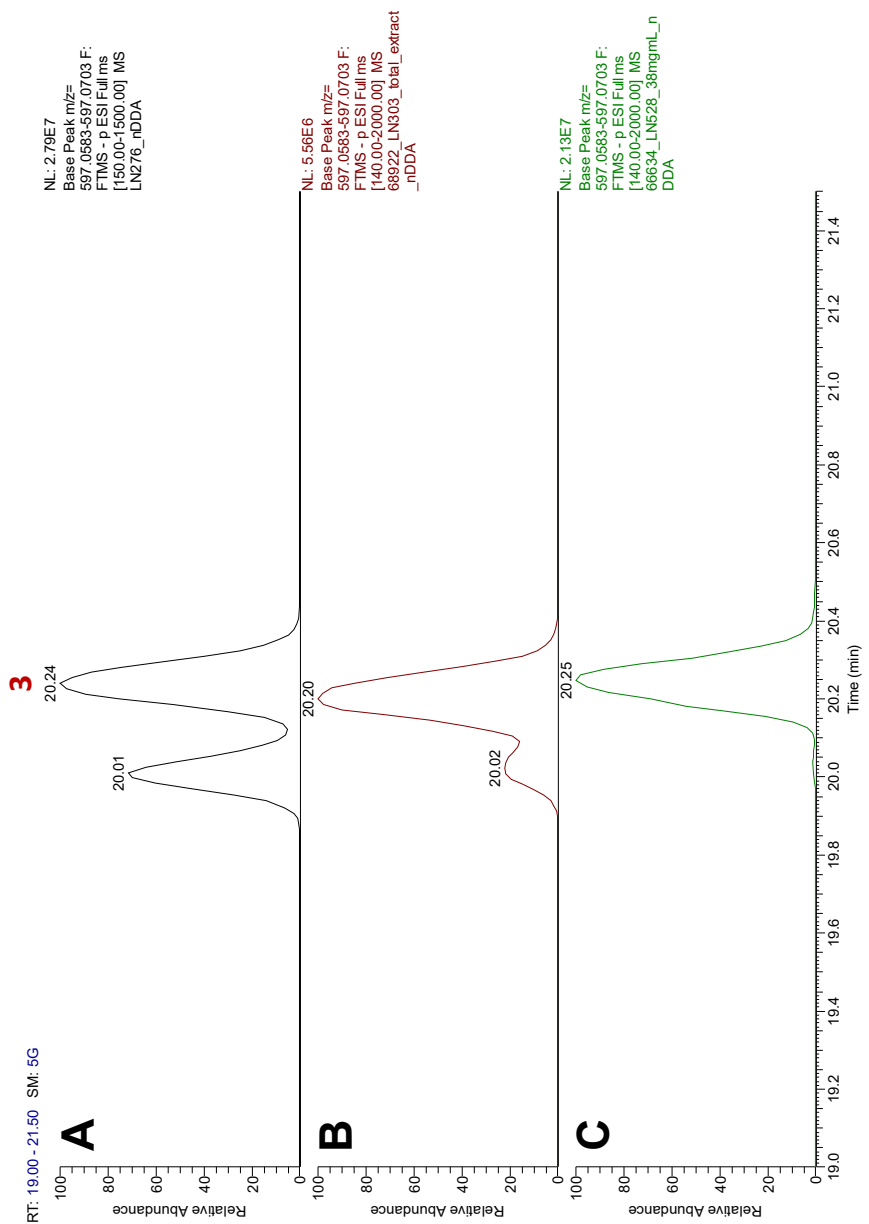


**Figure S12.** Extracted ion chromatograms ( $m/z$  597.0643 $\pm$ 0.0060) obtained by LC-MS in negative ion mode of the extracts from isolates LN276 (A), LN303 (B), and LN528 (C). The zoom shows the peak corresponding to emestrin (3) eluting at 20.2 min and the peak of an isomer eluting shortly earlier at 20.0 min.

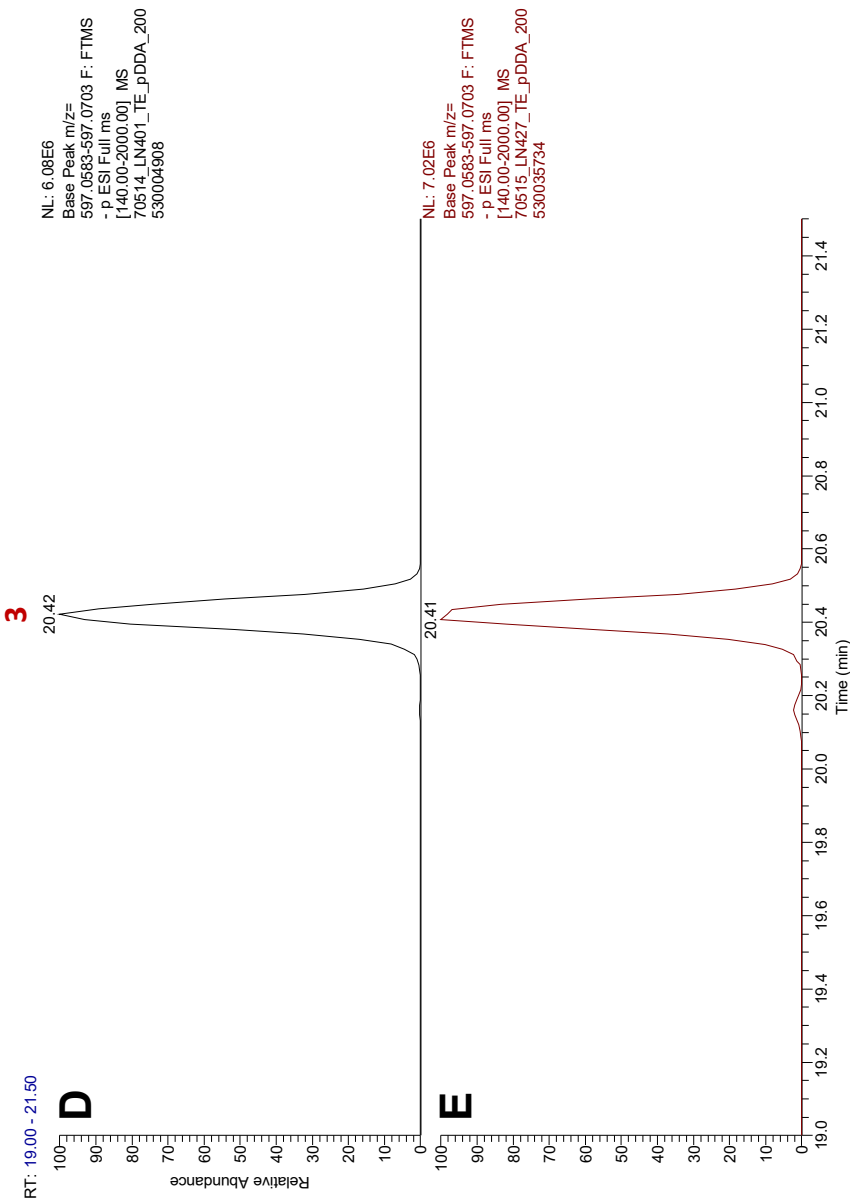


**Figure S12 (cont.).** Extracted ion chromatograms ( $m/z$  597.0643 $\pm$ 0.0060) obtained by LC-MS in negative ion mode of the extracts from isolates LN401 (D) and LN427 (E). The zoom shows the peak corresponding to emestrin (3) eluting at 20.4 min and the peak of an isomer eluting shortly earlier at 20.2 min.

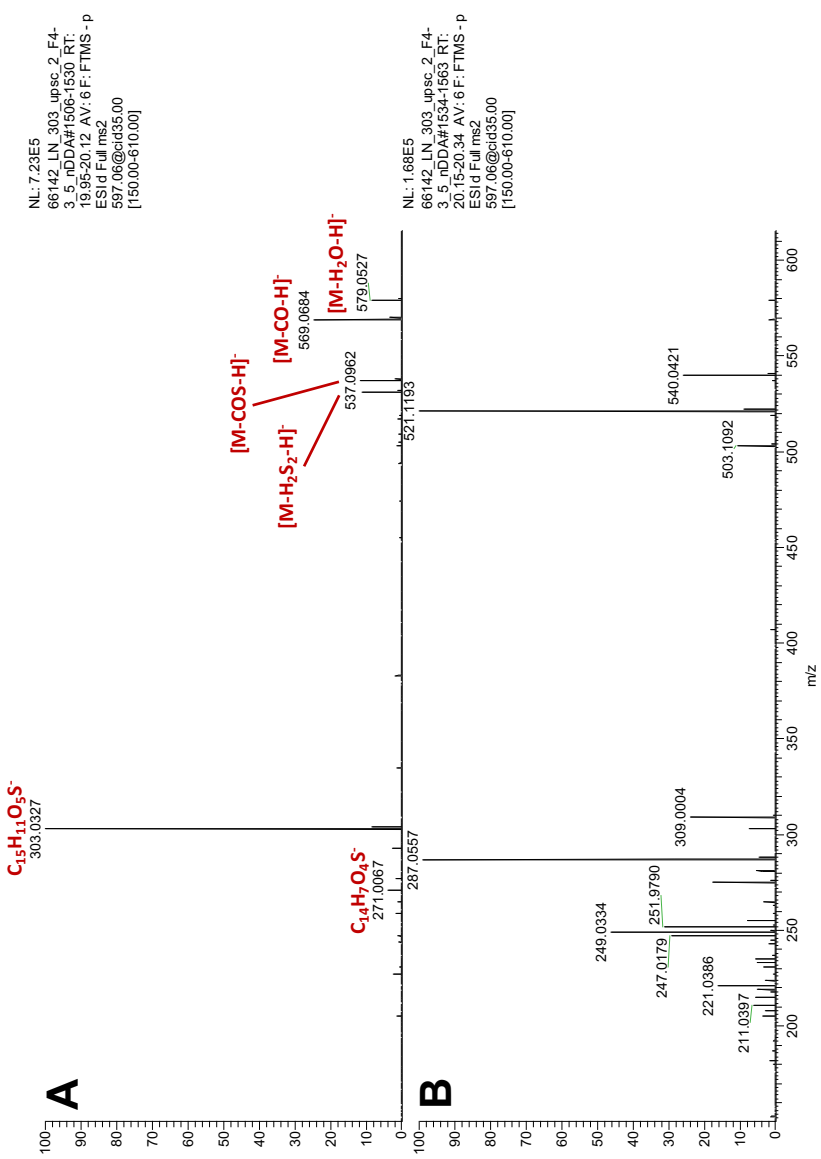
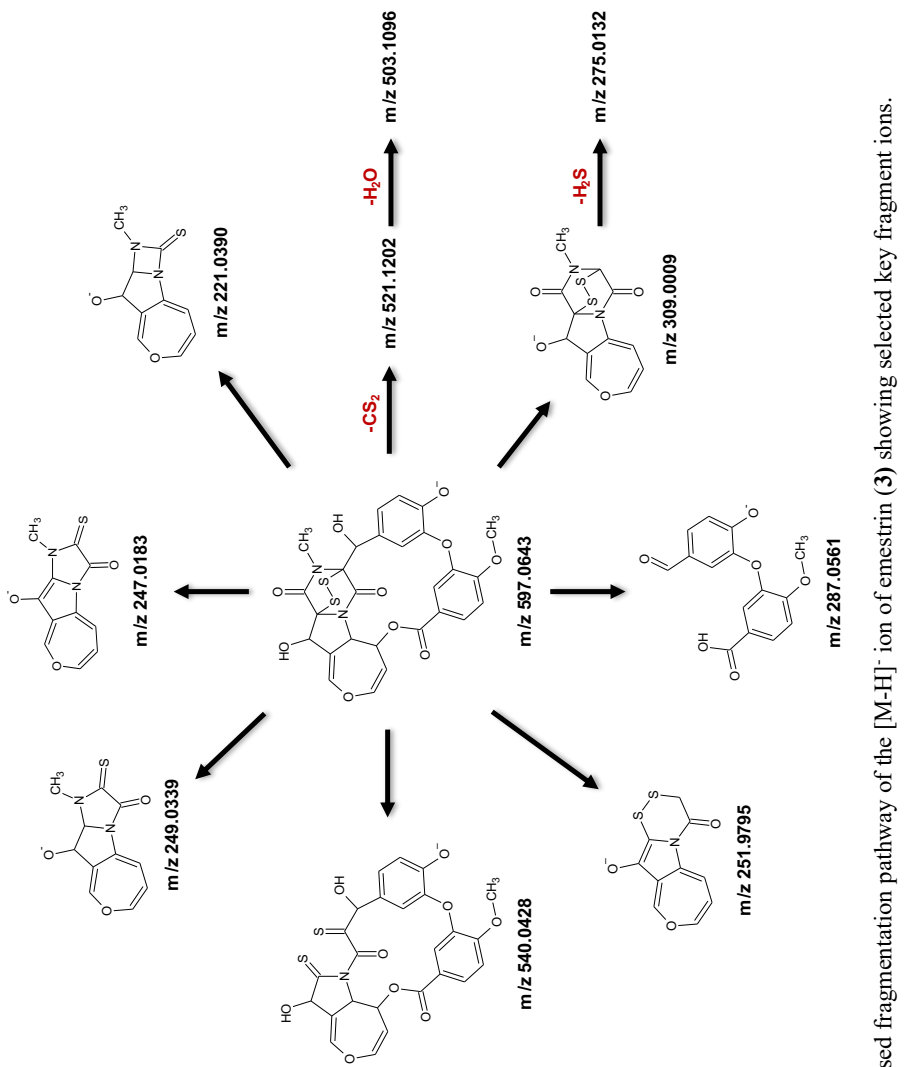


**Figure S13.** HRESIMS/MS spectrum of the  $[\text{M}-\text{H}]^-$  ion of the non-isolated emestrin isomer eluting at 20.0. min (A) and emestrin (3) eluting at 20.2 min (B) obtained by LC-MS in negative ion mode.



**Scheme S6.** Proposed fragmentation pathway of the  $[M-H]^-$  ion of emestrin (3) showing selected key fragment ions.

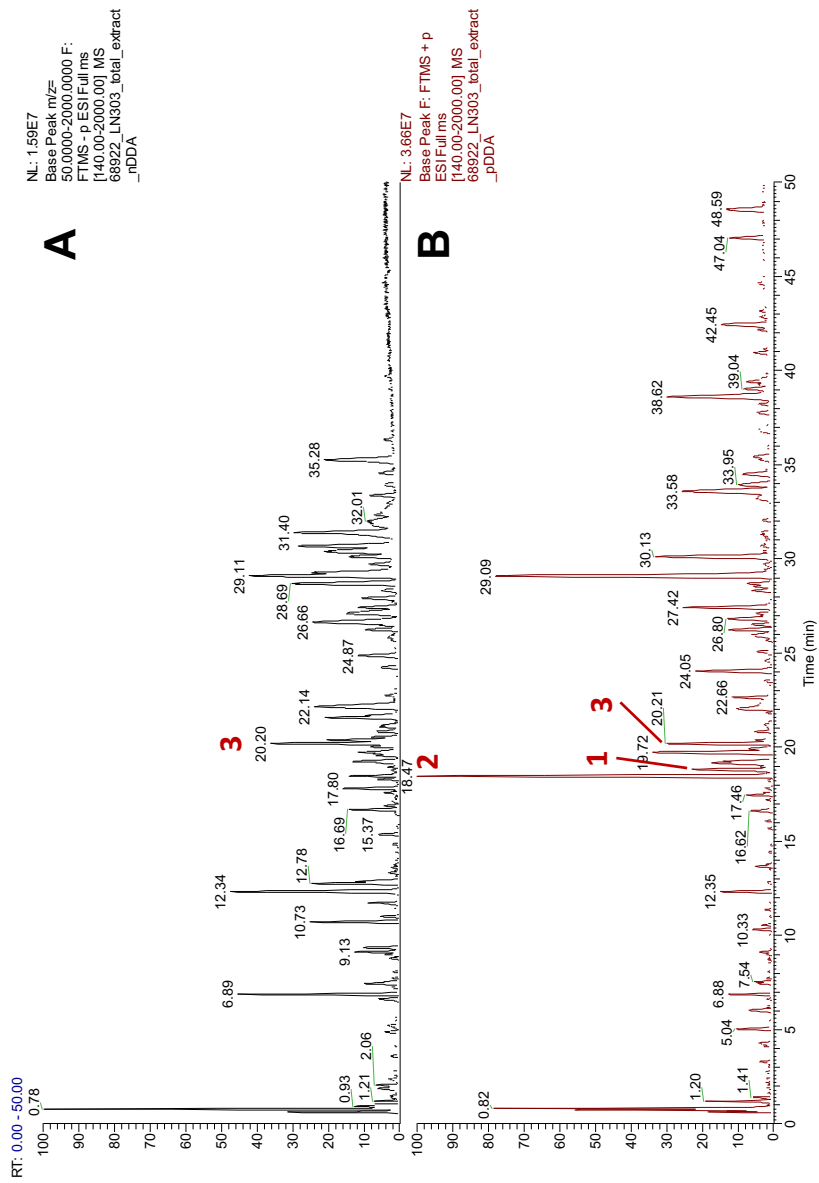


**Figure S14.** Base peak chromatograms obtained by LC-MS in negative ion mode (A) and positive ion mode (B) of the total extract from isolate LN303. The peaks corresponding toakanthenin A,akanthenin B, and emestrin are marked with **1**, **2**, and **3**, respectively.

**Table S1.** Experimental parameters and CCDC-Code of emestrin.

Sample	Machine	Source	Temp.	Detector Distance	Time/ Frame	#Frames	Frame width	CCDC
	Bruker		[K]	[mm]	[s]		[°]	
<b>Emestrin</b>	D8	Mo	100	40	60	4309	0.300	2040245

**Table S2.** Sample and crystal data.

Radiation [Å]	MoK $\alpha$ ( $\lambda = 0.71073$ )	Z	2	Measurement method	\f and \w scans
Crystal habit	clear colorless block	a [Å]	12.0970(12)		
Crystal size [mm <sup>3</sup> ]	0.08 × 0.02 × 0.01	b [Å]	7.7388(8)	Abs. correction type	multiscan
Empirical formula	C <sub>29</sub> H <sub>30</sub> N <sub>2</sub> O <sub>12</sub> S <sub>2</sub>	c [Å]	15.2512(15)	Abs. correction Tmin	0.6477
Formula weight [g/mol]	662.67	$\alpha$ [°]	90	Abs. correction Tmax	0.5913
Temperature [K]	100.0	$\beta$ [°]	98.357(4)	Density (calculated) [g/cm <sup>3</sup> ]	1.378
Crystal system	monoclinic	$\gamma$ [°]	90	Absorption coefficient [mm <sup>-1</sup> ]	0.095
Space group	<i>P</i> 2 <sub>1</sub>	Volume [Å <sup>3</sup> ]	1412.6(2)	F (000) [e <sup>-</sup> ]	784.0

**Table S3.** Data collection and structure refinement.

2 $\Theta$ range for data collection [°]	4.642 to 60.228	Index ranges		Goodness-of-fit on F <sup>2</sup>	1031
Reflections collected	73456	h -17 ≤ h ≤ 17		Diff. peak and hole [e <sup>-</sup> Å <sup>-3</sup> ]	0.36/-0.47
Data / restraints / parameters	8218/1/415	k -10 ≤ k ≤ 10			
Refinement method	Least squares	l -21 ≤ l ≤ 21		Function minimized	$\Sigma w(F_o^2 - F_c^2)^2$
		all data	R1 = 0.0609, wR2 = 0.1169	Weighting scheme	where
		I>2σ(I)	R1 = 0.1094, wR2 = 0.1403	W = 1/[σ <sup>2</sup> (F <sub>o</sub> <sup>2</sup> ) + (0.0457P) <sup>2</sup> + 1.4439P]	P=(F <sub>o</sub> <sup>2</sup> +2F <sub>c</sub> <sup>2</sup> )/3

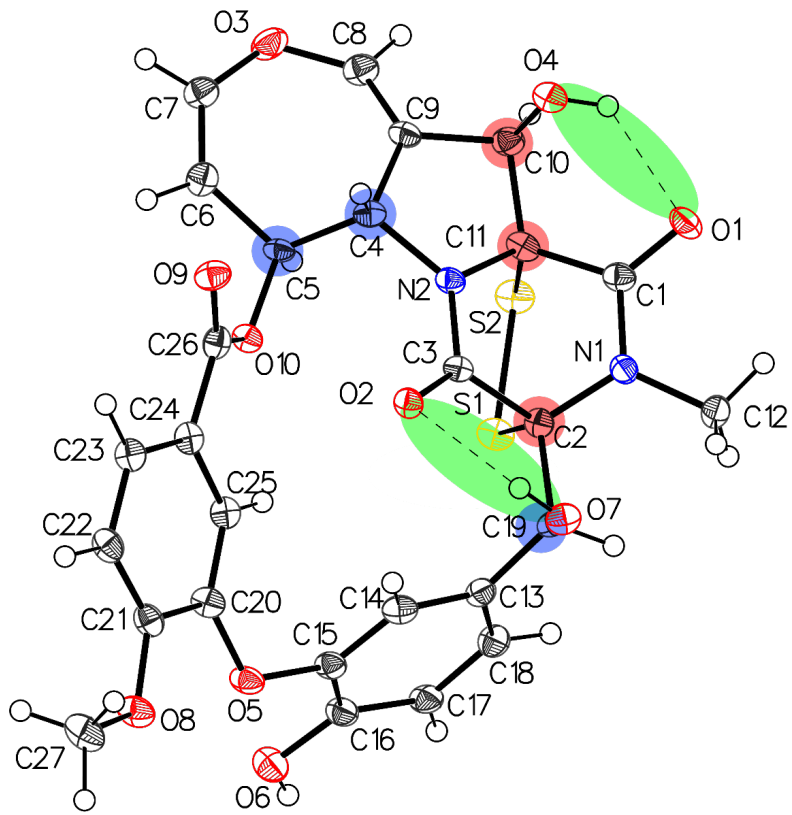


**Figure S15.** Asymmetric Unit of [emestrin]. C-C- Bond precision: 0.0070 Å. Chiral centres can be determined with the proof of Flack of -0.07(6). Red dotted are “R”, blue are “S”. Additional to the chiral information we can detect two intramolecular hydrogen bonds of moderate character (green highlighted). The structure is already at the CCDC at 1133525 & 1133526 but at RT. Both results are as well published and from good quality.

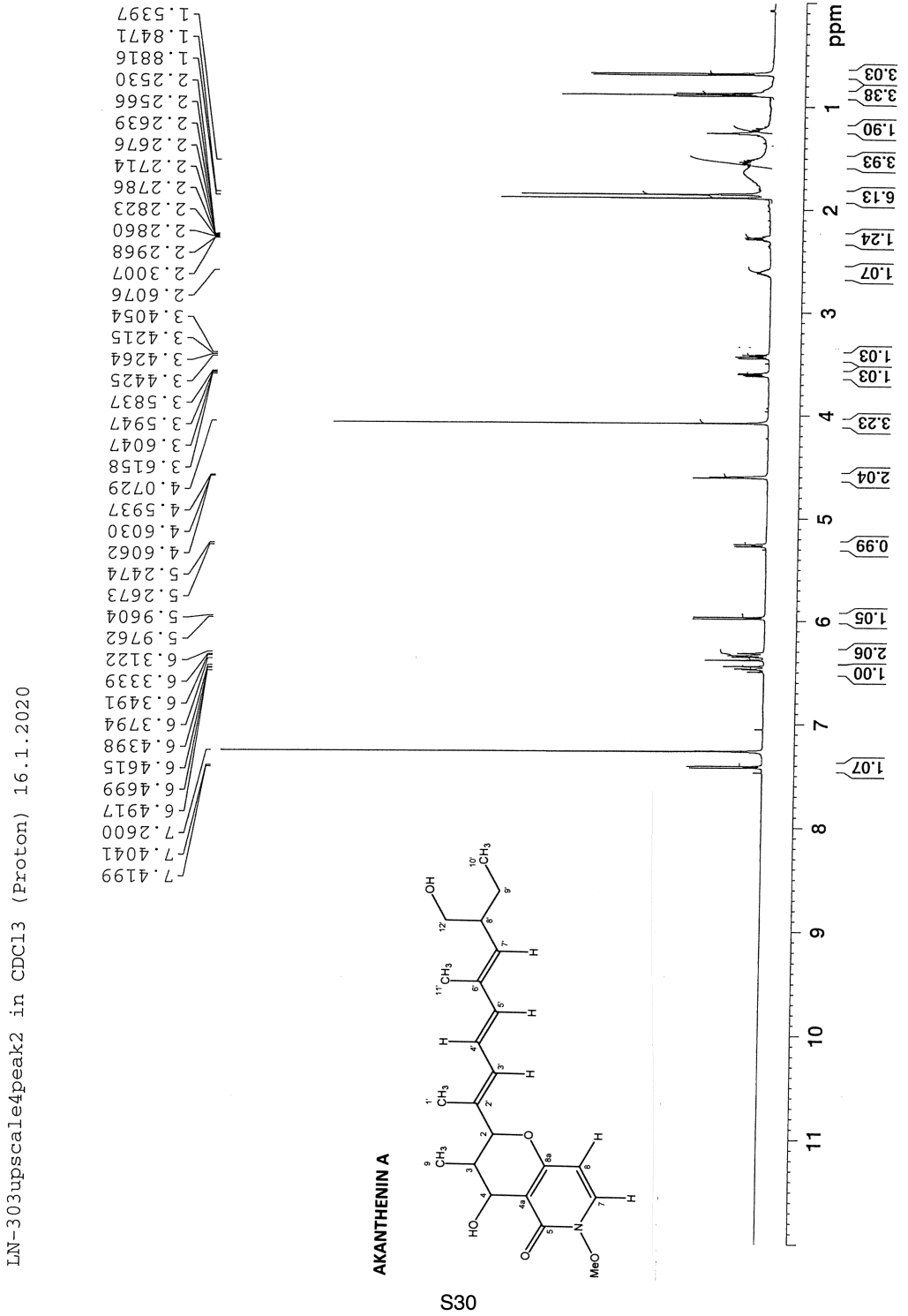
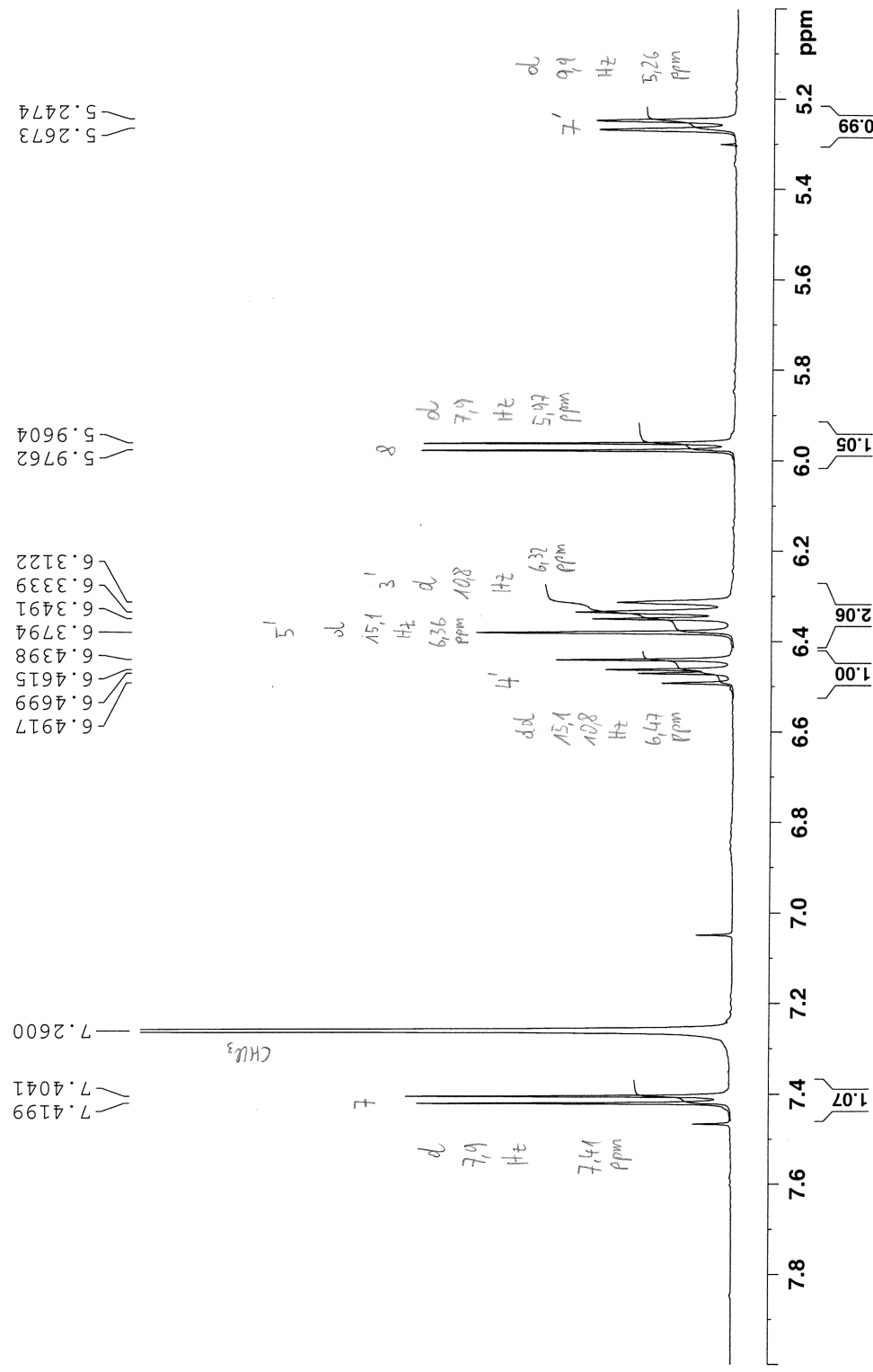
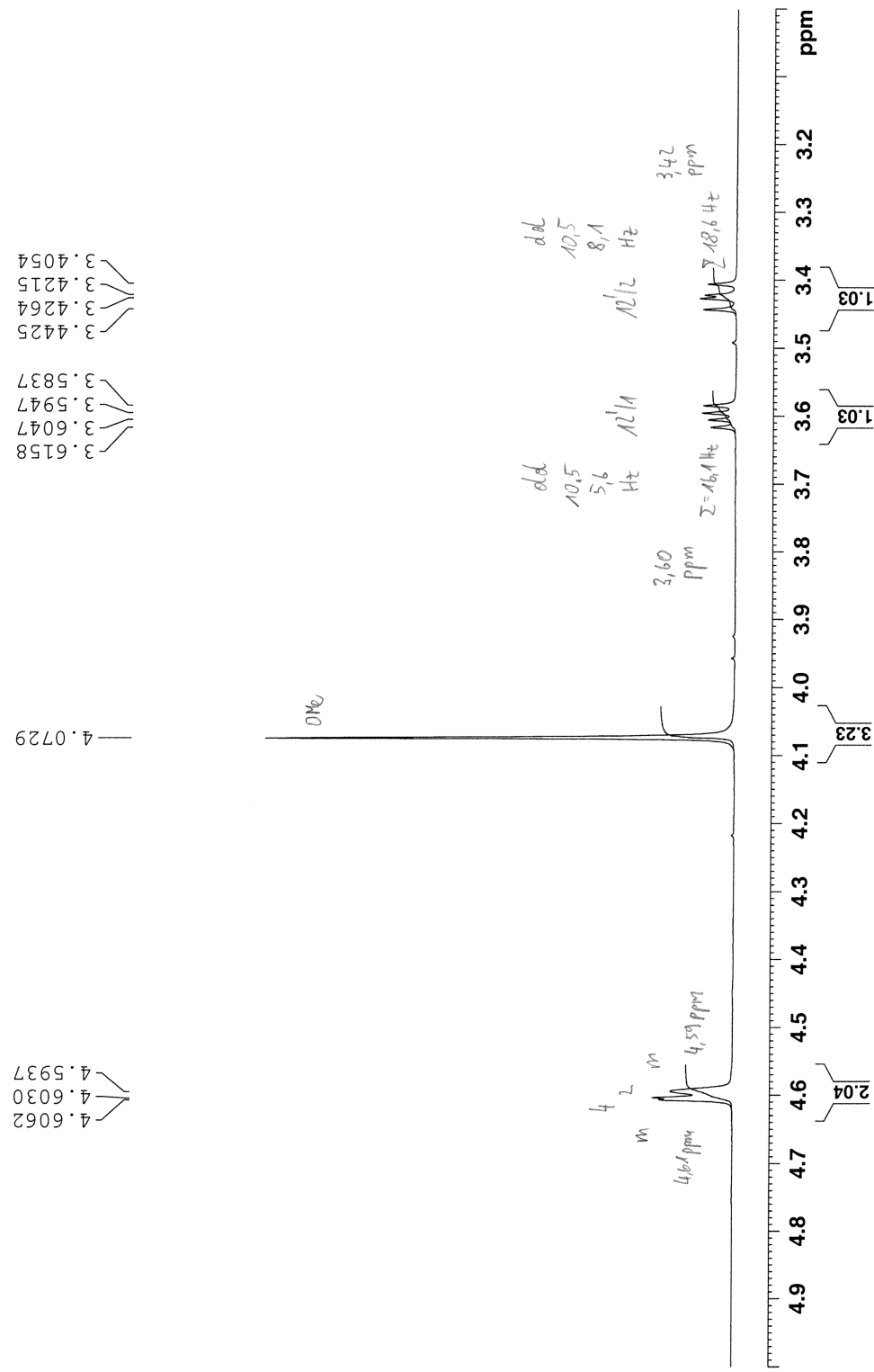


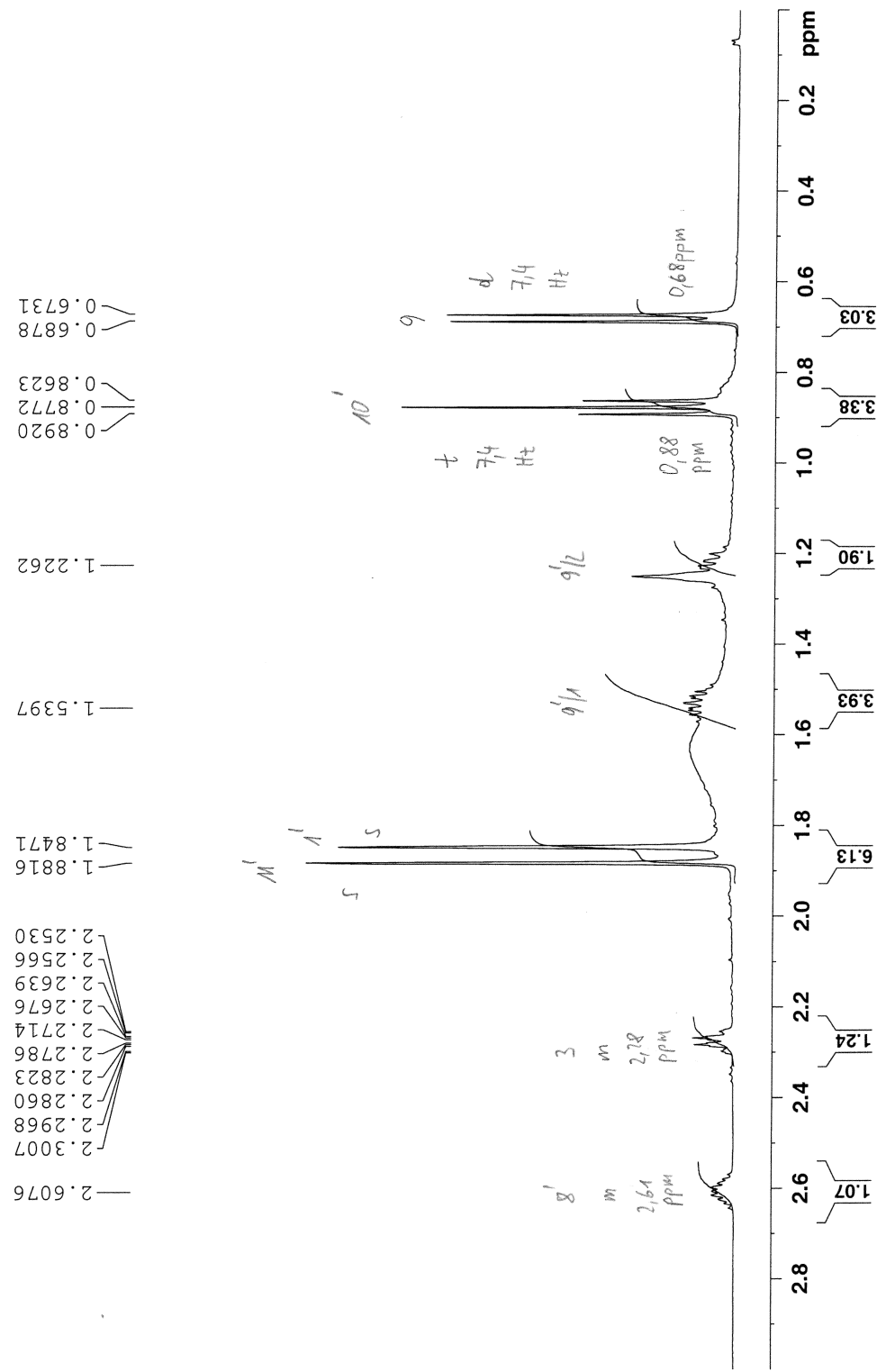
**Figure S16** (pages S30-S33).  $^1\text{H}$  NMR spectrum of 1 in  $\text{CDCl}_3$  ( $\delta$  in ppm).



LN-303upscale4peak2 in CDCl<sub>3</sub> (Proton) 16.1.2020



LN-303upscale4peak2 in CDCl<sub>3</sub> (Proton) 16.1.2020



AKANTHENIN A

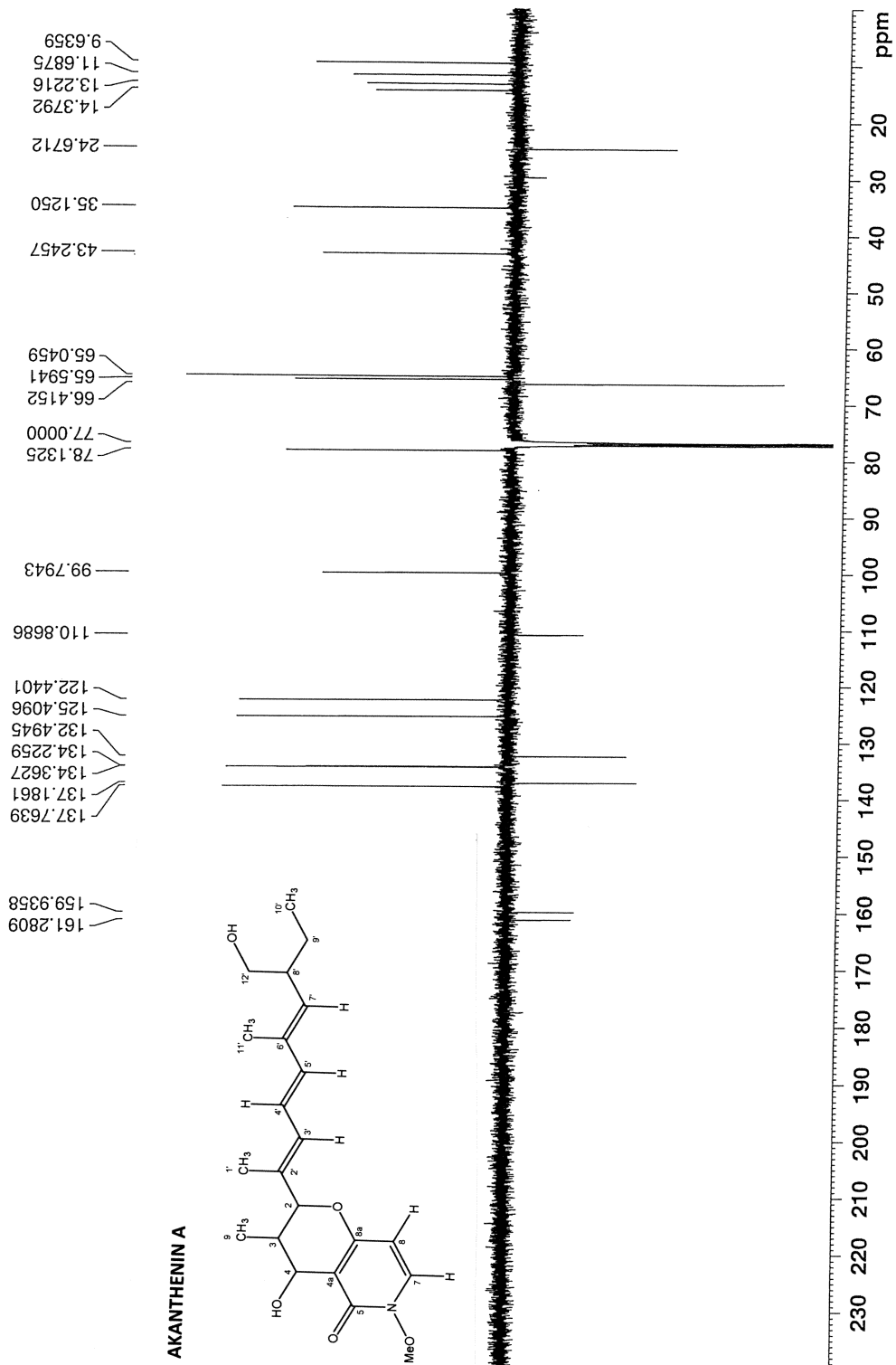
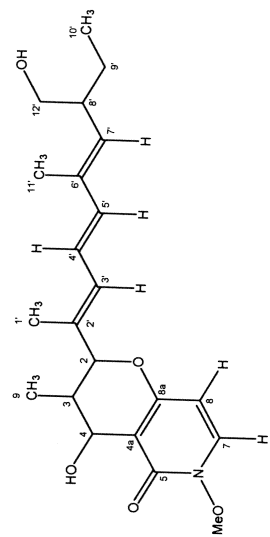
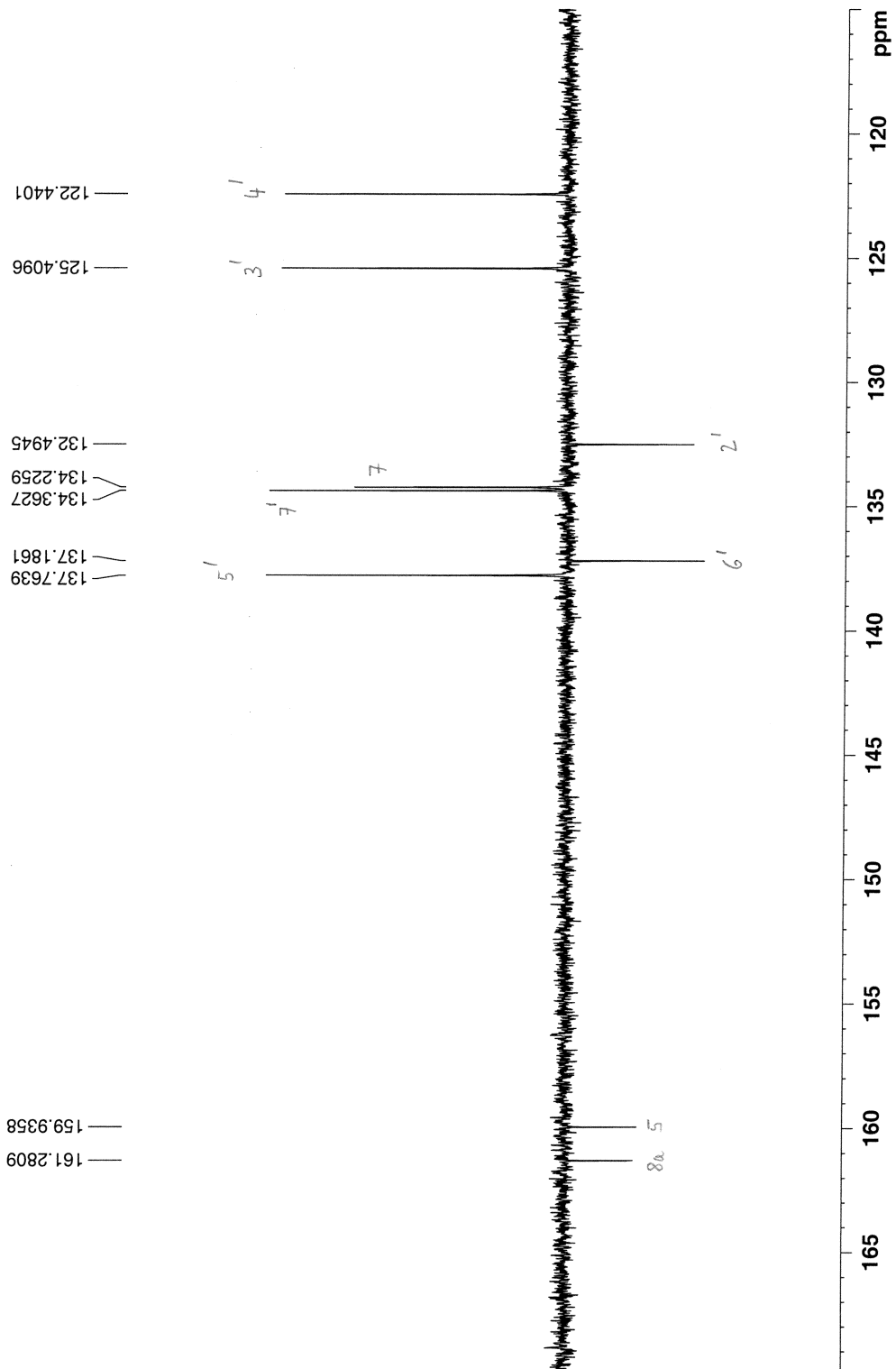
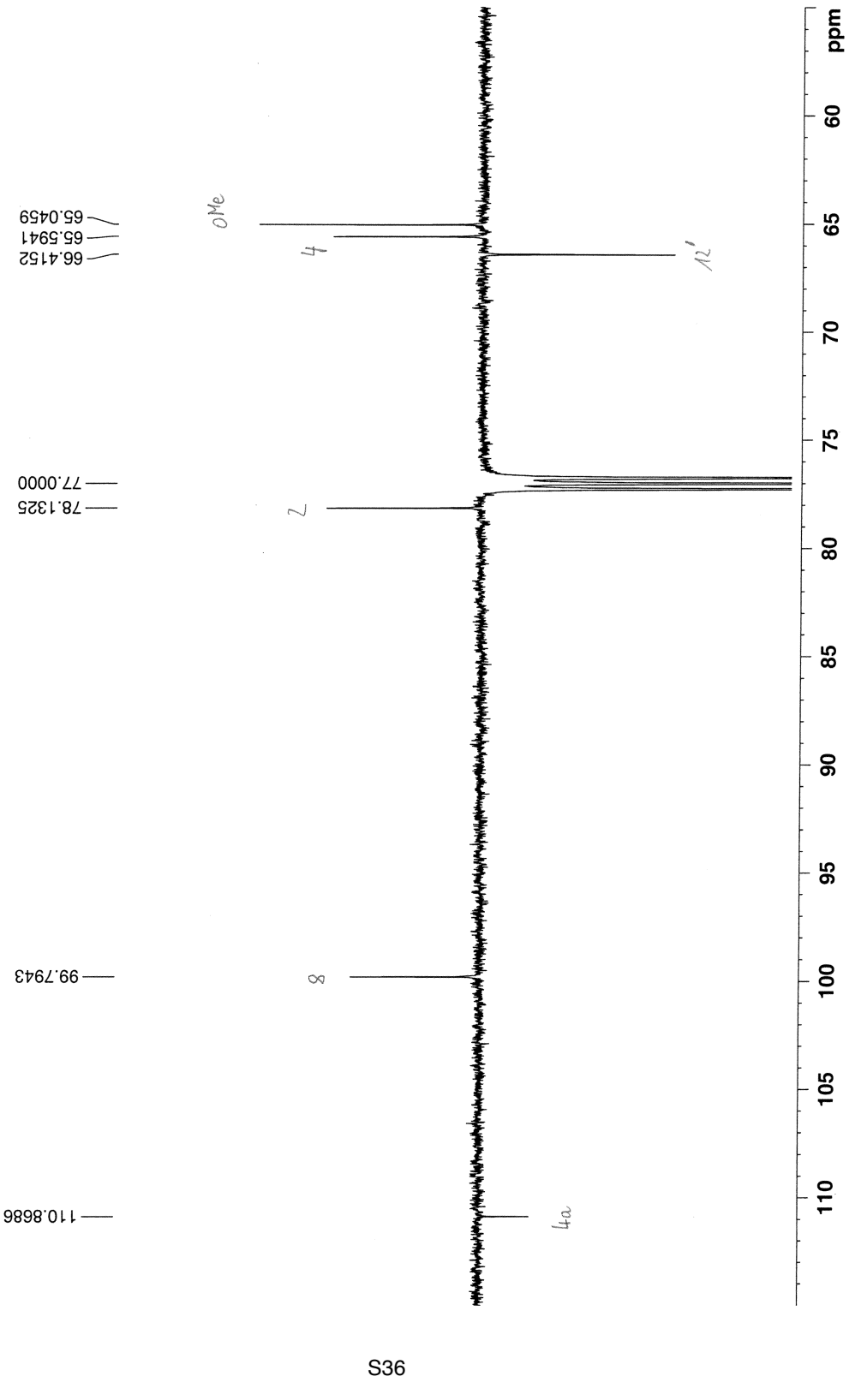
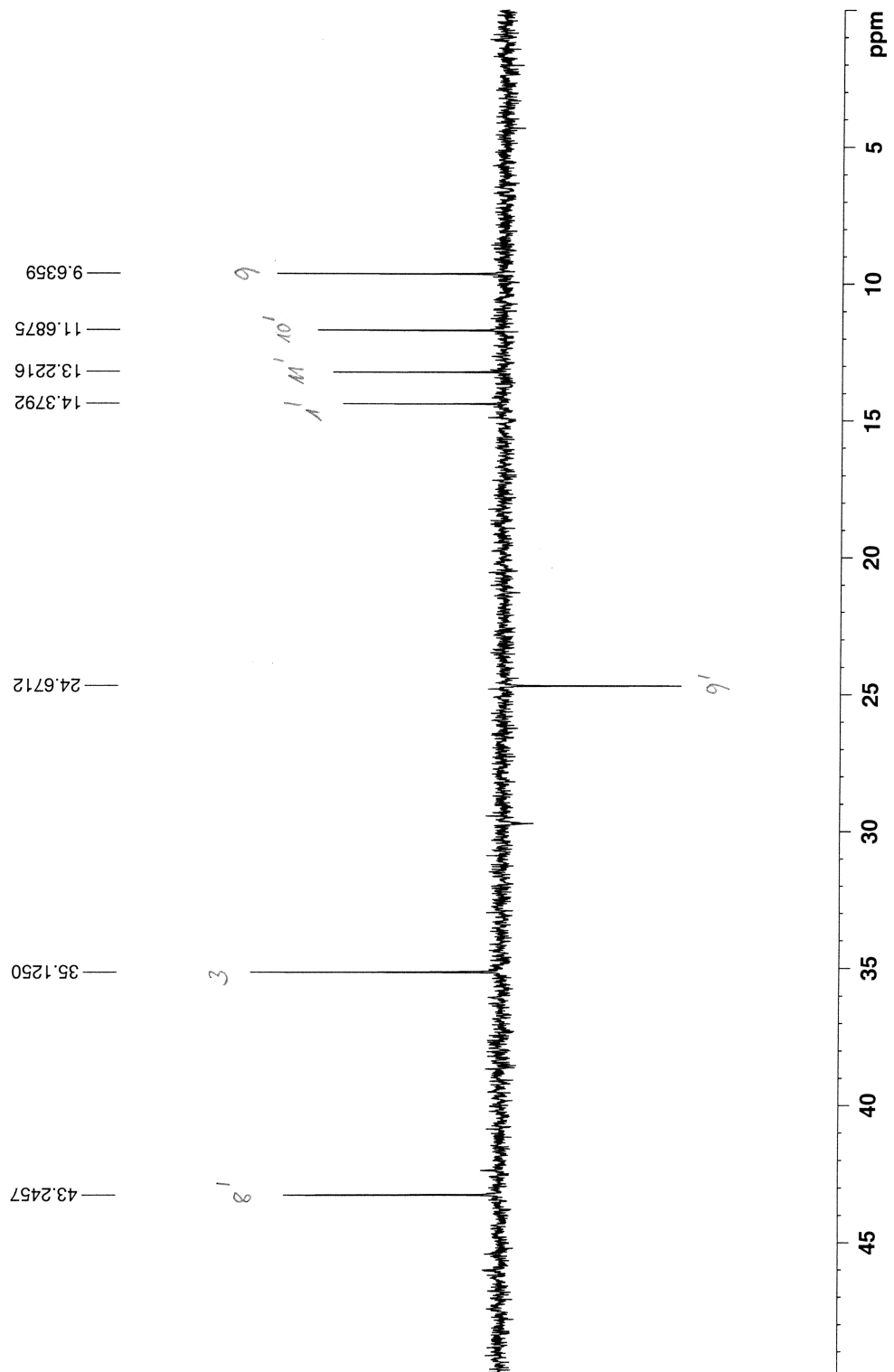


Figure S16 (pages S34-S37). <sup>13</sup>C NMR spectrum of **1** in CDCl<sub>3</sub> ( $\delta$  in ppm).







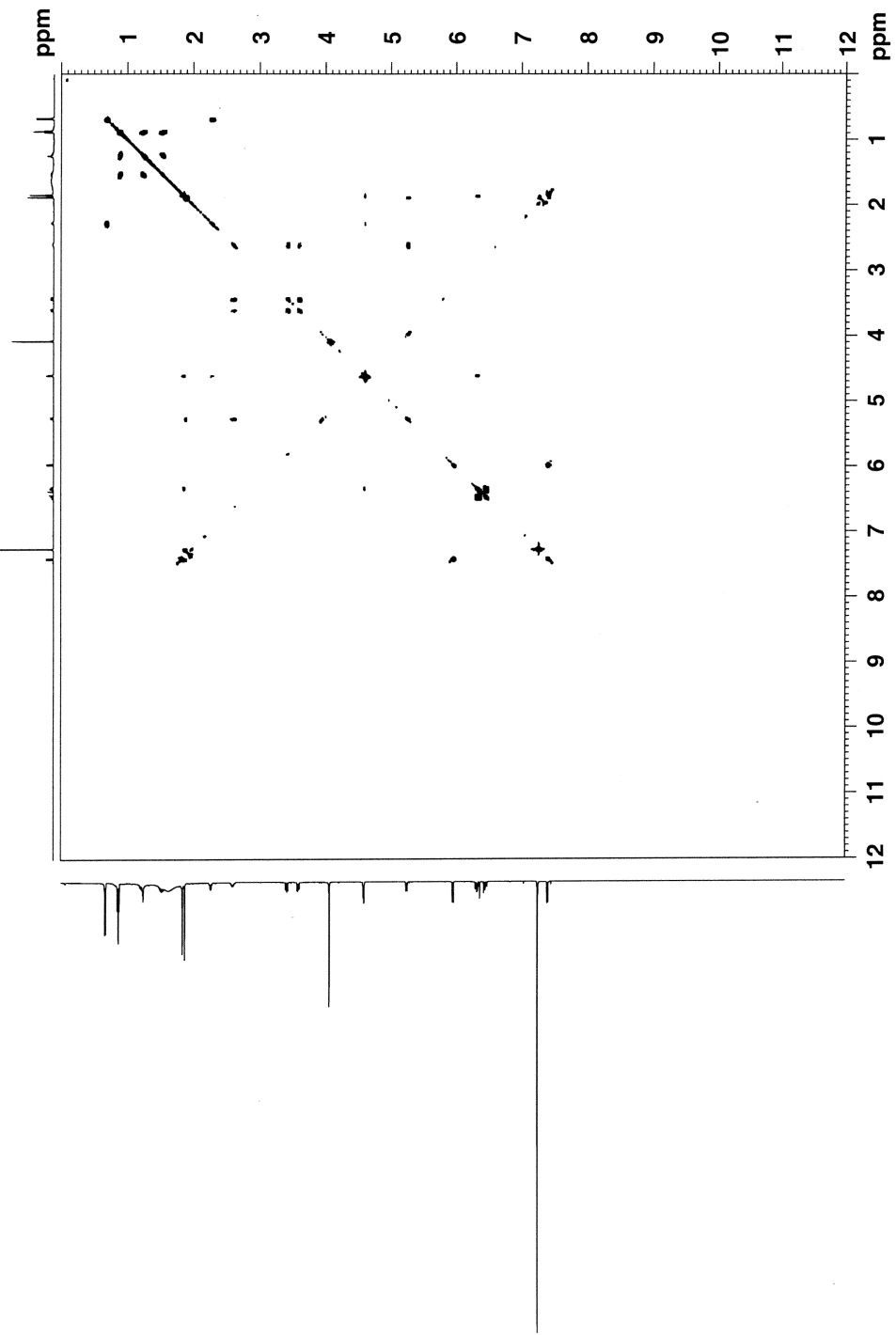
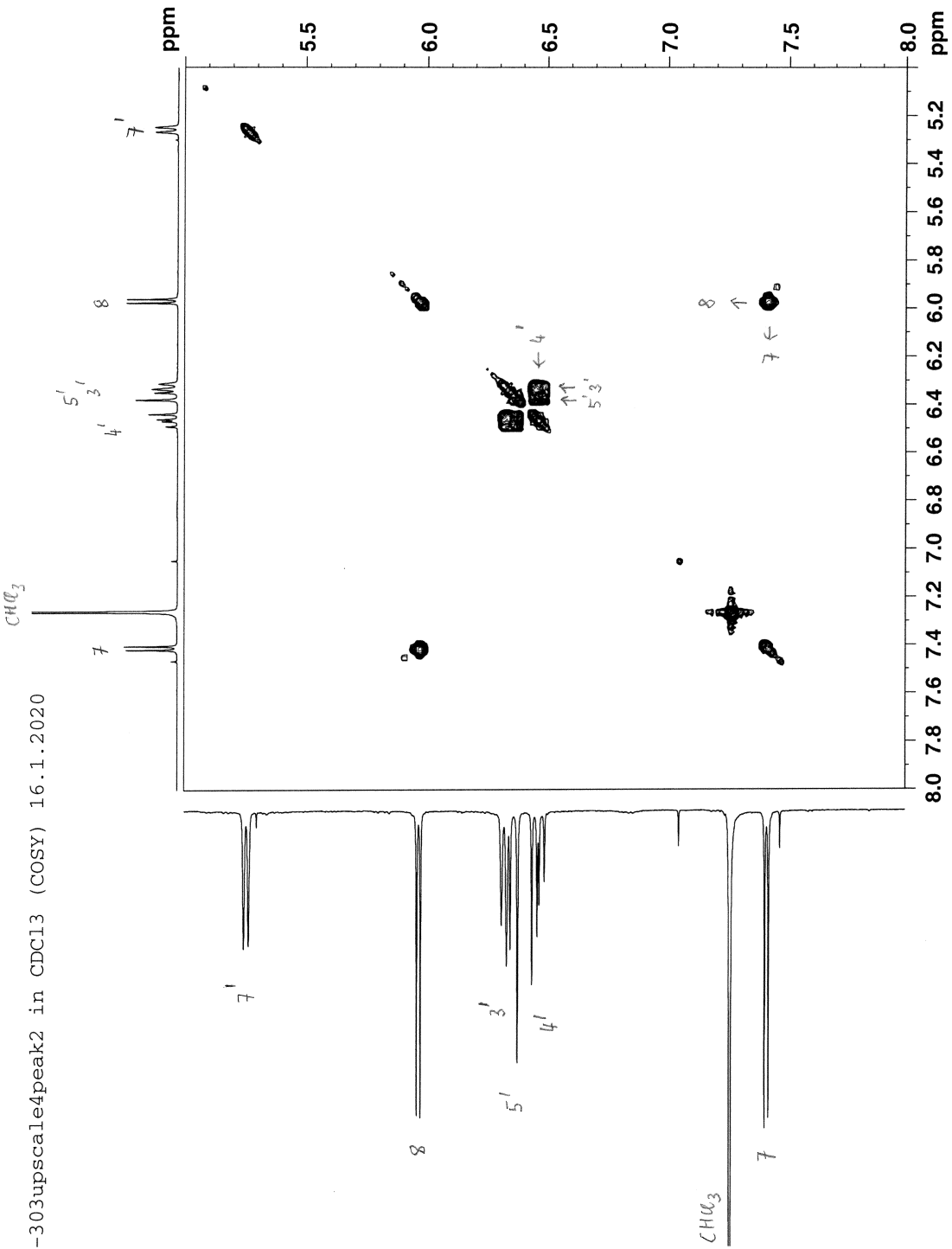
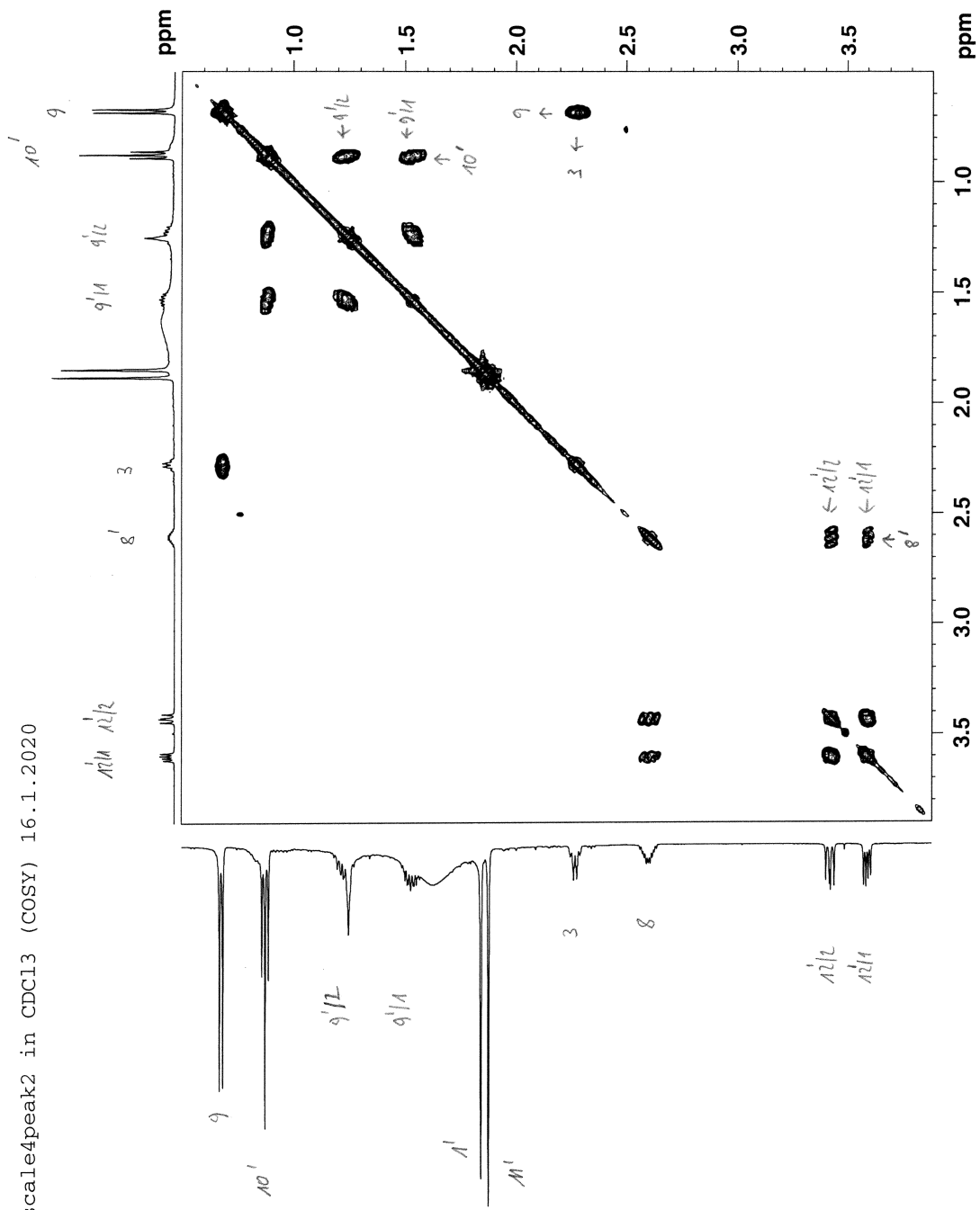


Figure S16 (pages S38-S41). COSY spectrum of **1** in CDCl<sub>3</sub> ( $\delta$  in ppm).

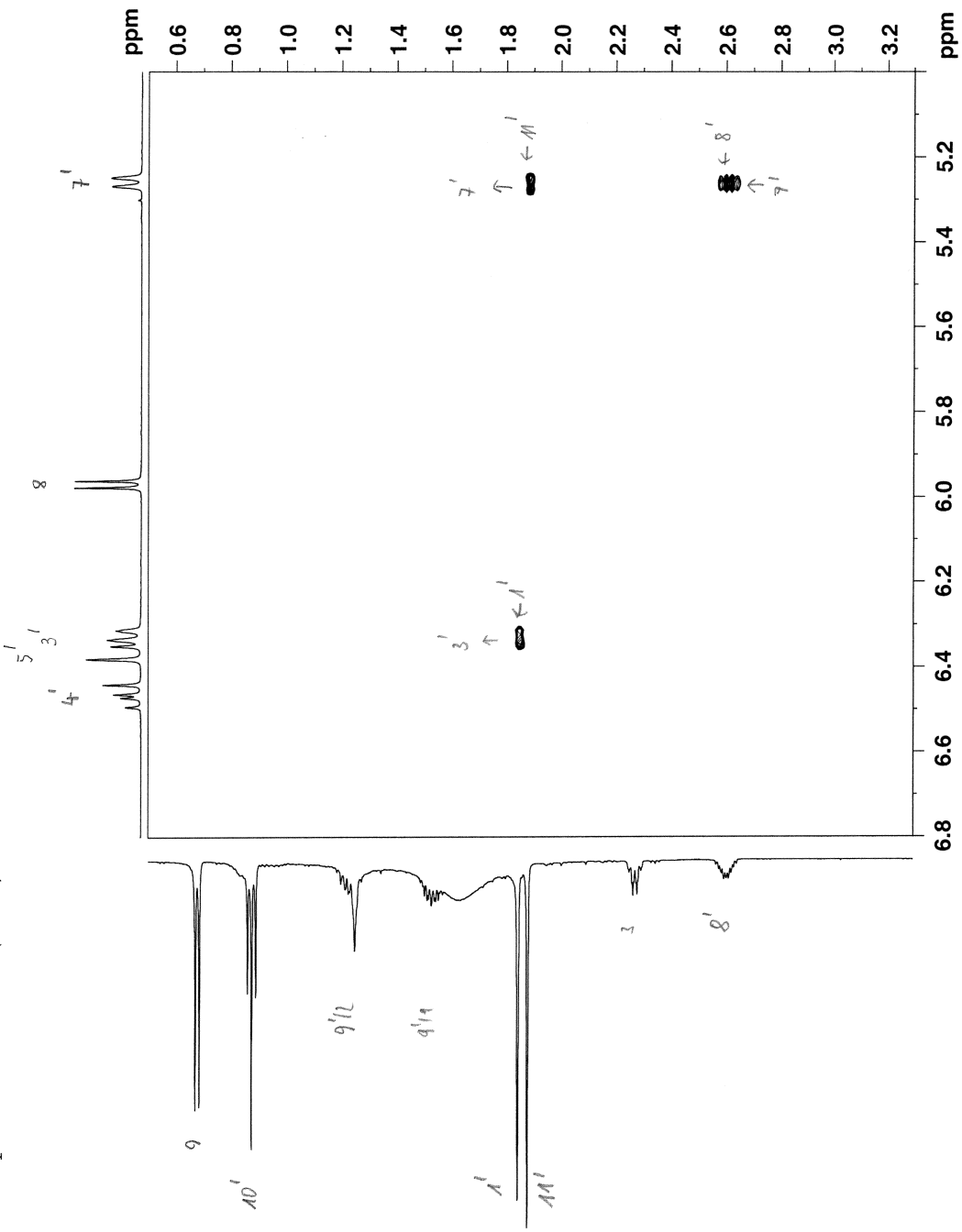
LN-303upscale4peak2 in CDCl<sub>3</sub> (COSY) 16.1.2020



LN-303upscale4peak2 in CDCl<sub>3</sub> (COSY) 16.1.2020



LN-303upscale4peak2 in CDCl<sub>3</sub> (COSY) 16.1.2020



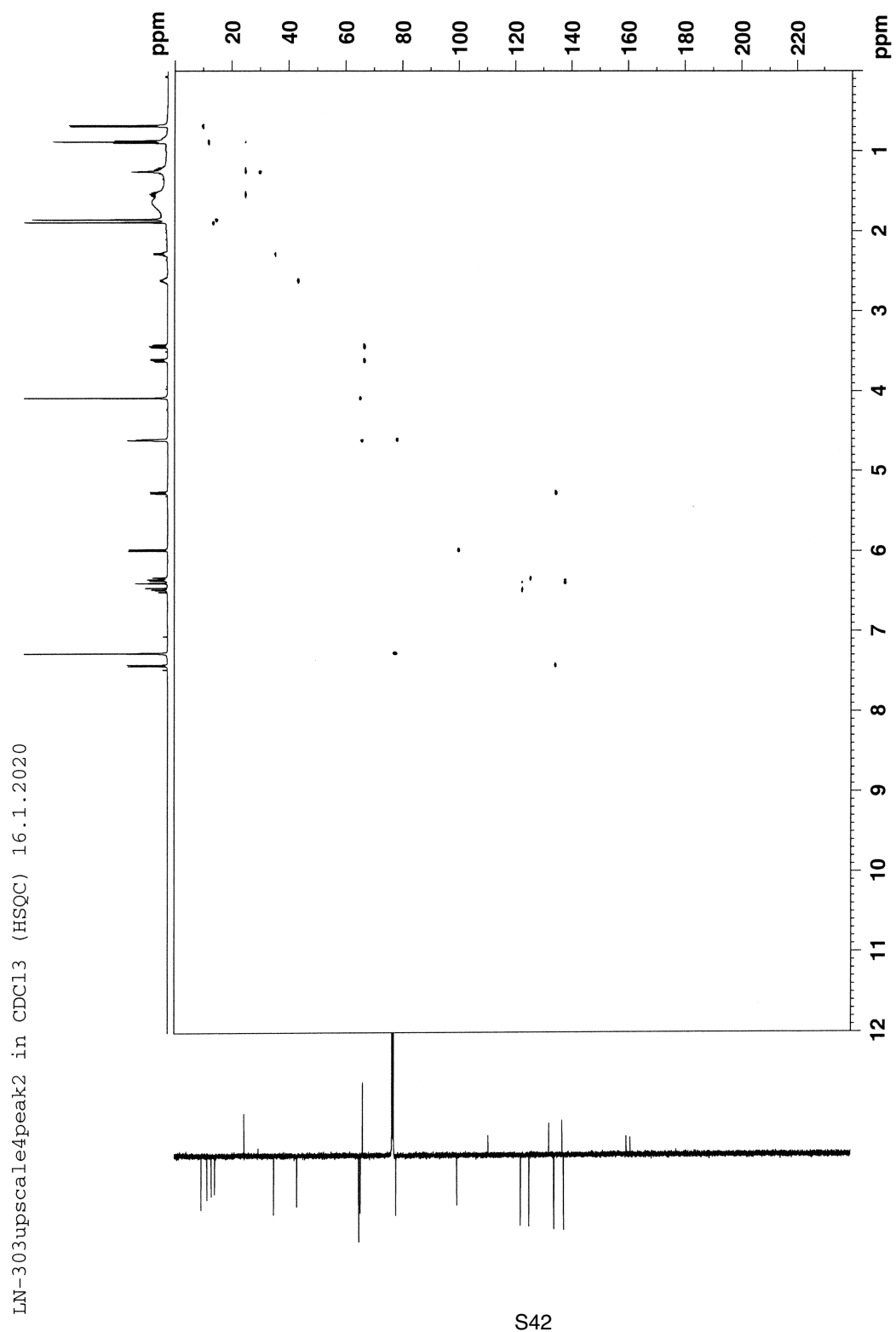
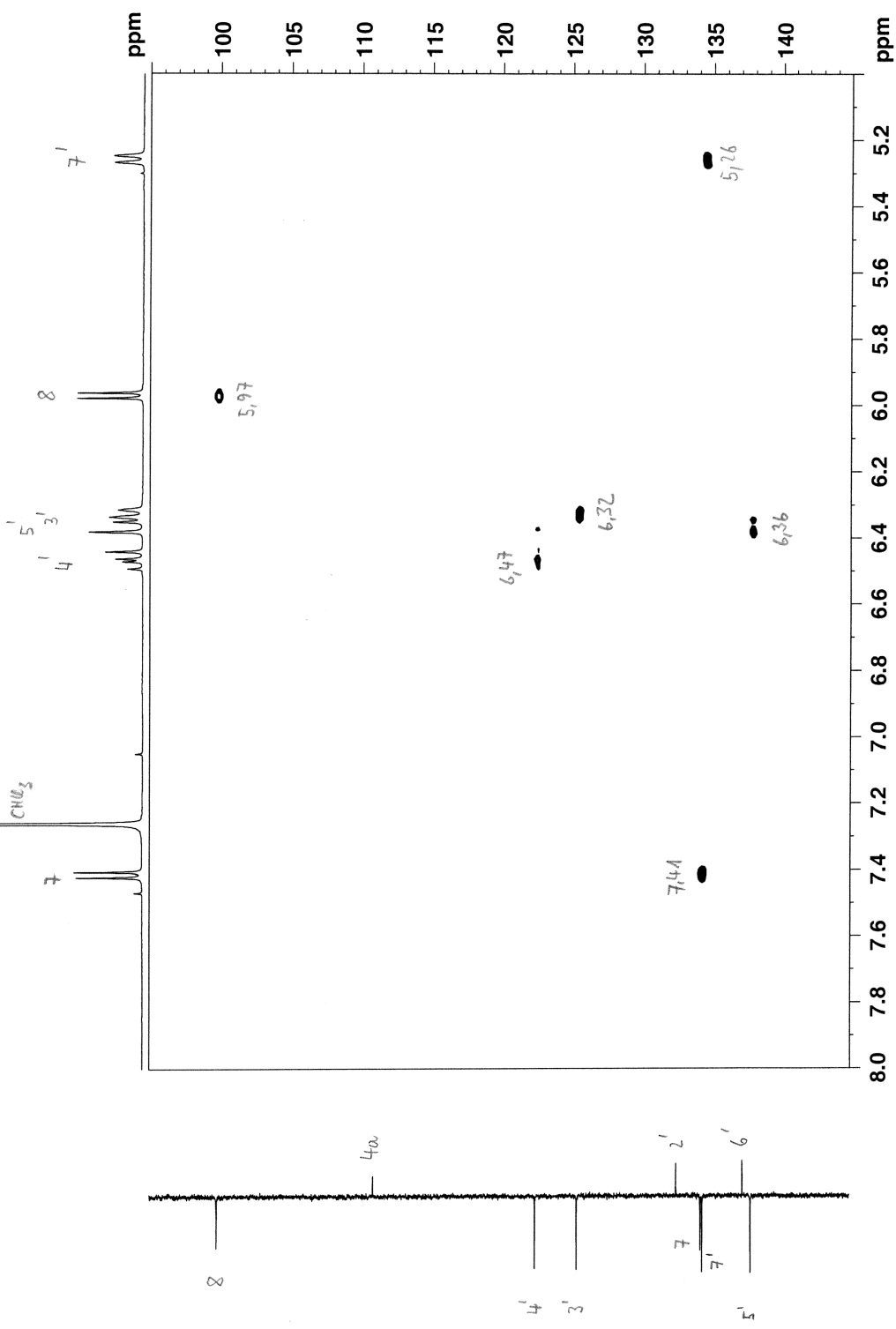
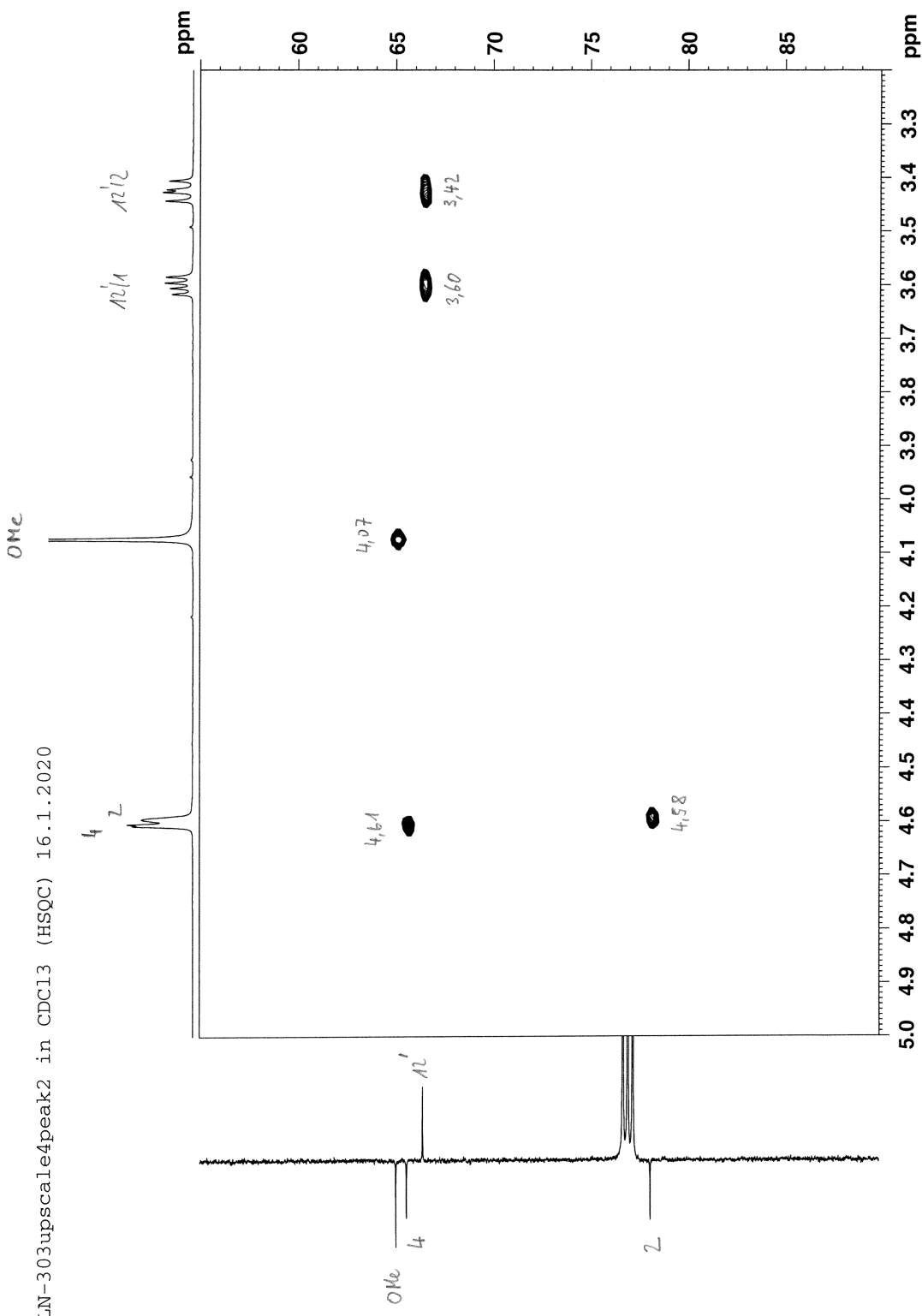


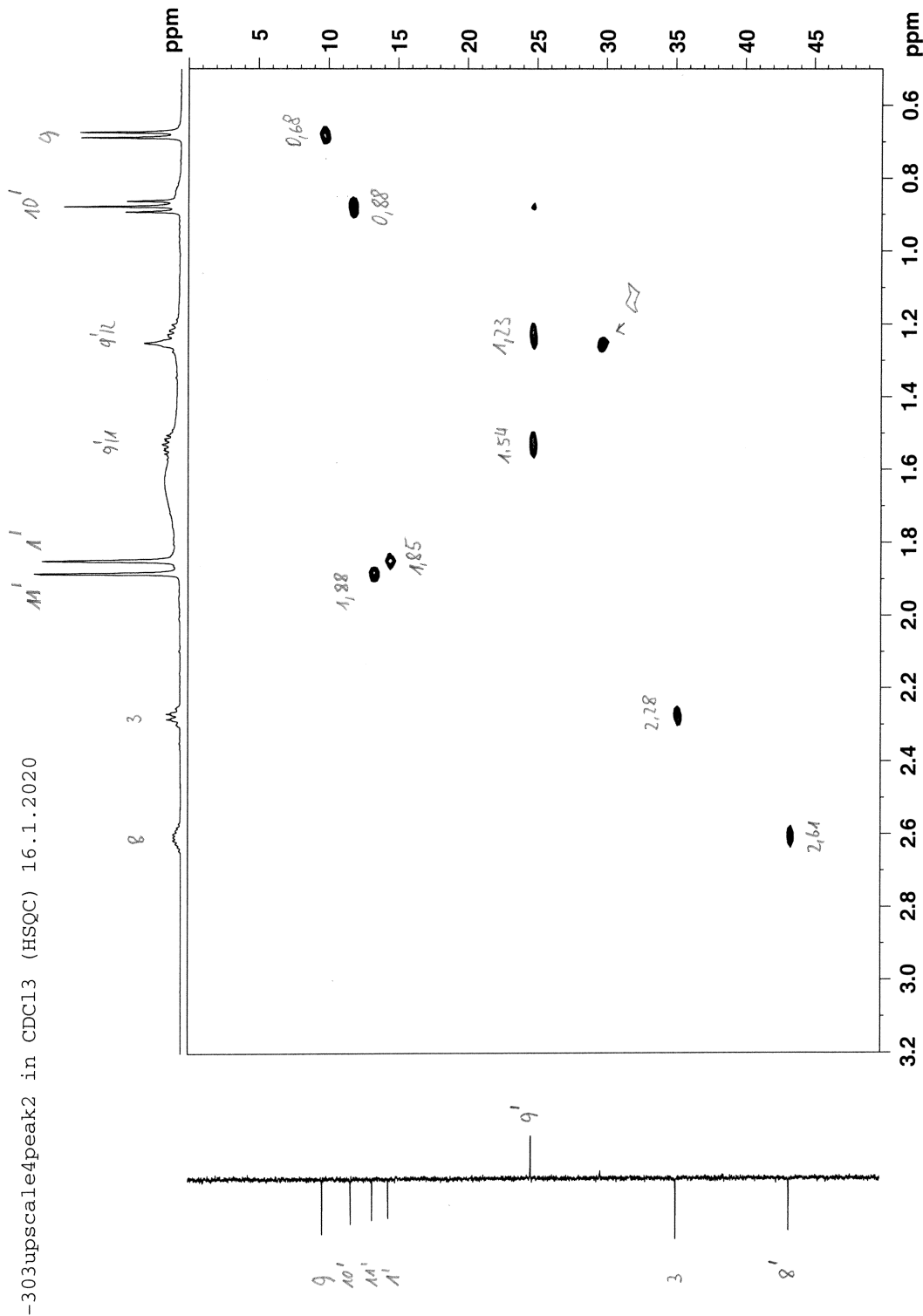
Figure S16 (pages S42-S45). HSQC spectrum of 1 in CDCl<sub>3</sub> ( $\delta$  in ppm).

LN-303upscale4peak2 in CDCl<sub>3</sub> (HSQC) 16.1.2020



LN-303upscale4peak2 in CDCl<sub>3</sub> (HSQC) 16.1.2020





LN-303upscale4peak2 in CDCl<sub>3</sub> (HMBC) 16.1.2020

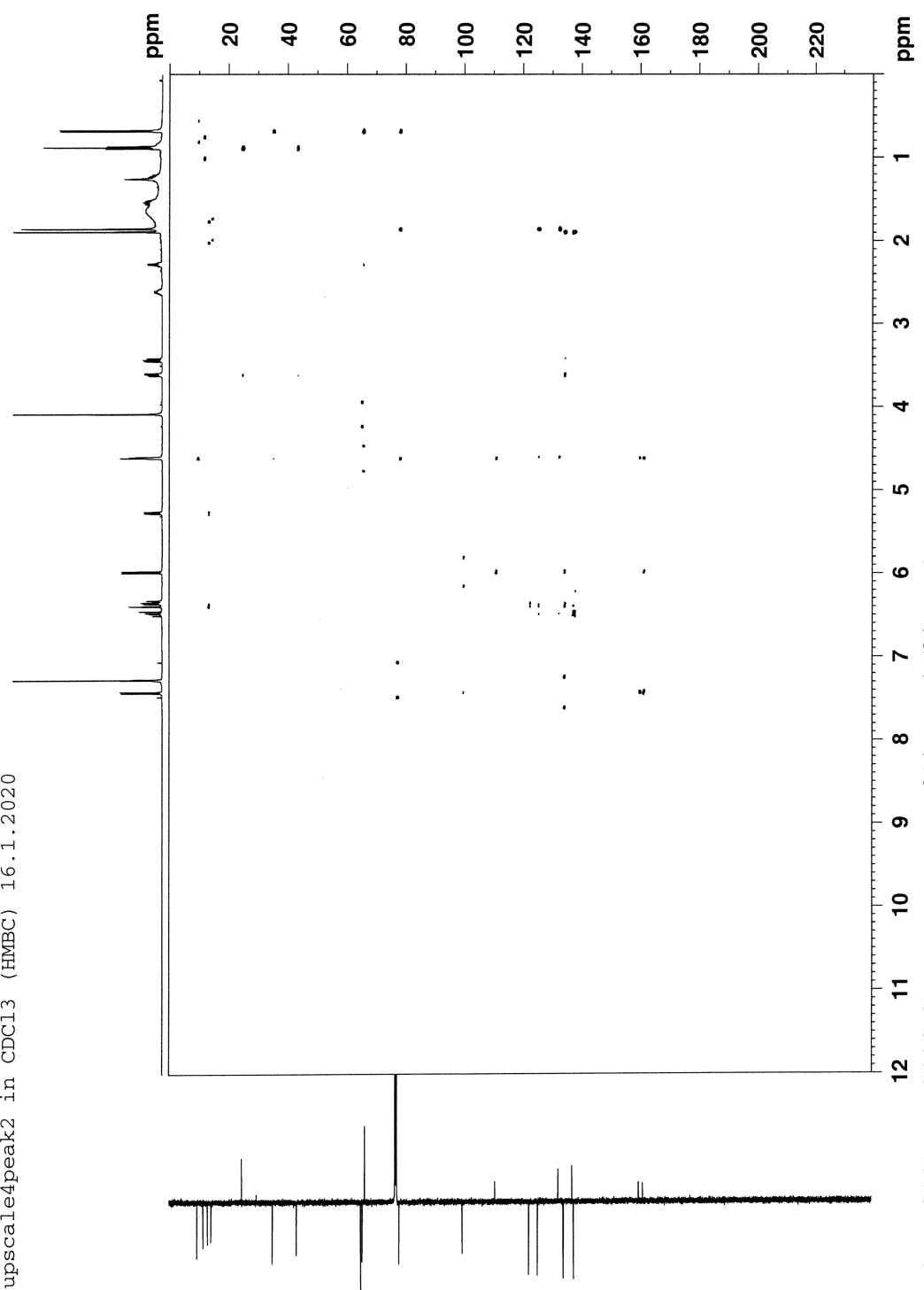
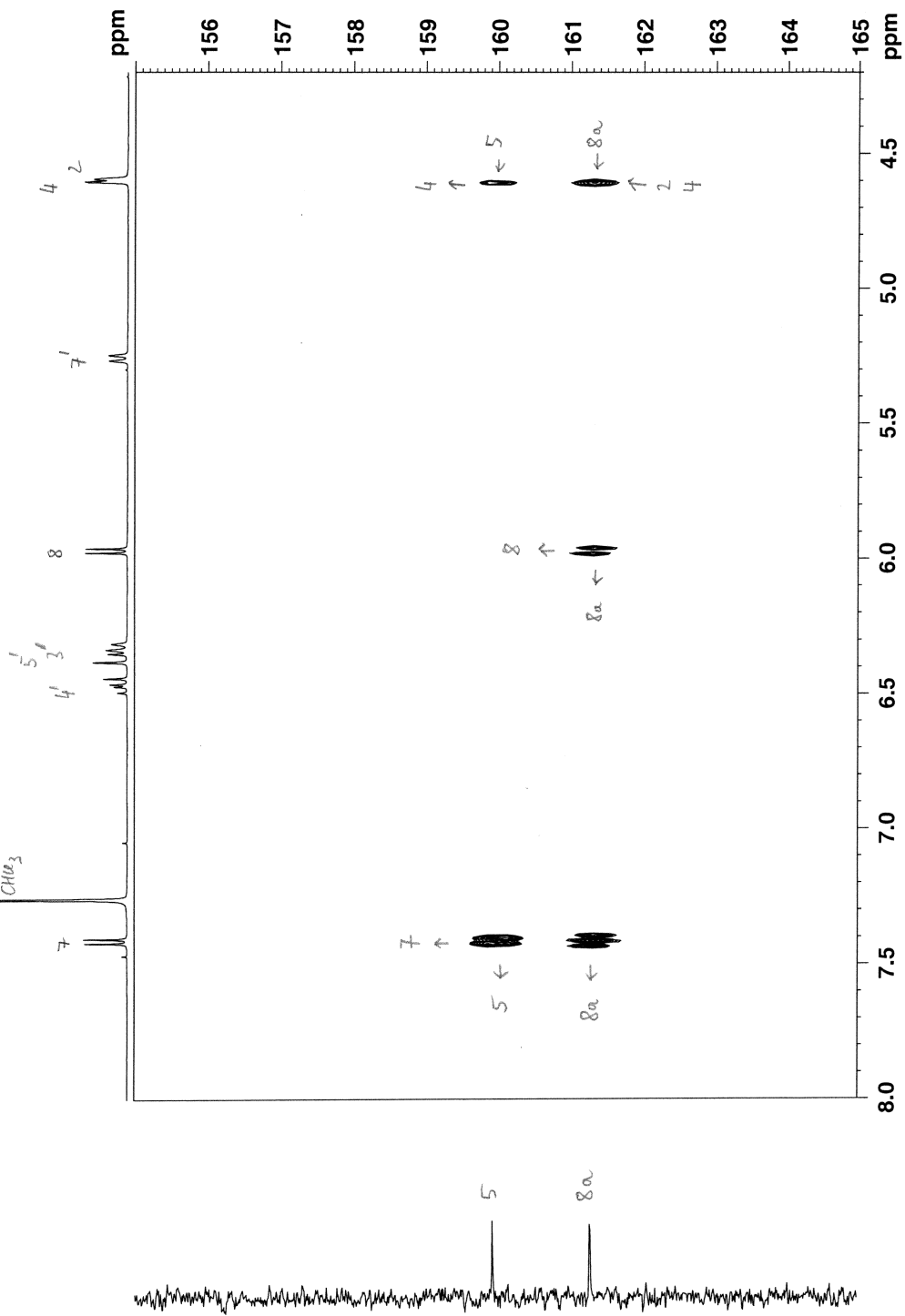
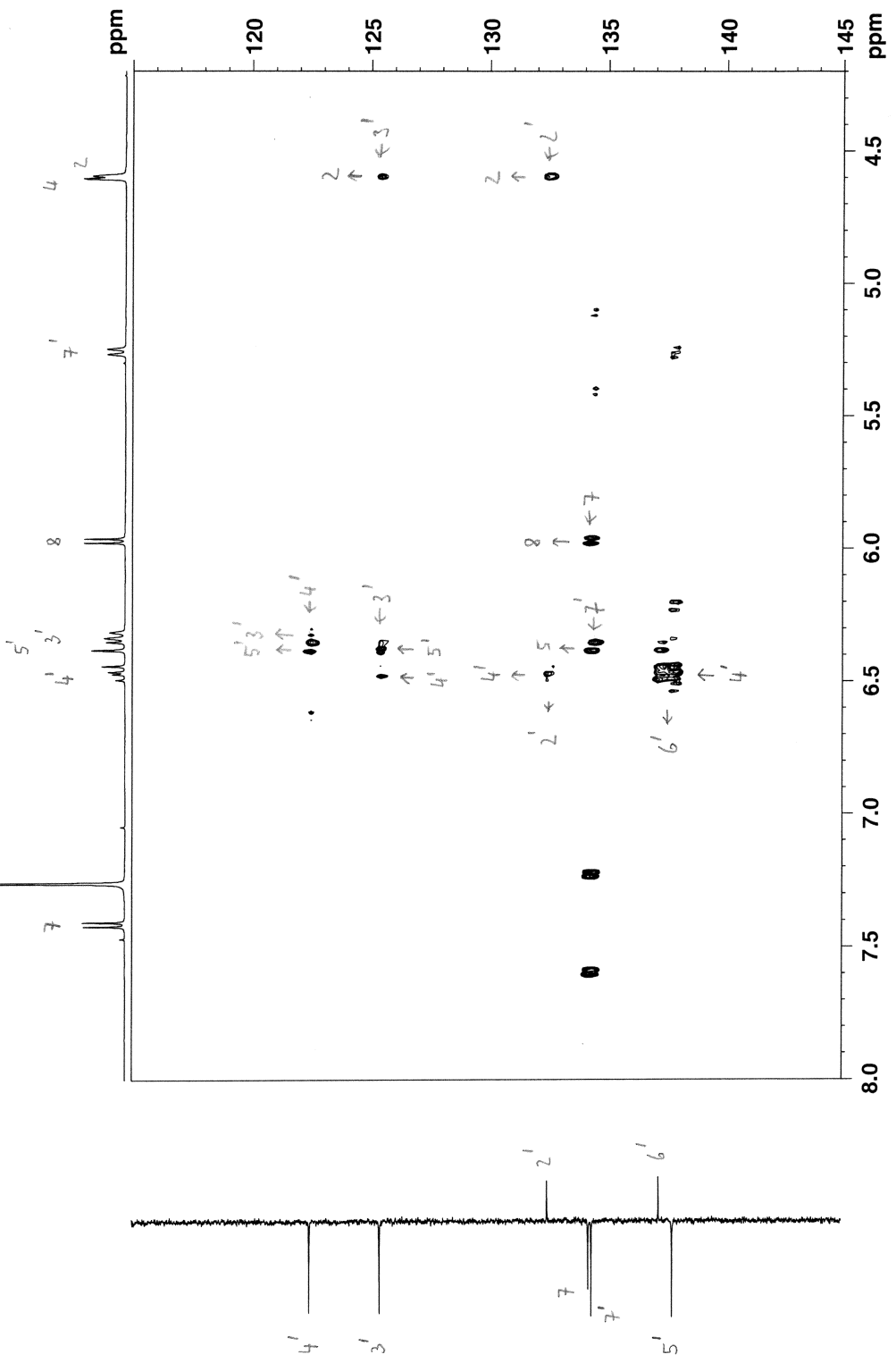


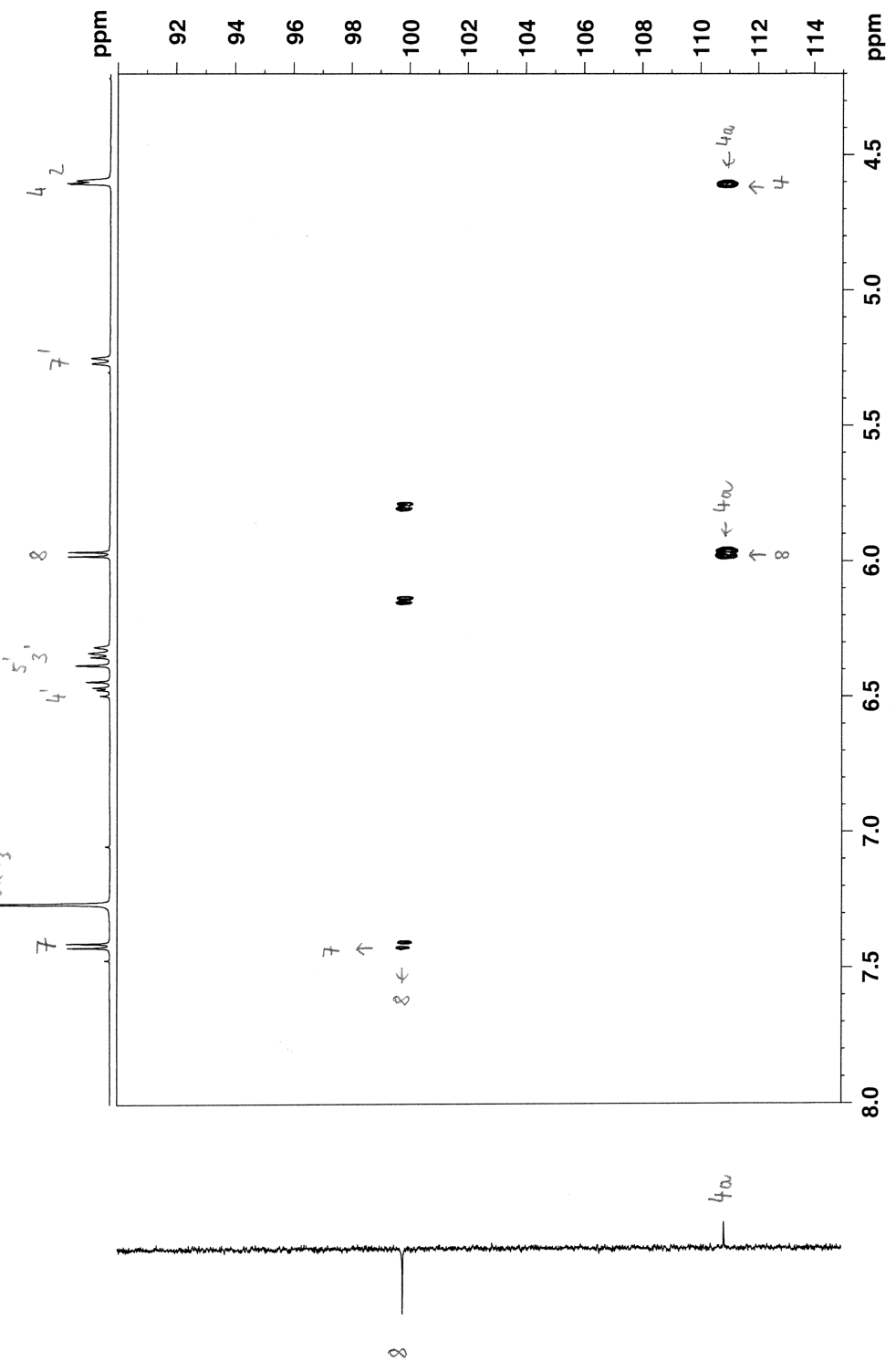
Figure S16 (pages S46-S59). HMBC spectrum of **1** in CDCl<sub>3</sub> ( $\delta$  in ppm).

LN-303upscale4peak2 in CDCl<sub>3</sub> (HMBC) 16.1.2020

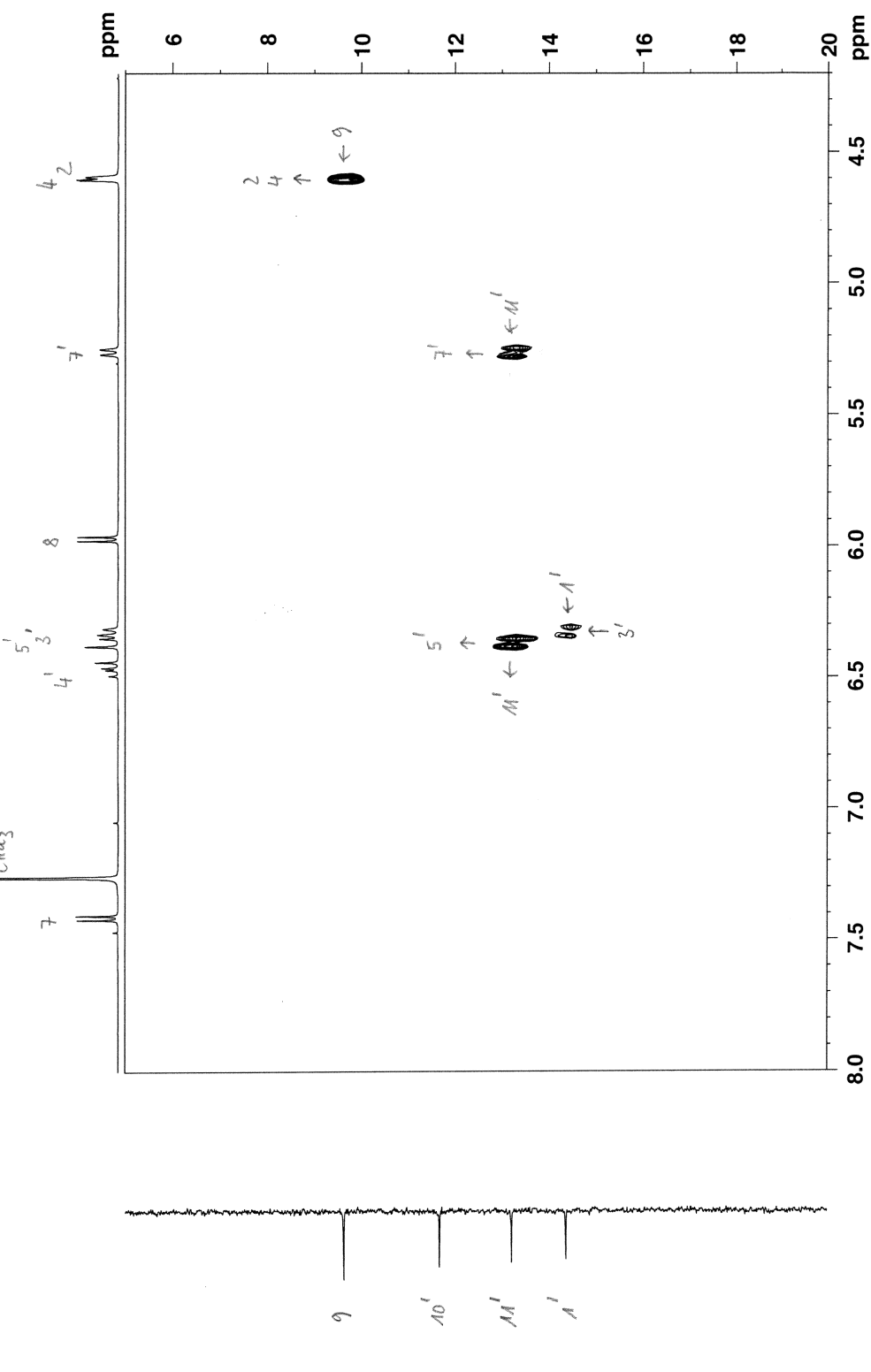




LN-303upscale4peak2 in CDC13 (HMBC) 16.1.2020

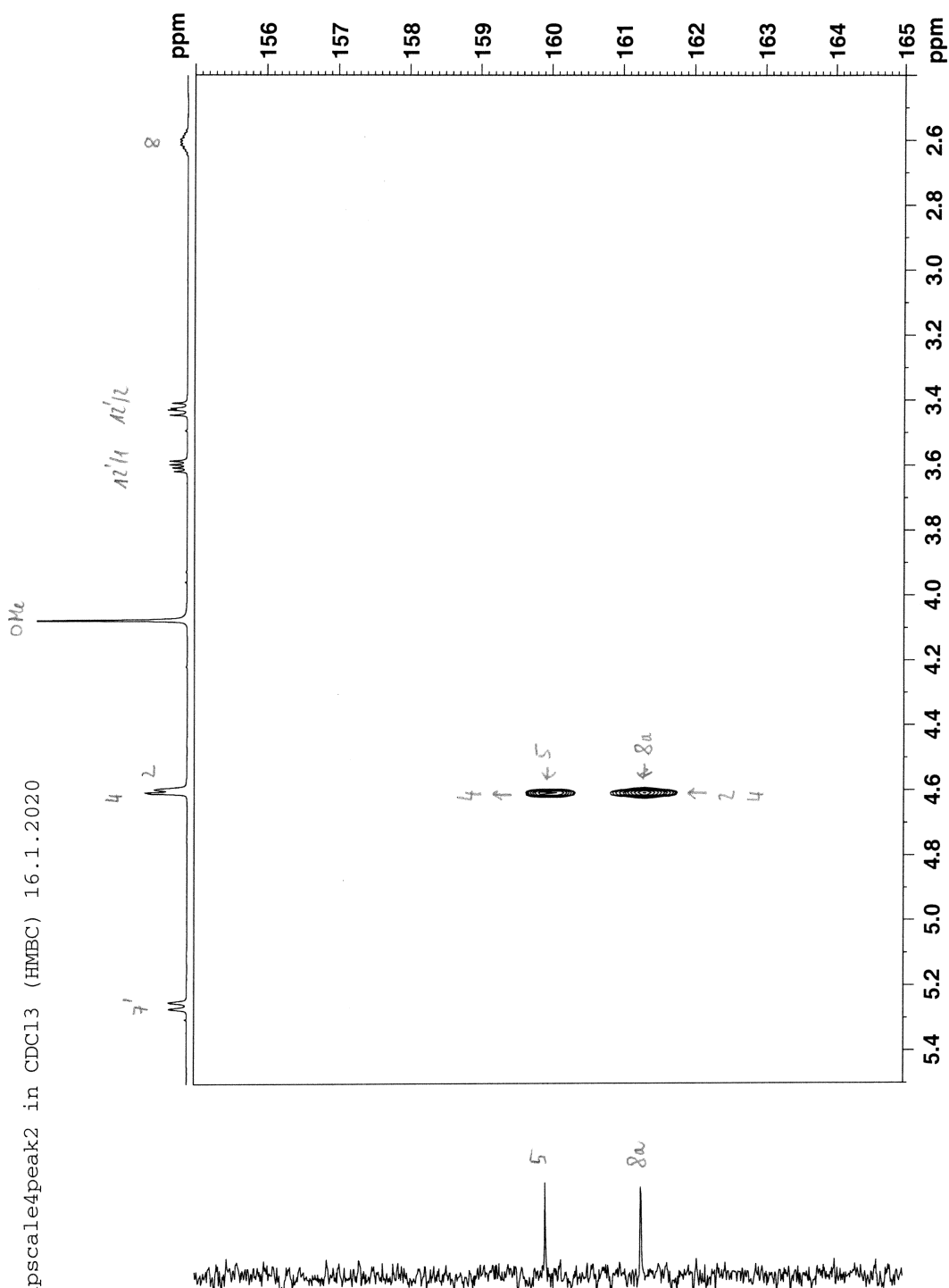


LN-303upscale4peak2 in CDC13 (HMBC) 16.1.2020



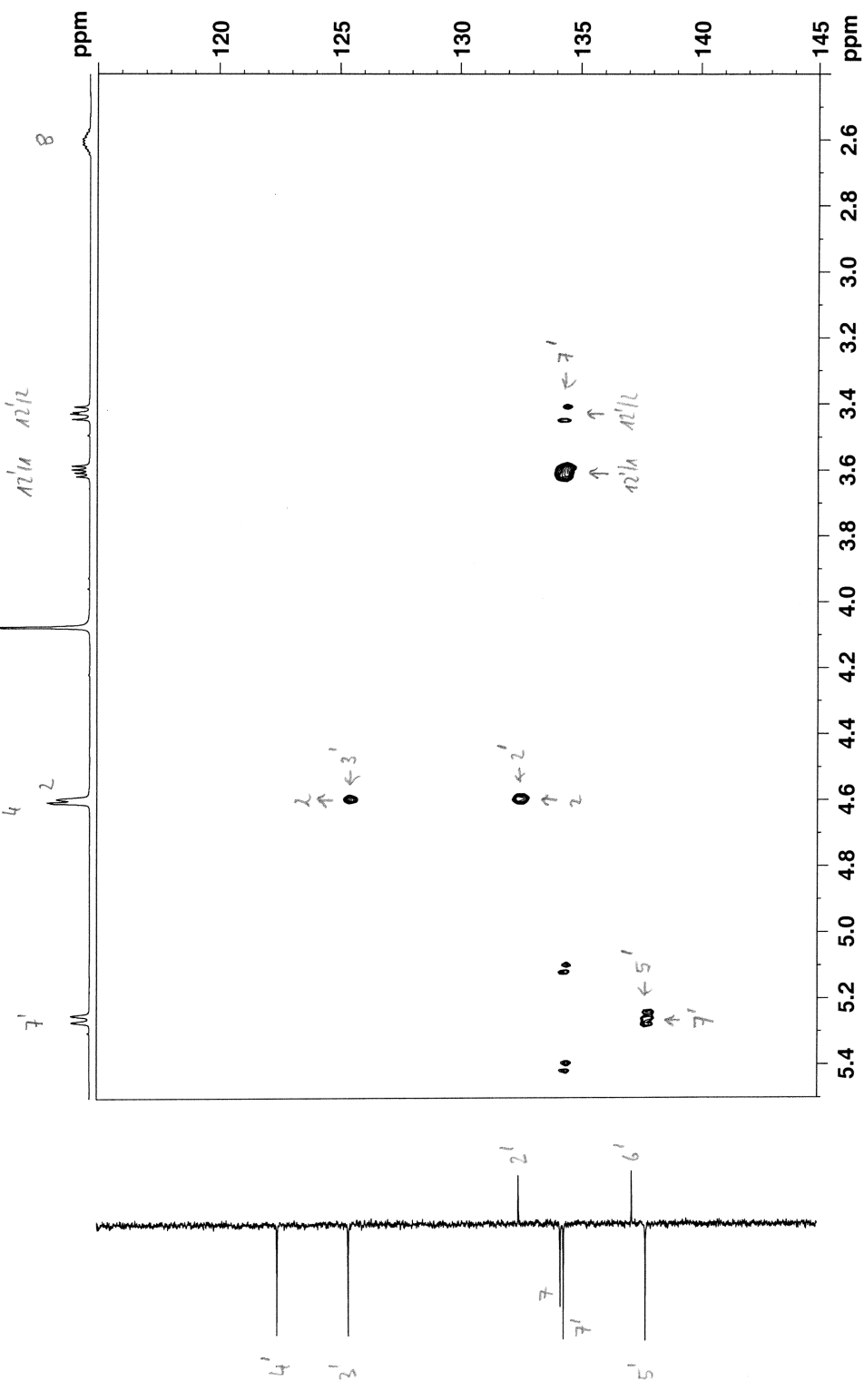
S50

LN-303upscale4peak2 in CDCl<sub>3</sub> (HMBC) 16.1.2020



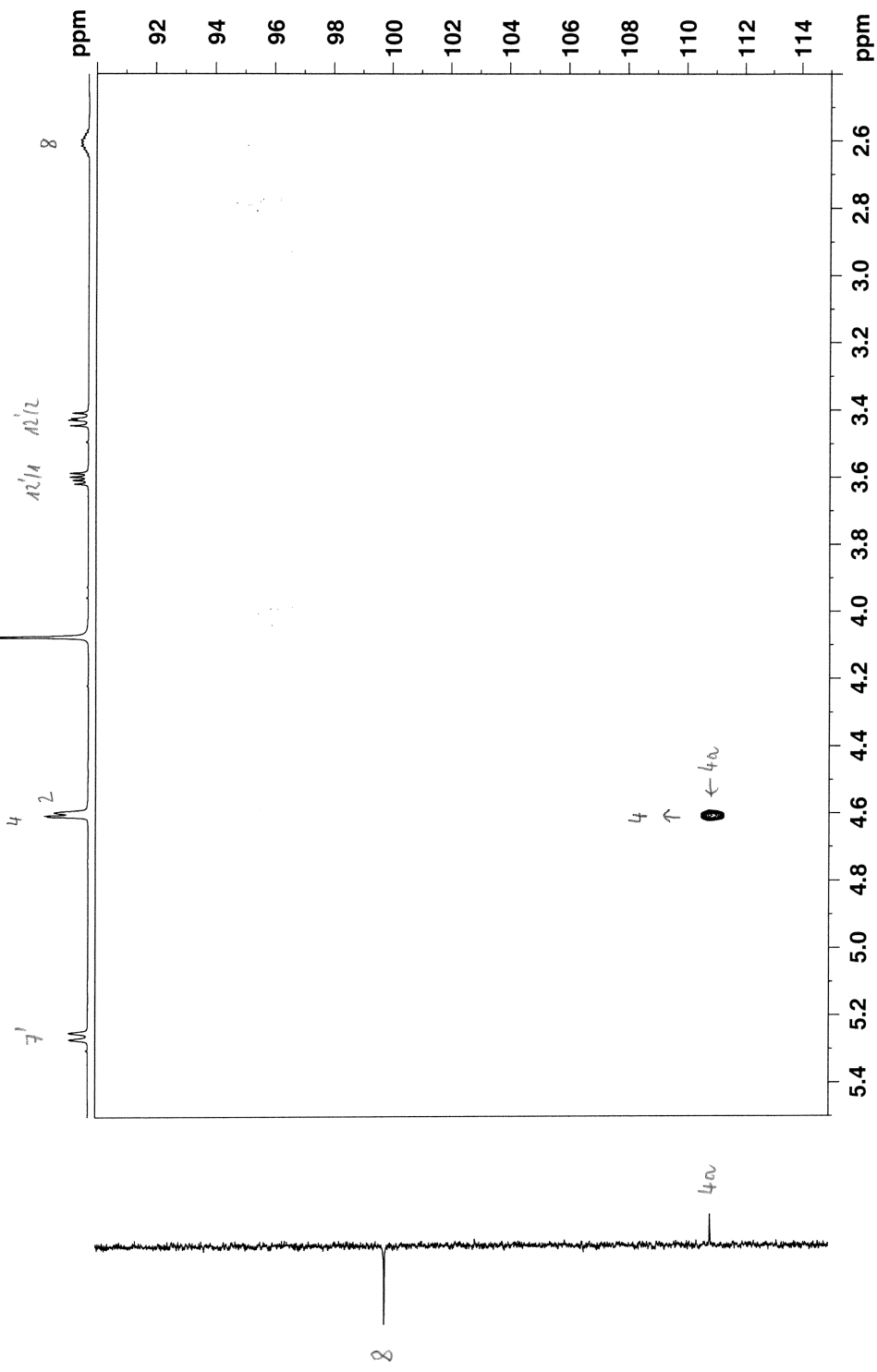
LN-303upscale4peak2 in CDC13 (HMBC) 16.1.2020

O Me

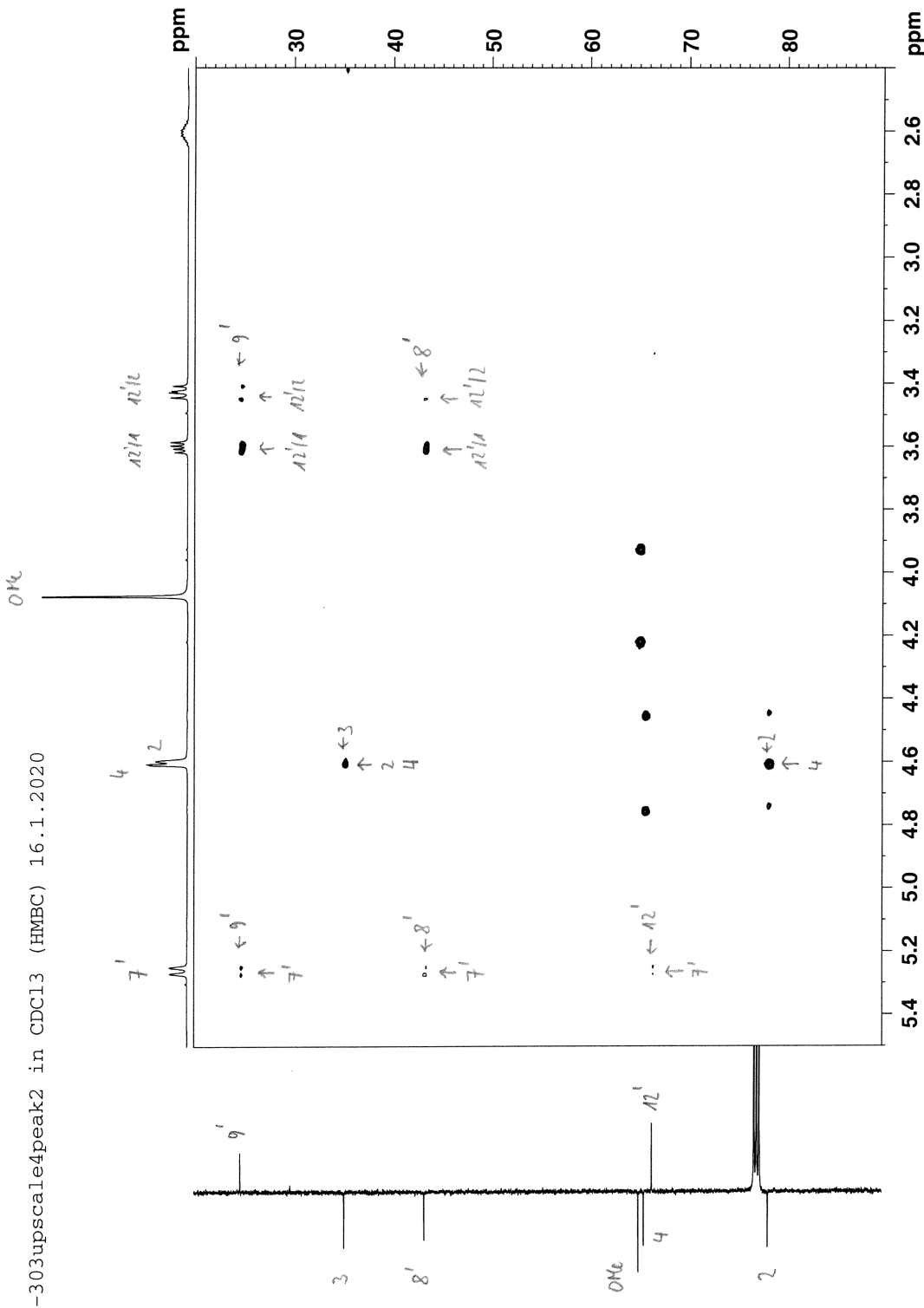


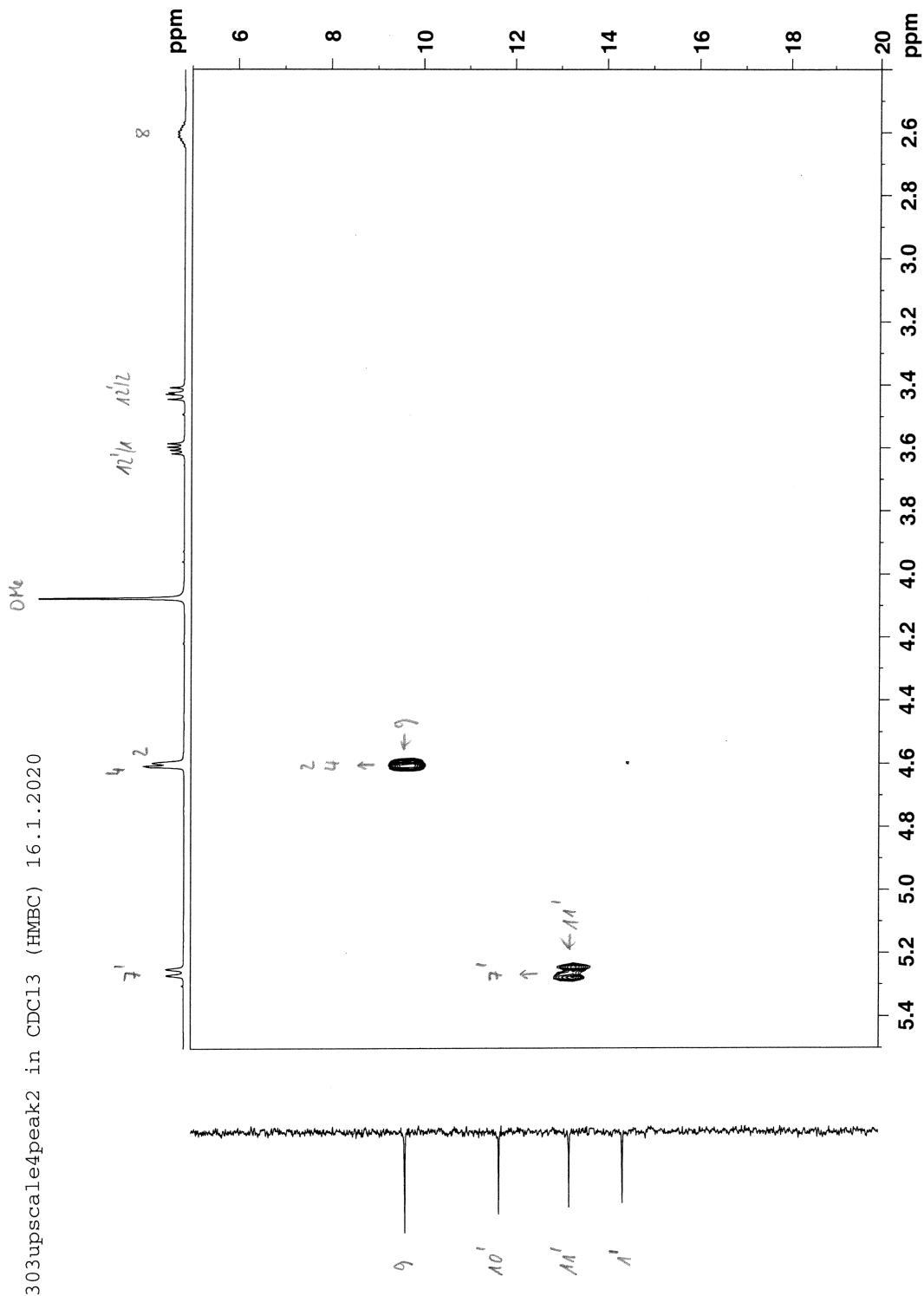
LN-303upscale4peak2 in CDC13 (HMBC) 16.1.2020

O Me

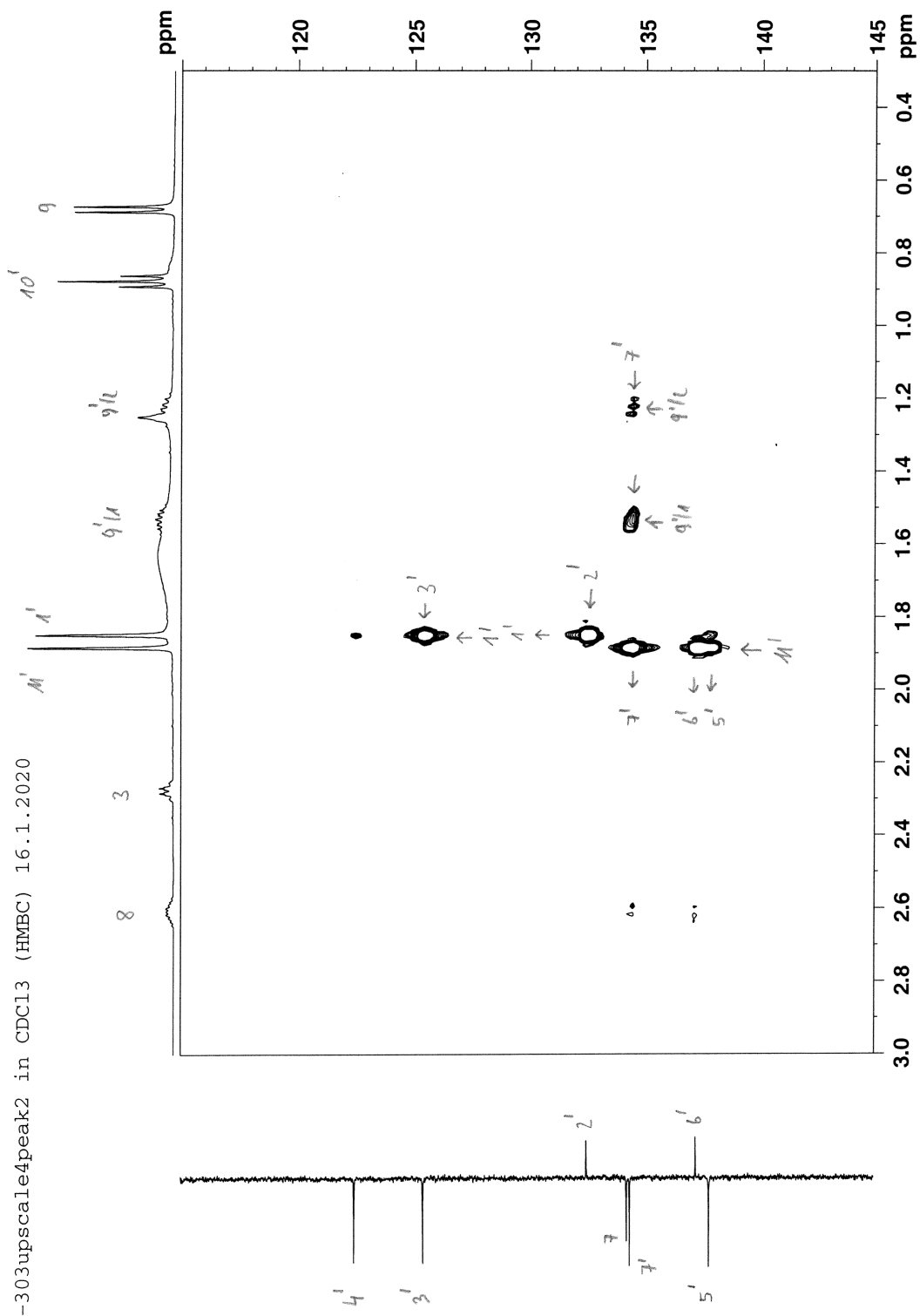


LN-303upscale4peak2 in CDCl<sub>3</sub> (HMBC) 16.1.2020

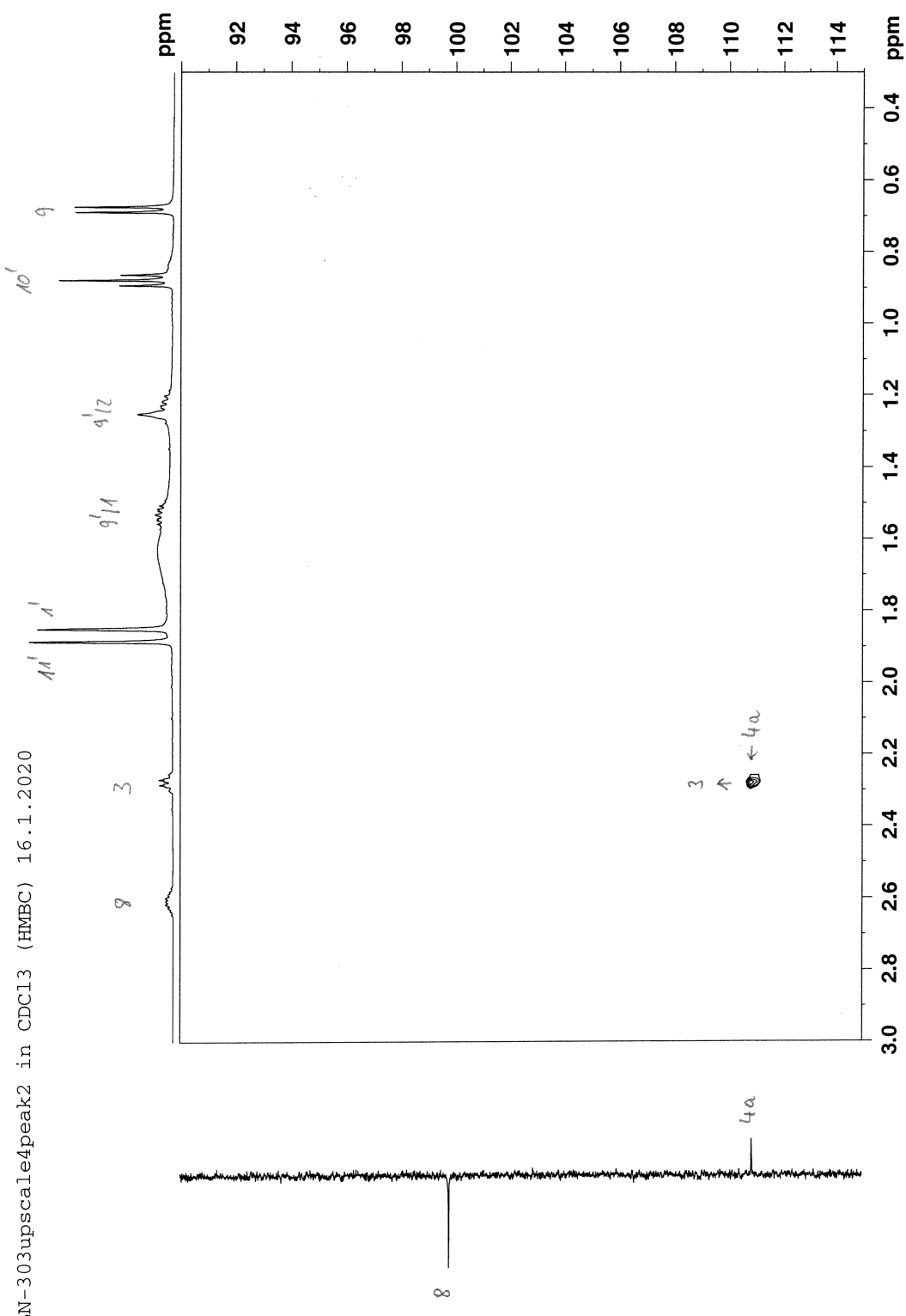




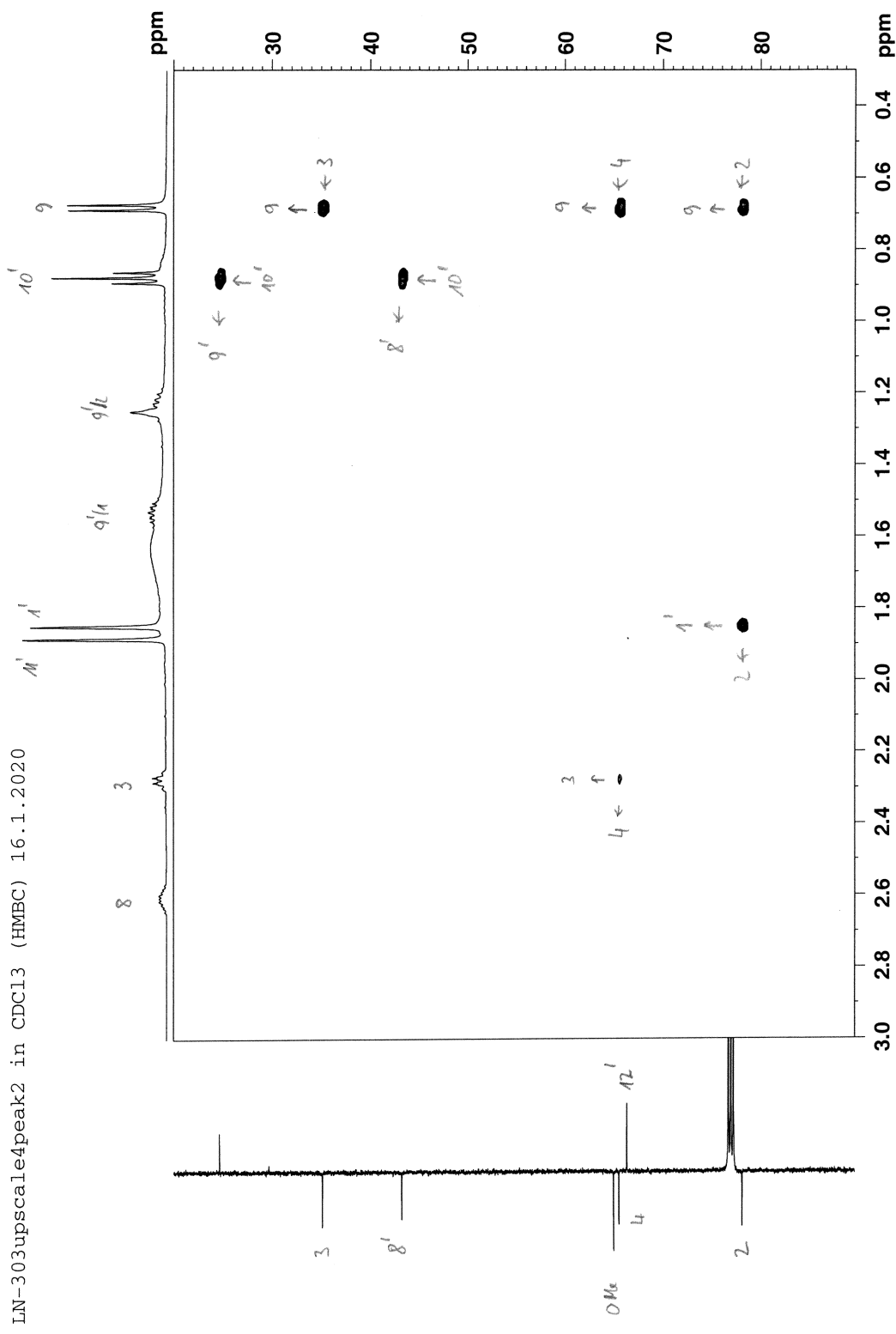
LN-303upscale4peak2 in CDCl<sub>3</sub> (HMBC) 16.1.2020



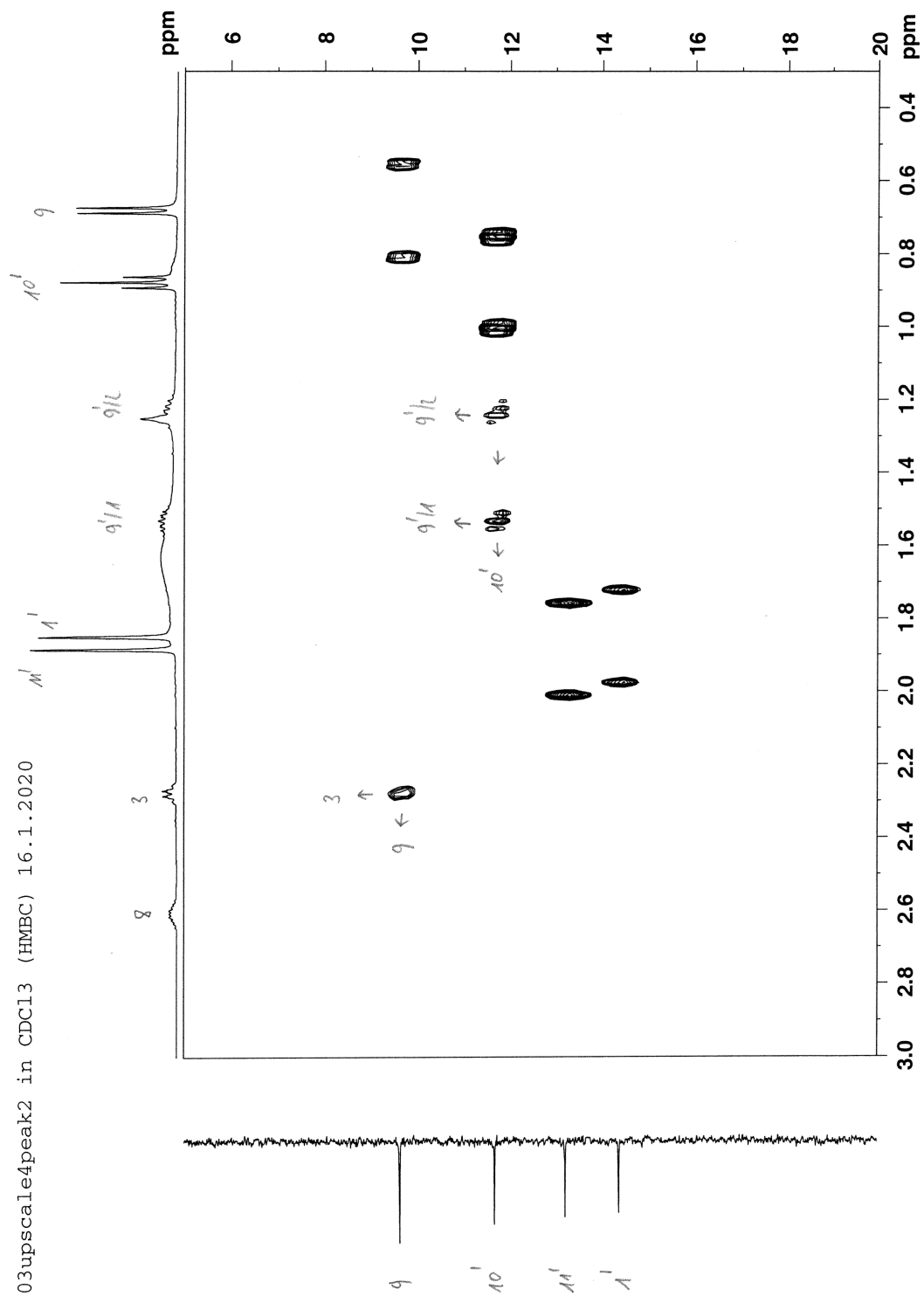
LN-303upscale4peak2 in CDCl<sub>3</sub> (HMBC) 16.1.2020



LN-303upscale4peak2 in CDCl<sub>3</sub> (HMBC) 16.1.2020



LN-303upscale4peak2 in CDCl<sub>3</sub> (HMBC) 16.1.2020



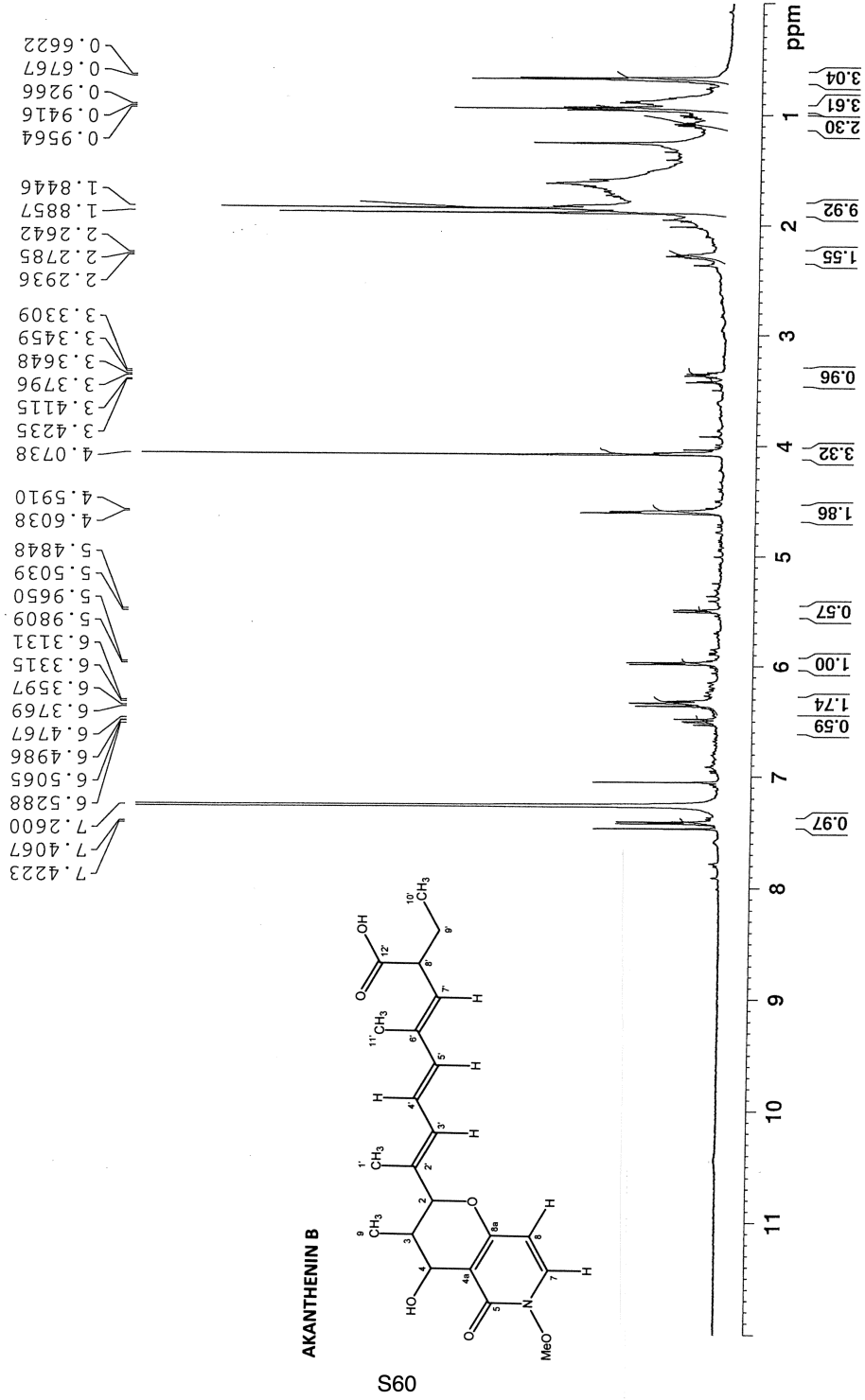
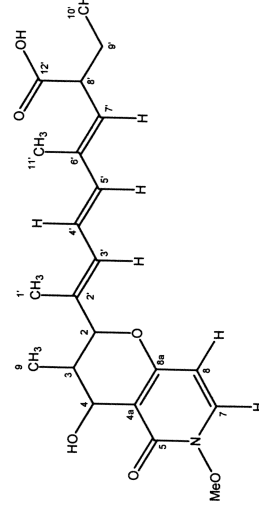
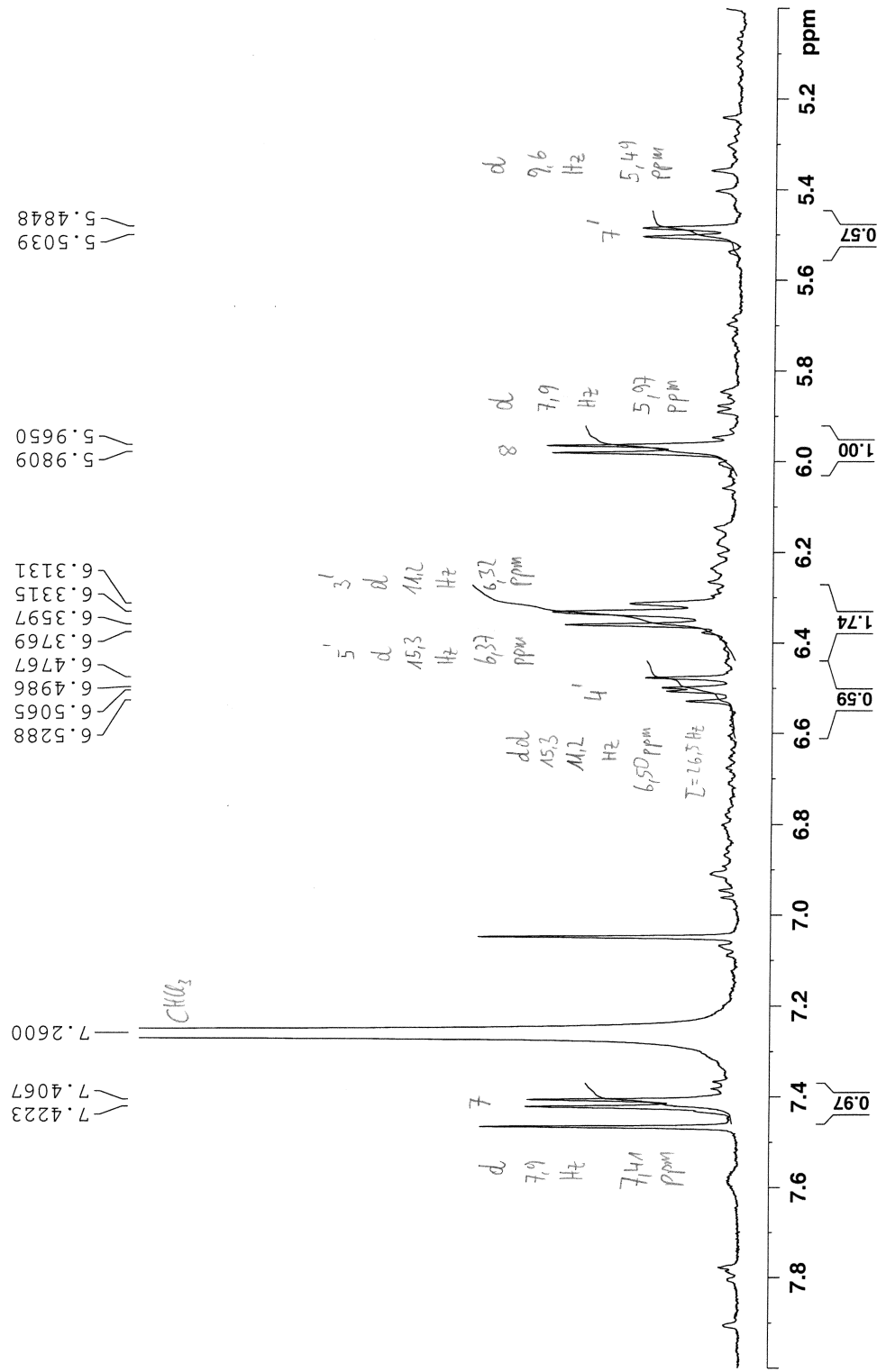
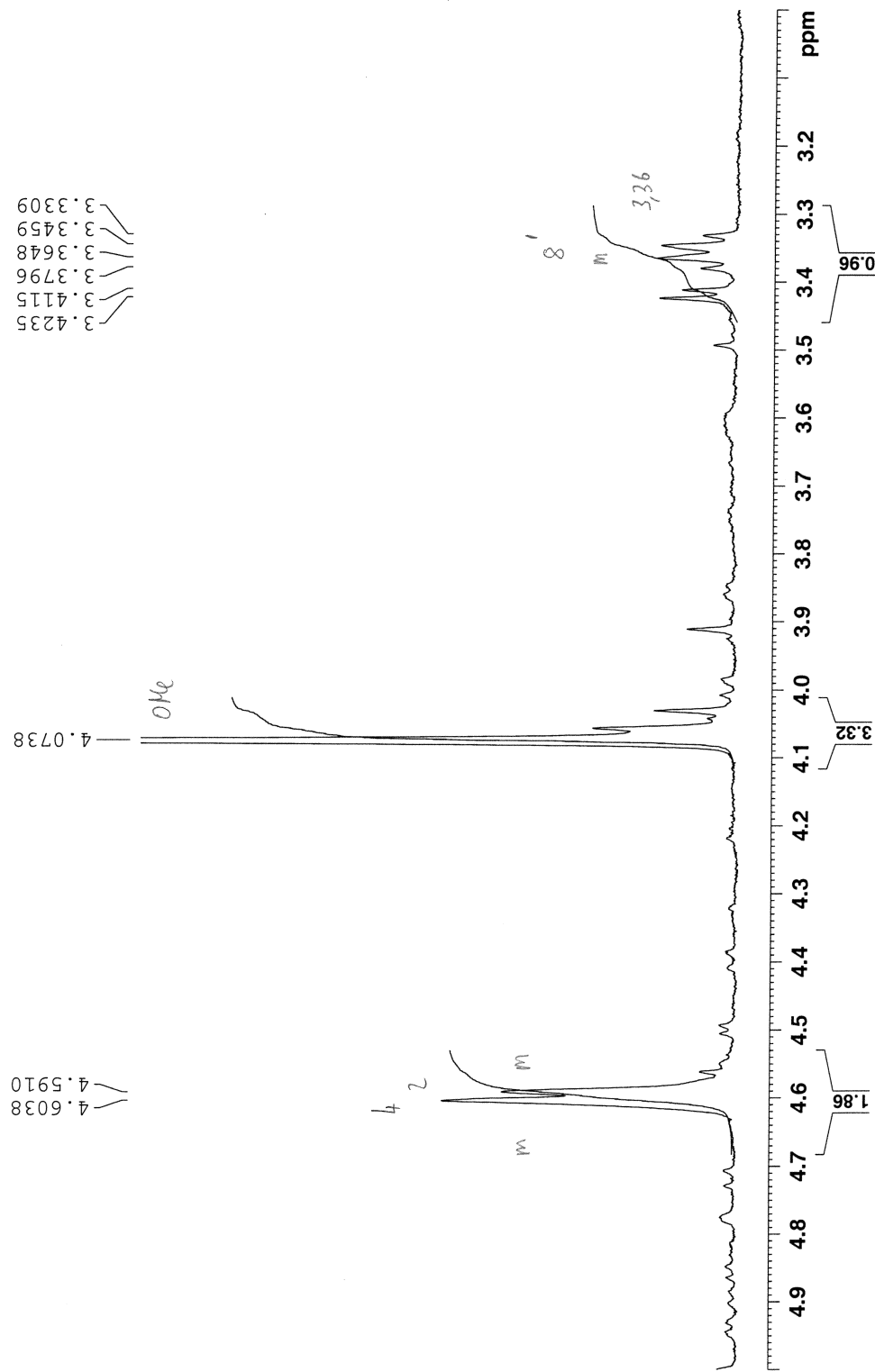
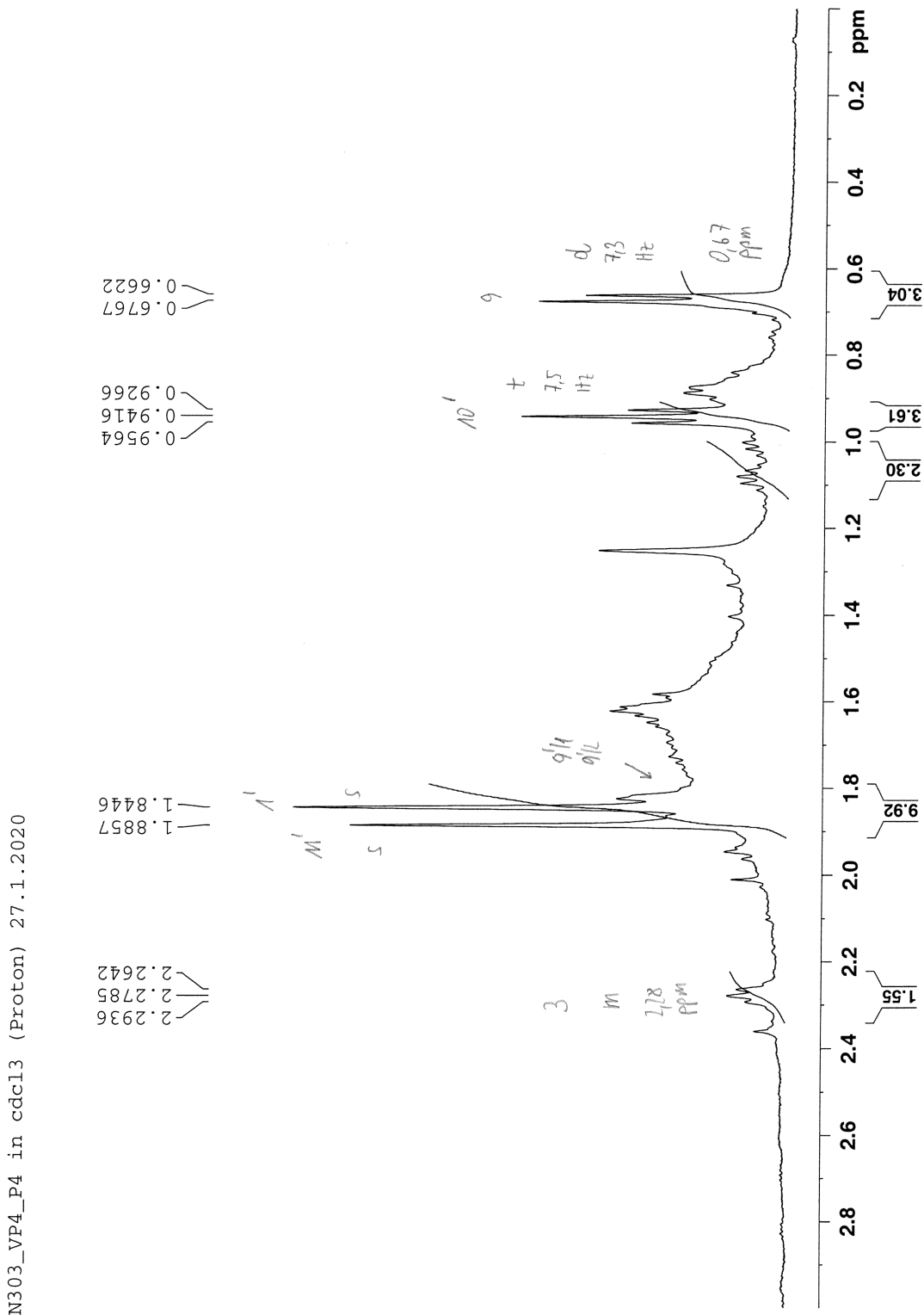


Figure S17 (pages S60-S63). <sup>1</sup>H NMR spectrum of **2** in CDCl<sub>3</sub> (δ in ppm).









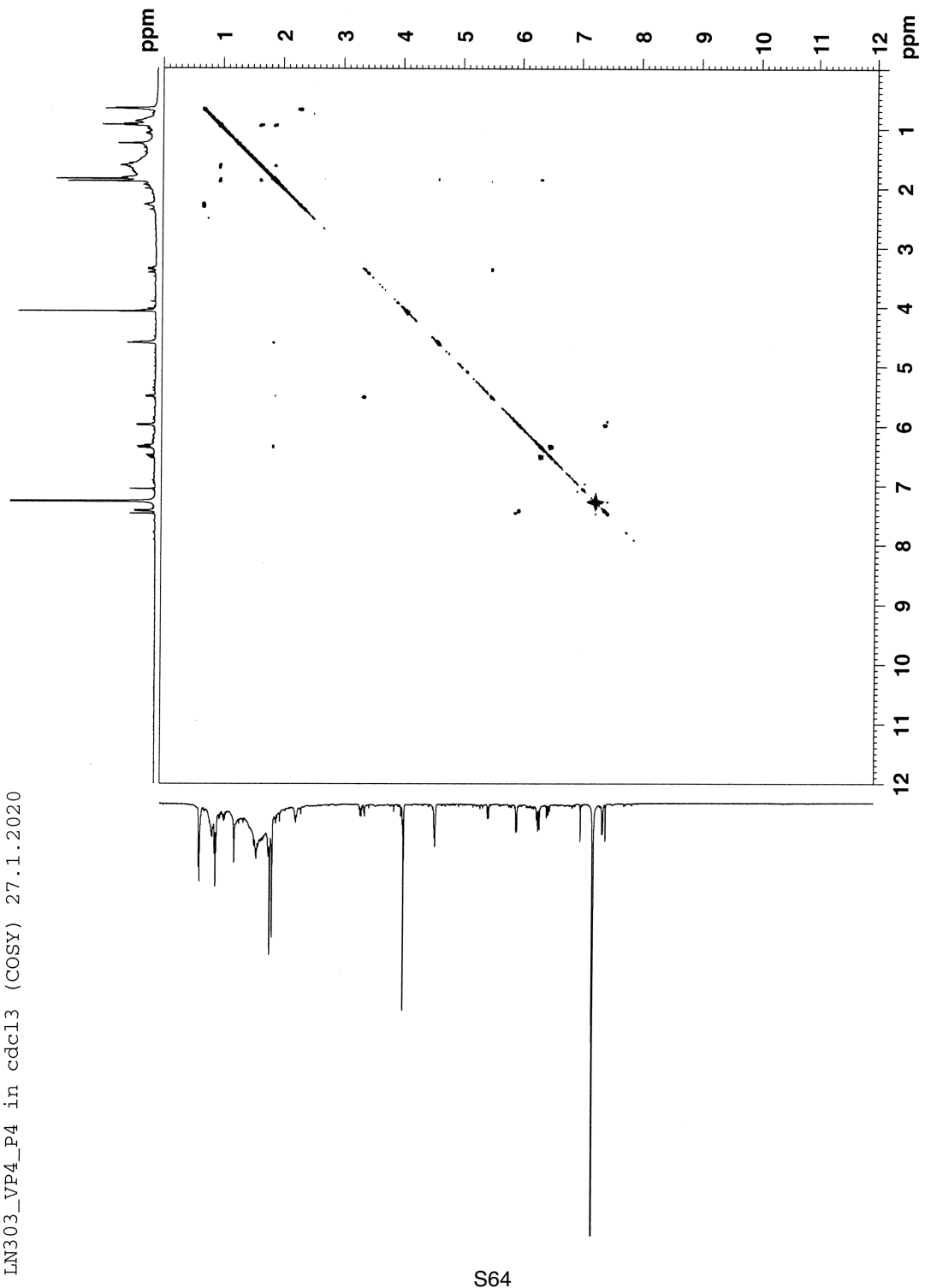
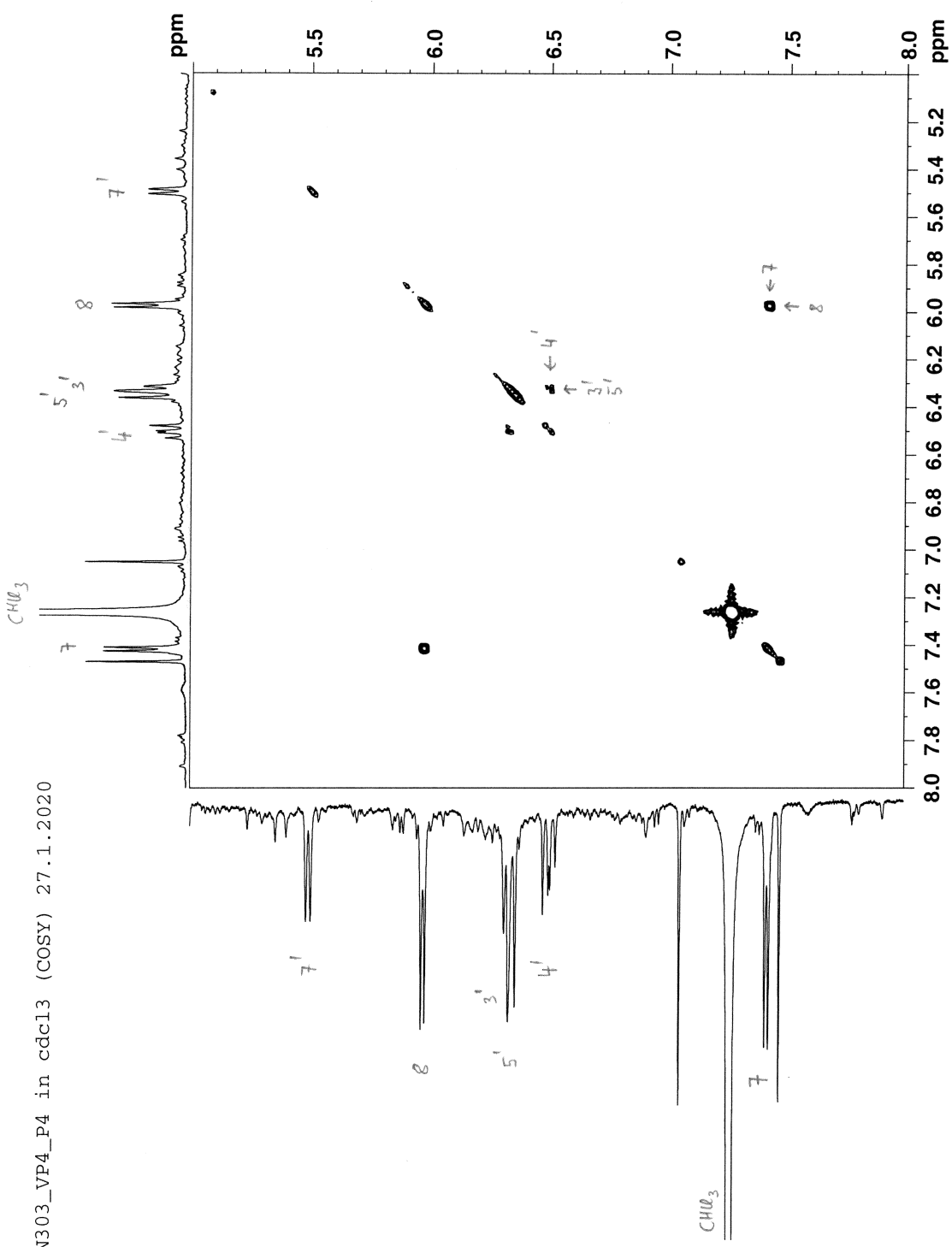
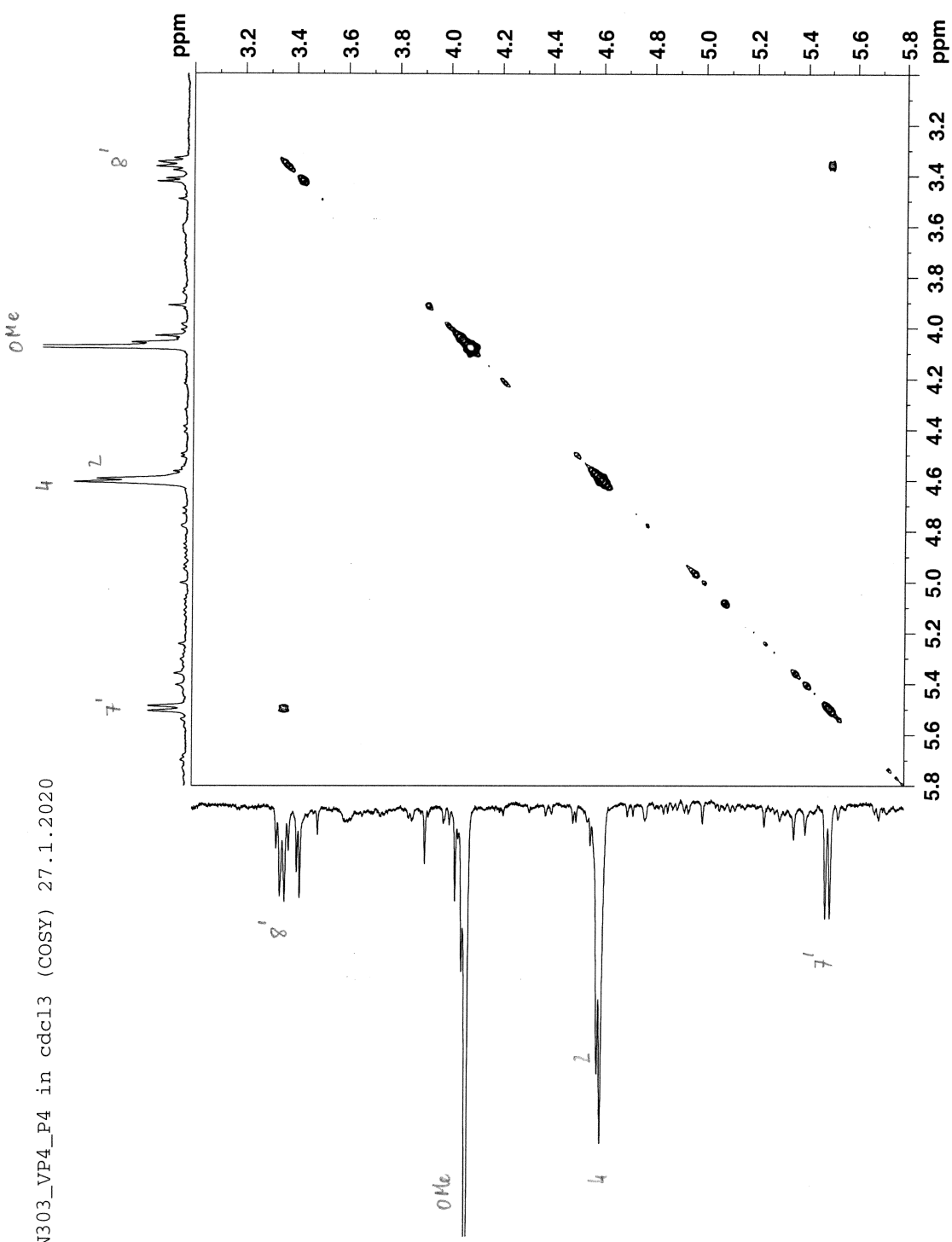
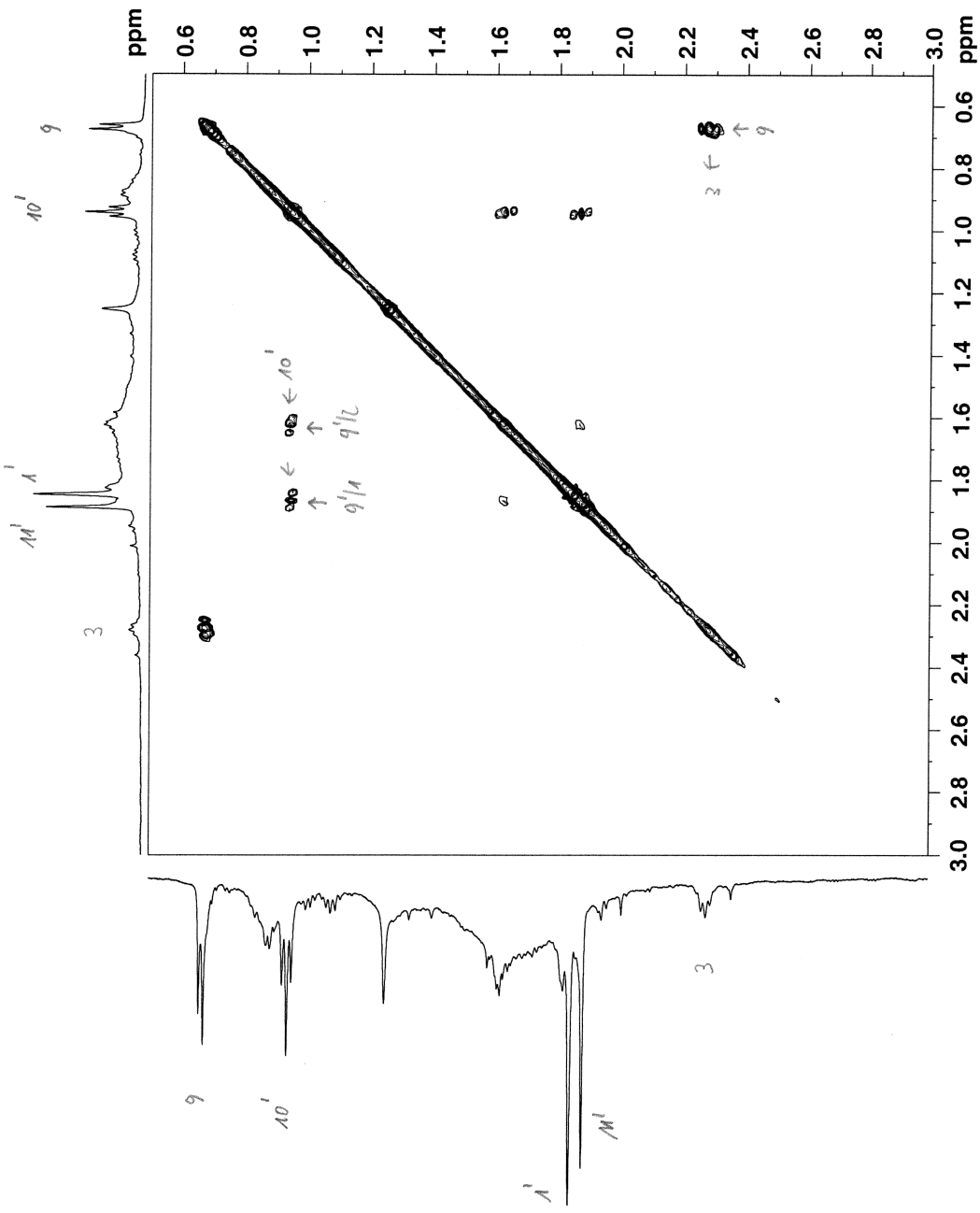


Figure S17 (pages S64-S67). COSY spectrum of **2** in  $\text{CDCl}_3$  ( $\delta$  in ppm).



LN303\_VP4\_P4 in cdcl3 (COSY) 27.1.2020





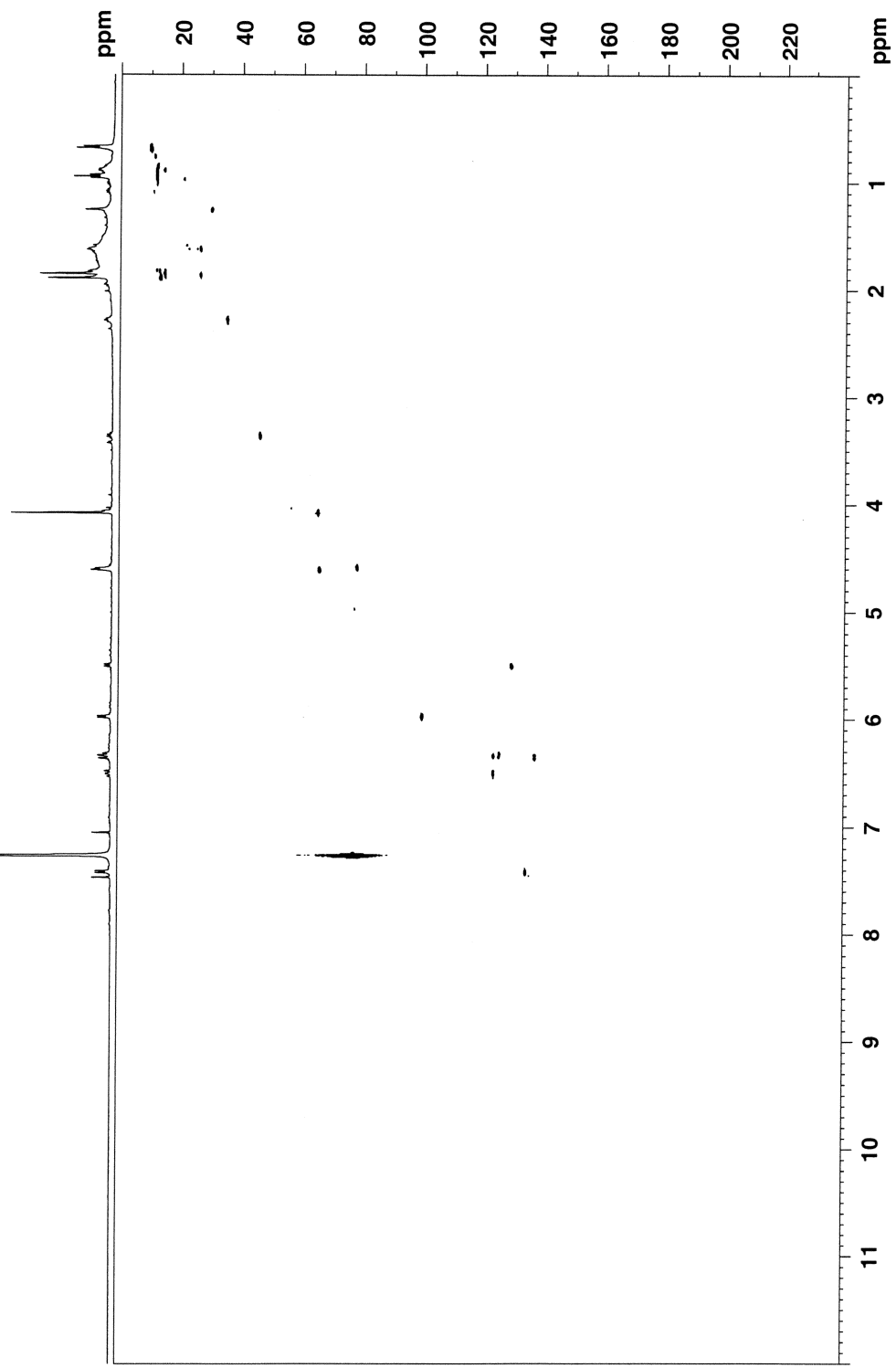
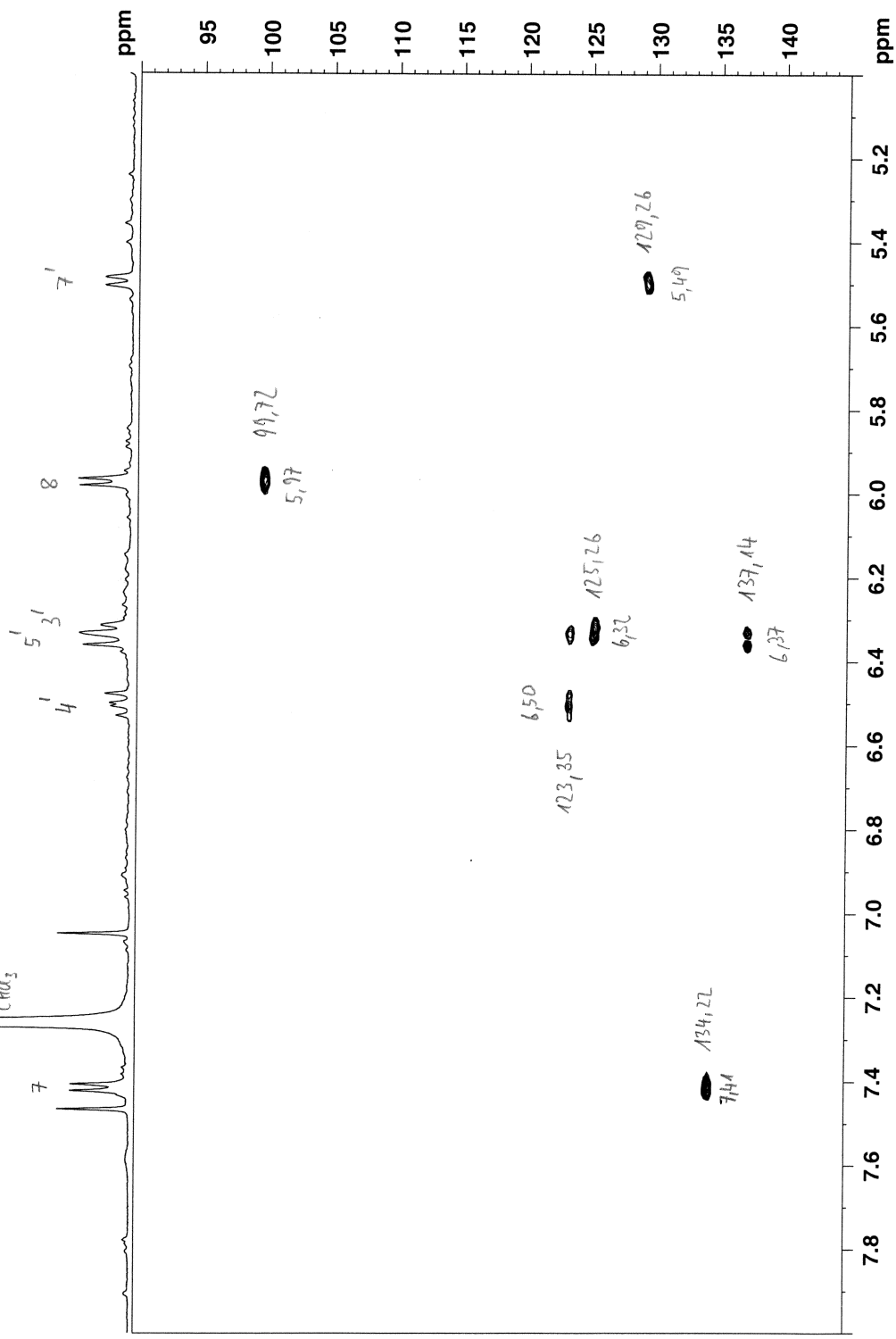
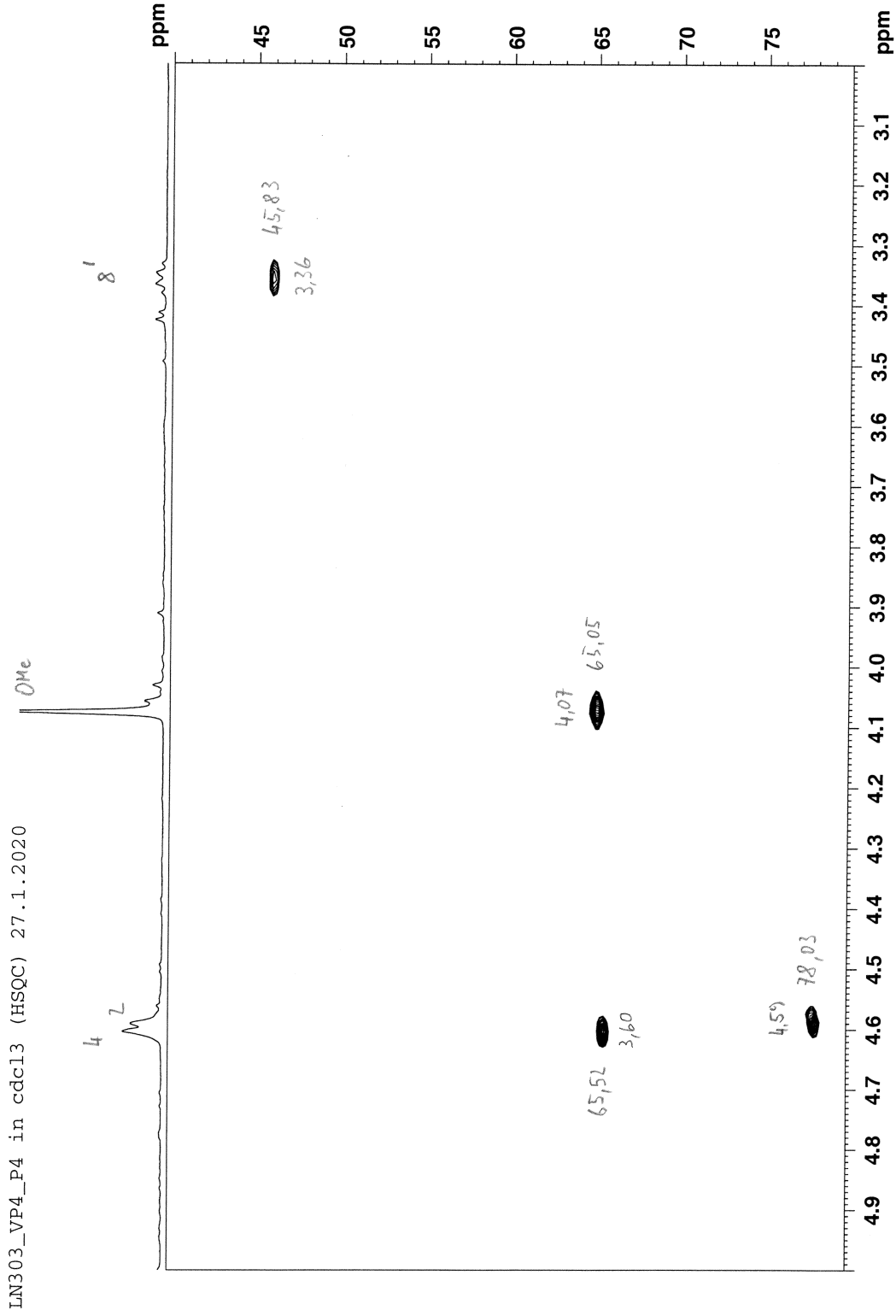
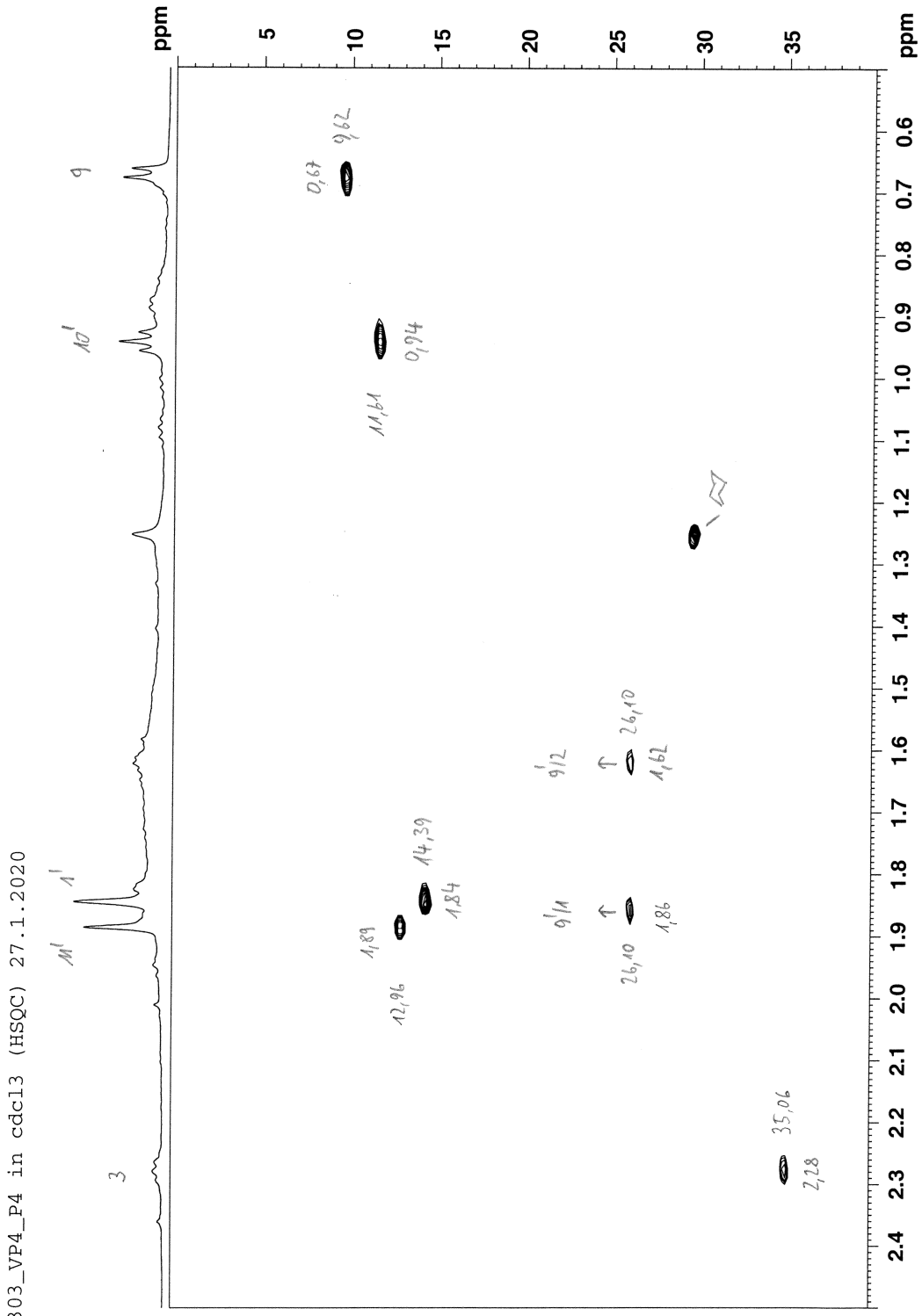


Figure S17 (pages S68-71). HSQC spectrum of **2** in  $\text{CDCl}_3$  ( $\delta$  in ppm).

LN303\_VP4\_P4 in cdcl3 (HSQC) 27.1.2020







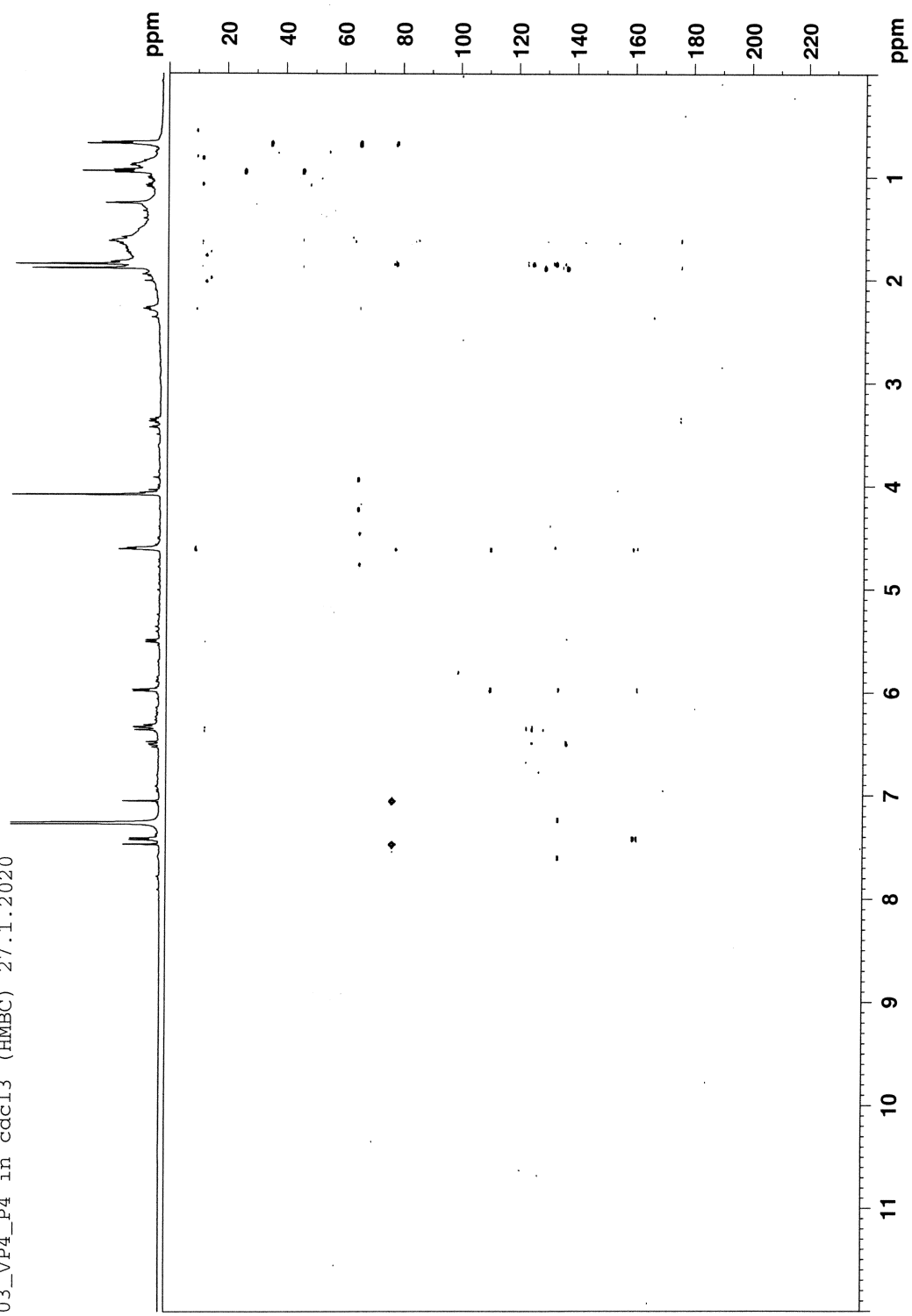
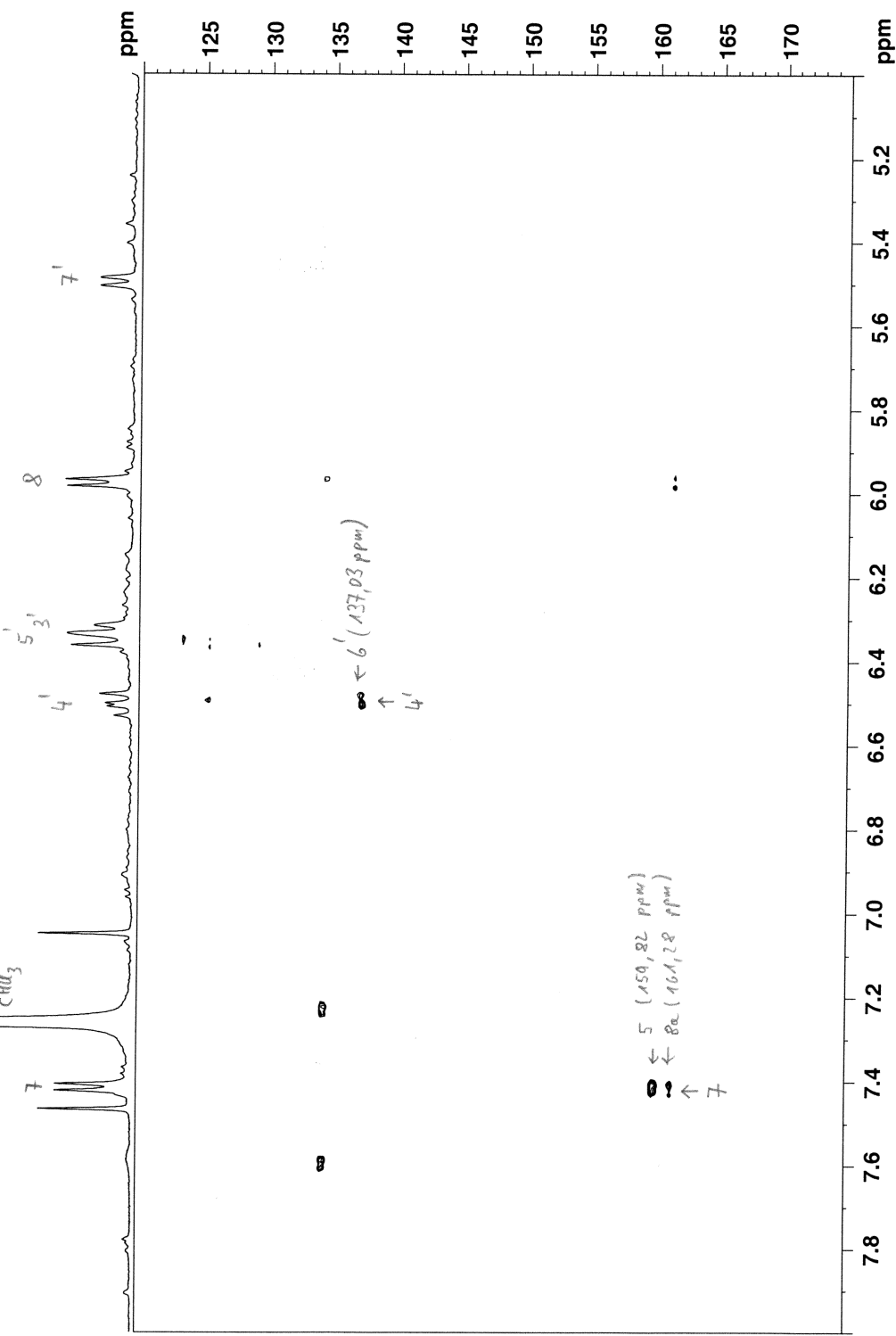
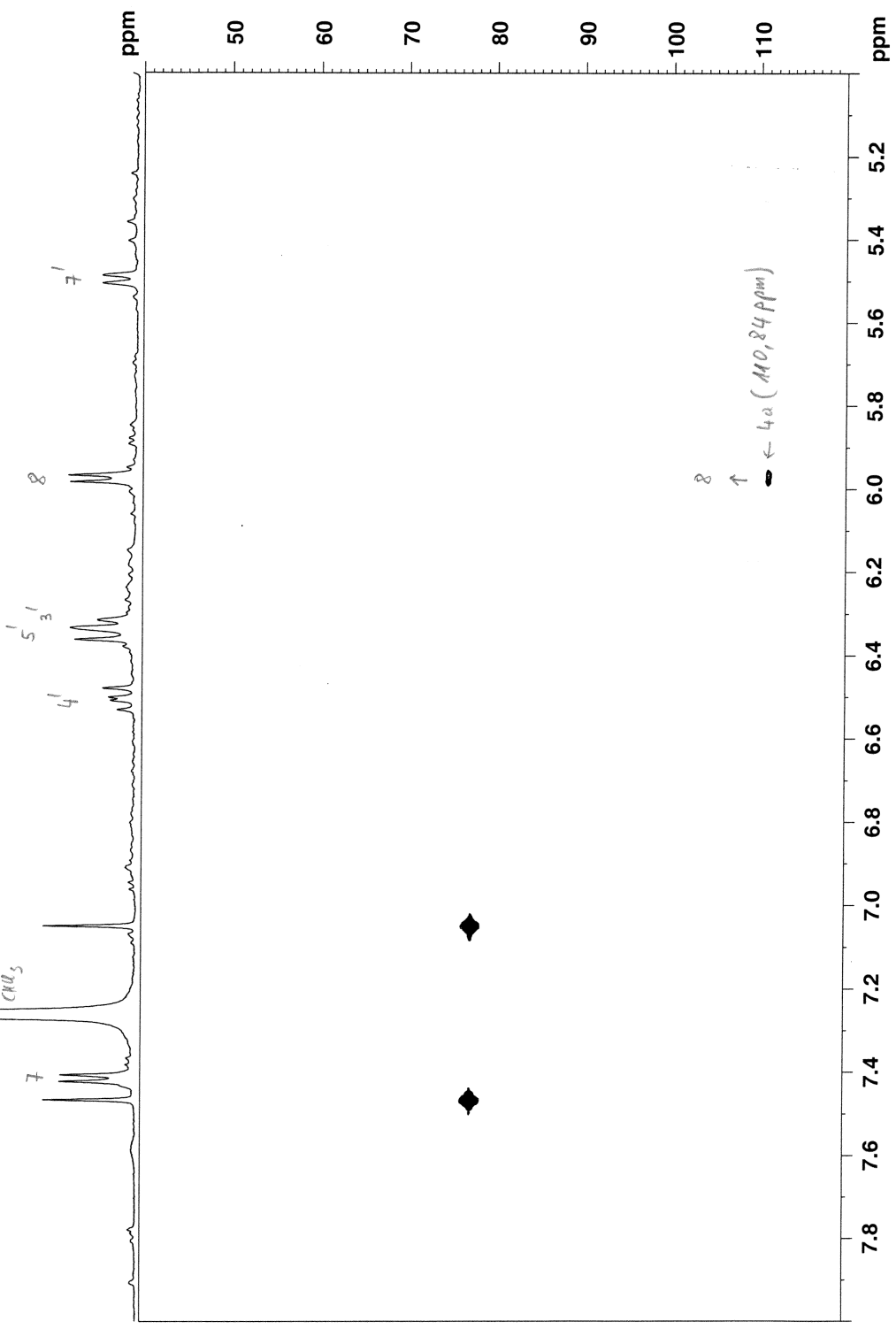


Figure S17 (pages S72-S82). HMBC spectrum of **2** in  $\text{CDCl}_3$  ( $\delta$  in ppm).

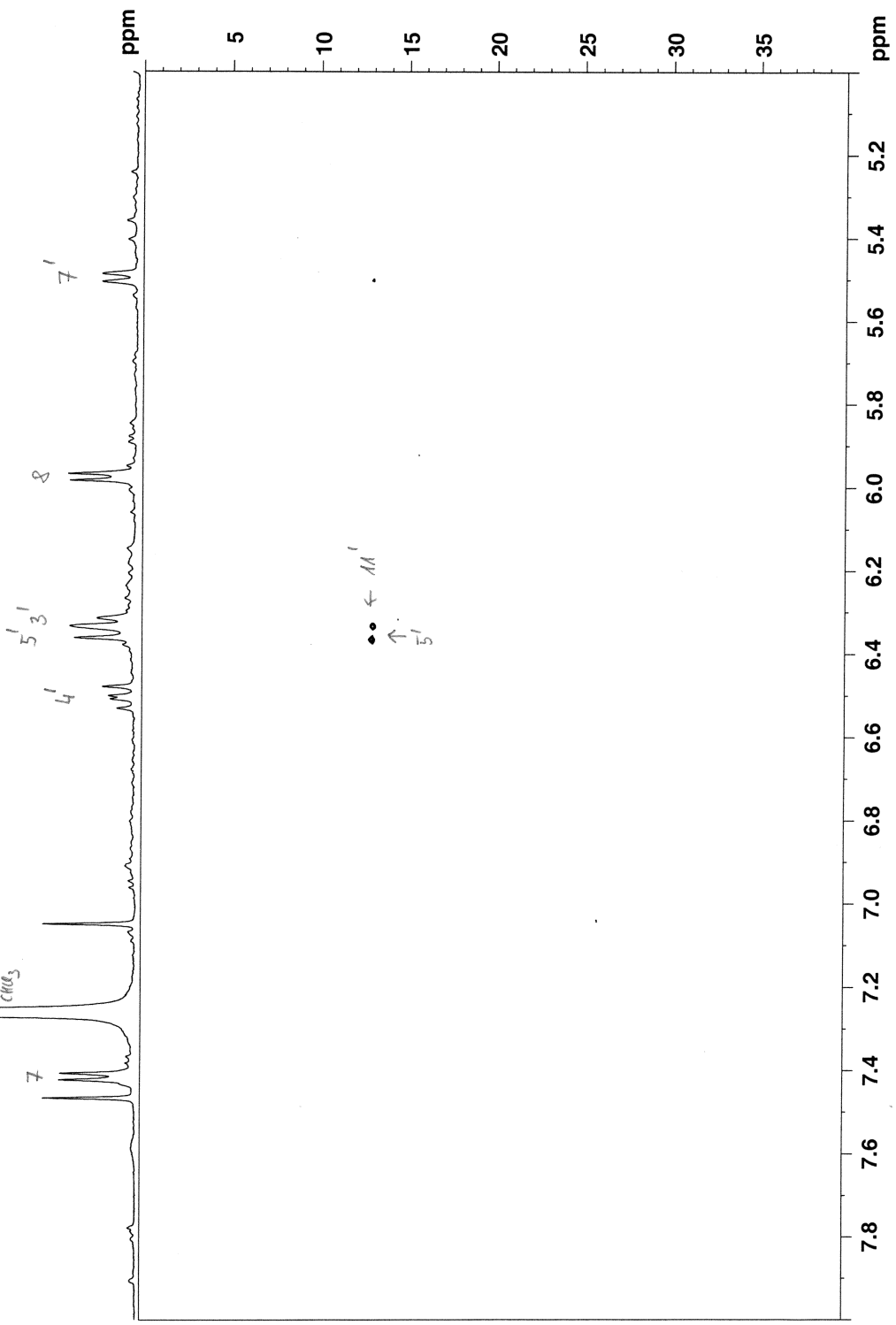
LN303\_VP4\_P4 in cdc13 (HMBC) 27.1.2020



LNN303\_VP4\_P4 in cdc13 (HMBQ) 27.1.2020

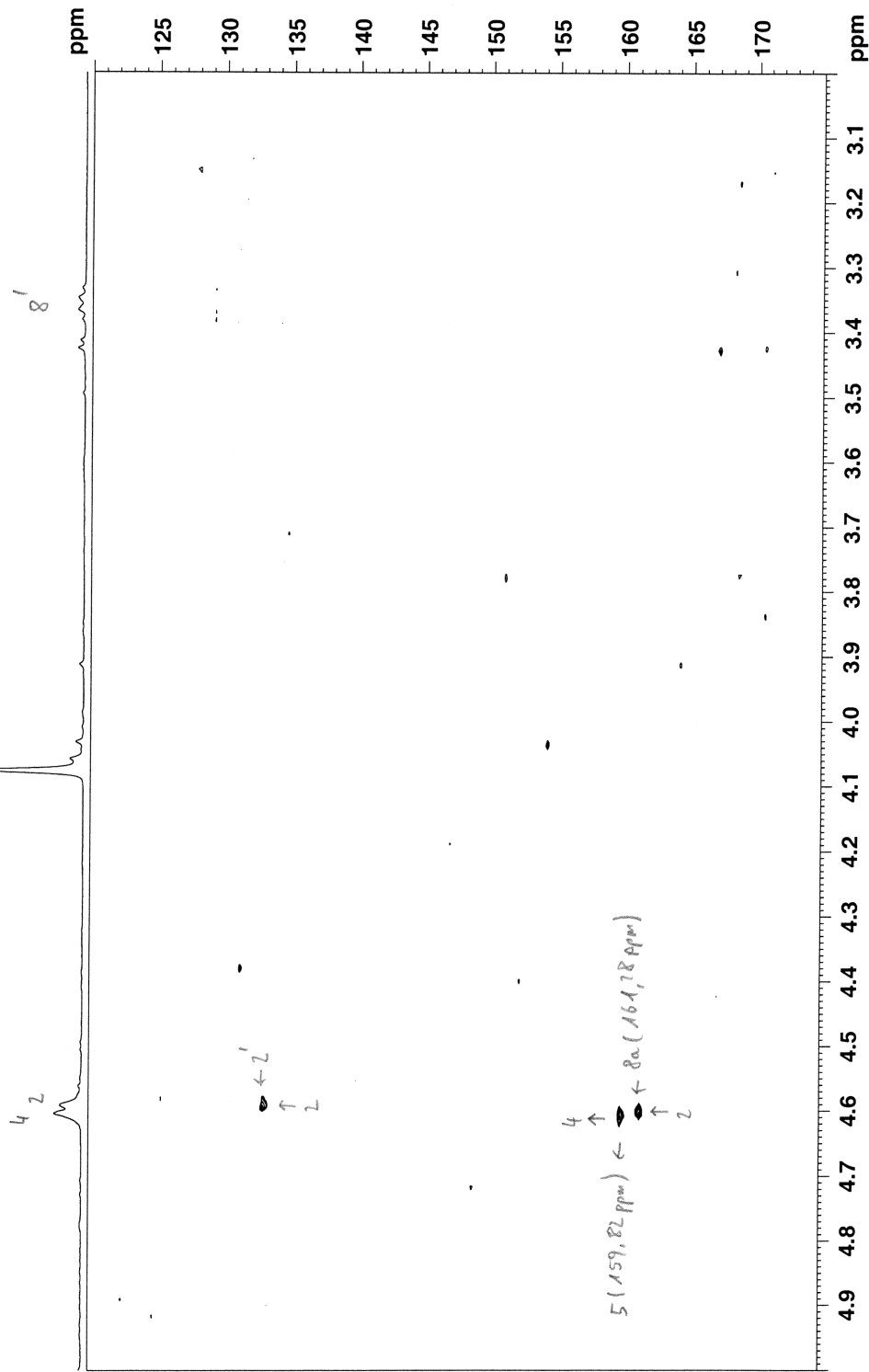


LN303\_VP4\_P4 in cdc13 (HMBG) 27.1.2020



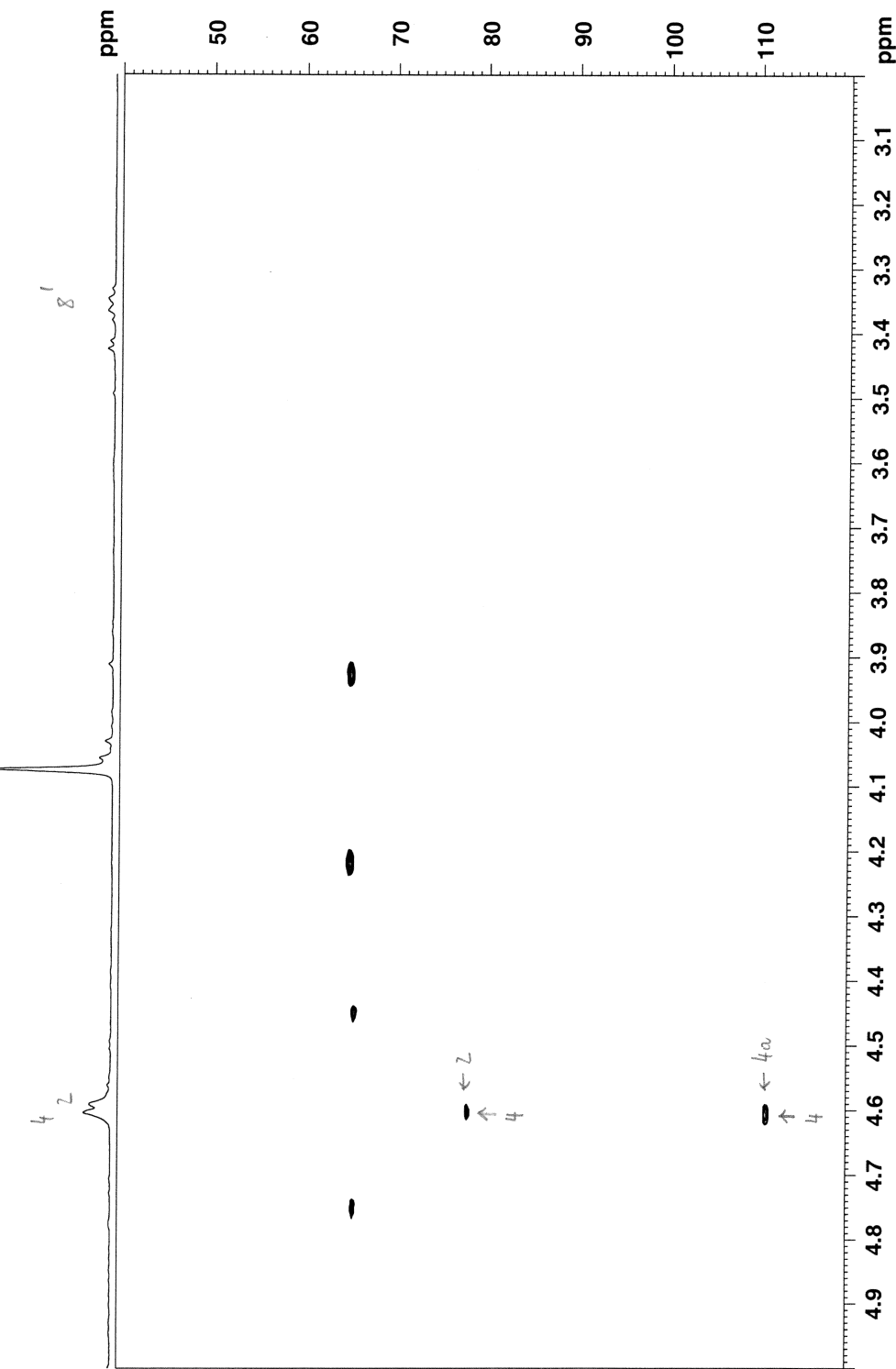
LN303\_VP4\_P4 in cdc13 (HMBC) 27.1.2020

0  $\mu$ t



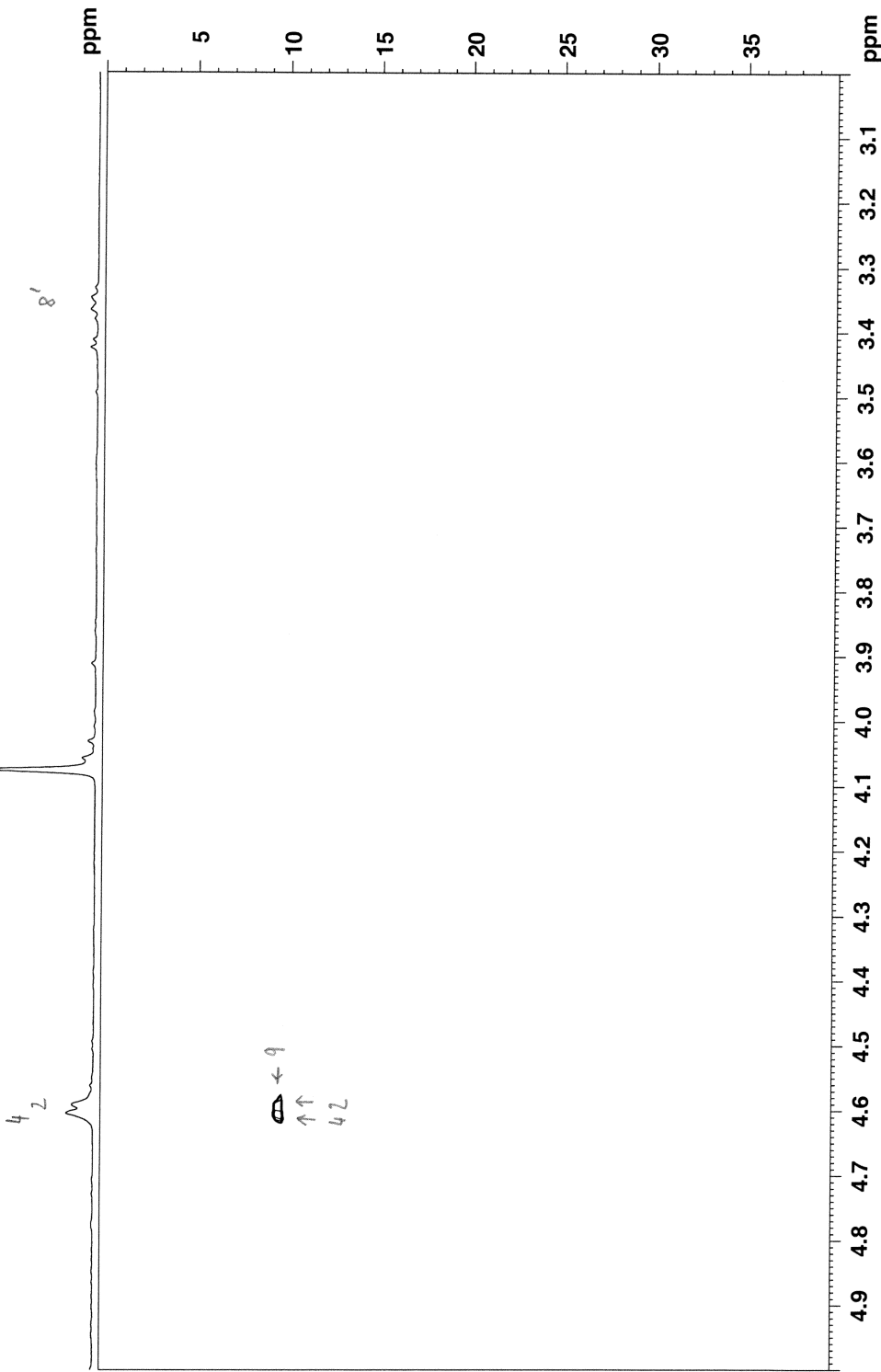
LN303\_VP4\_P4 in cdc13 (HMBC) 27.1.2020

0Hz

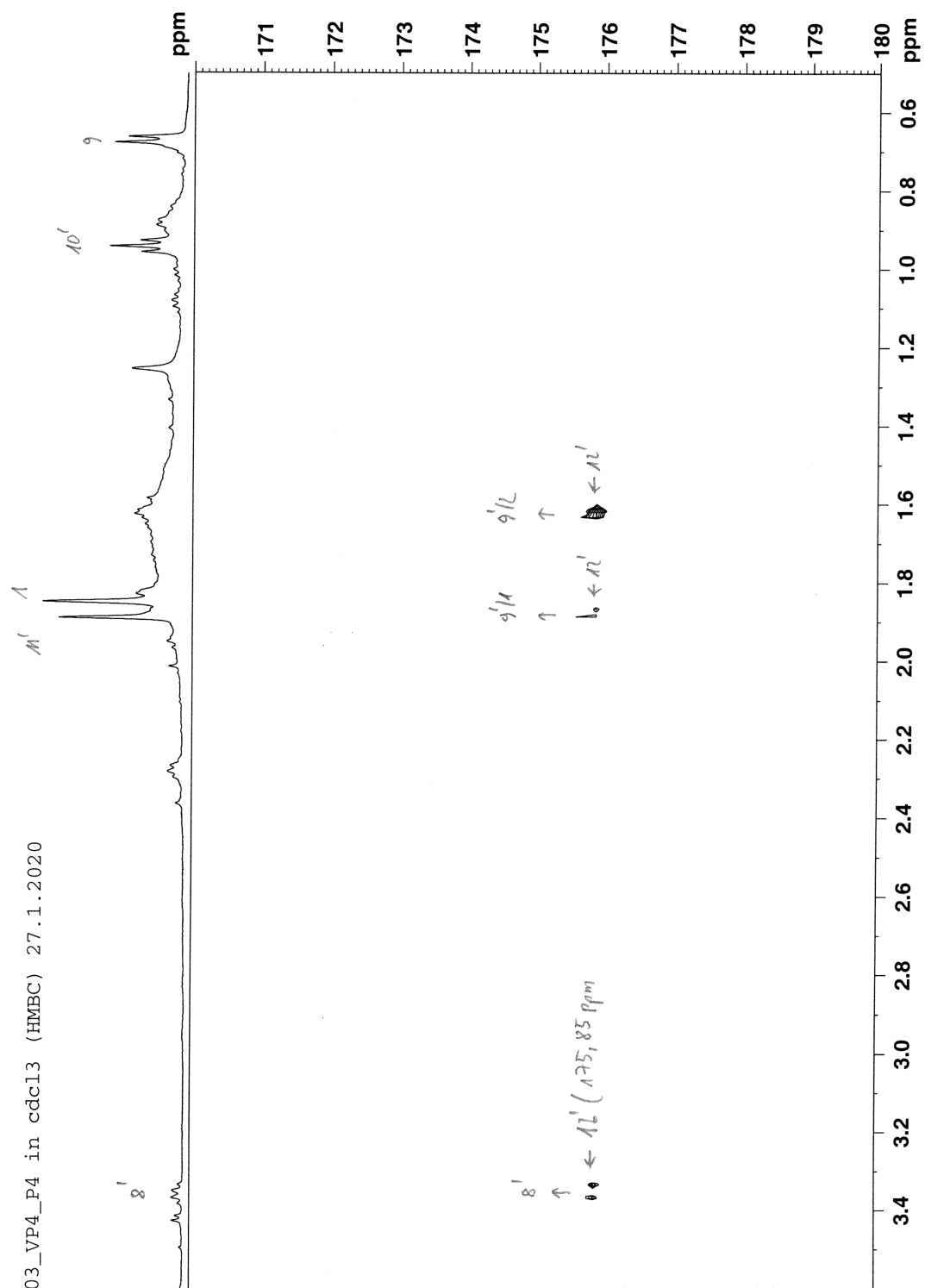


LNN303\_VP4\_P4 in cdc13 (HMBC) 27.1.2020

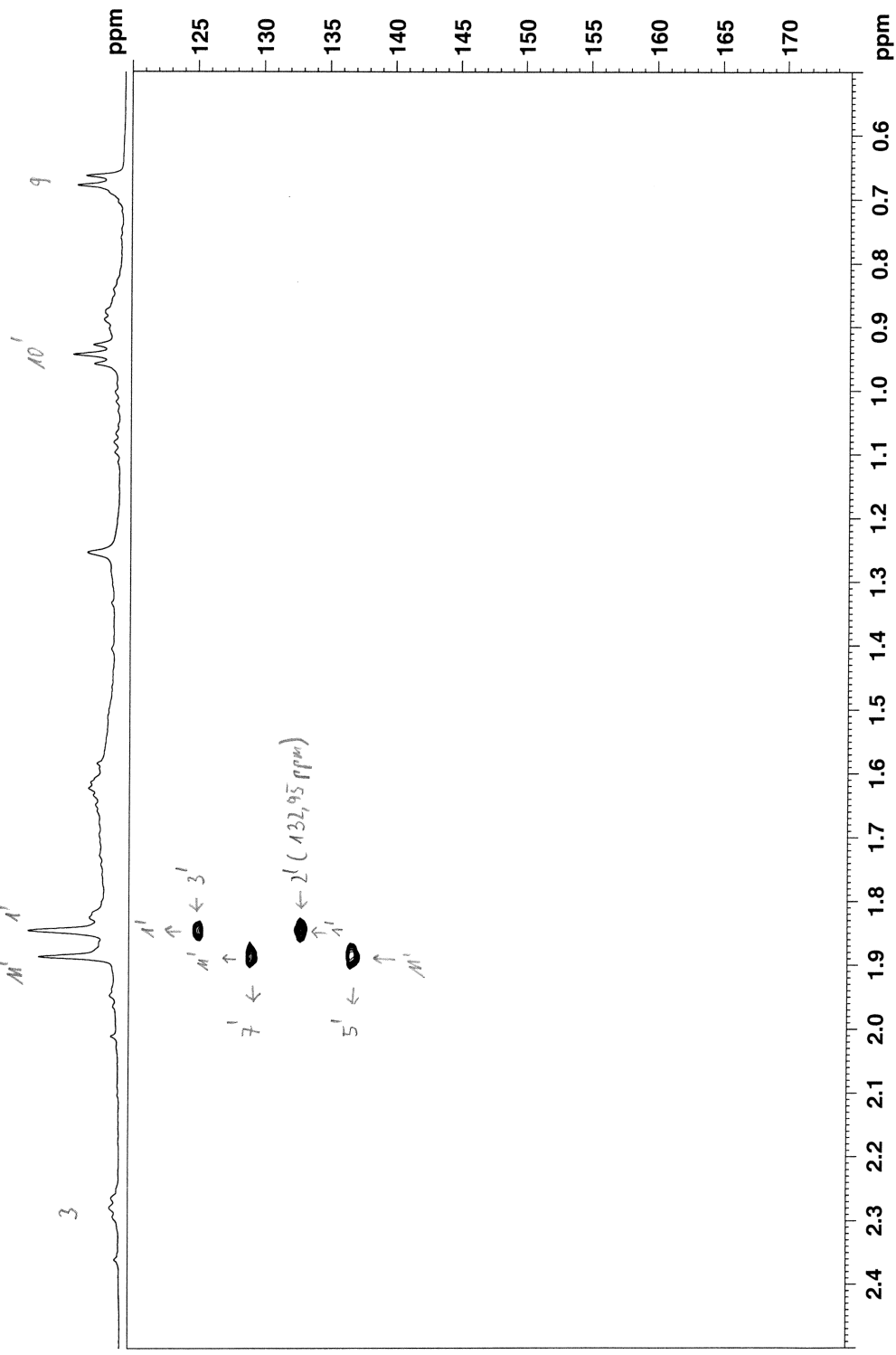
OHC



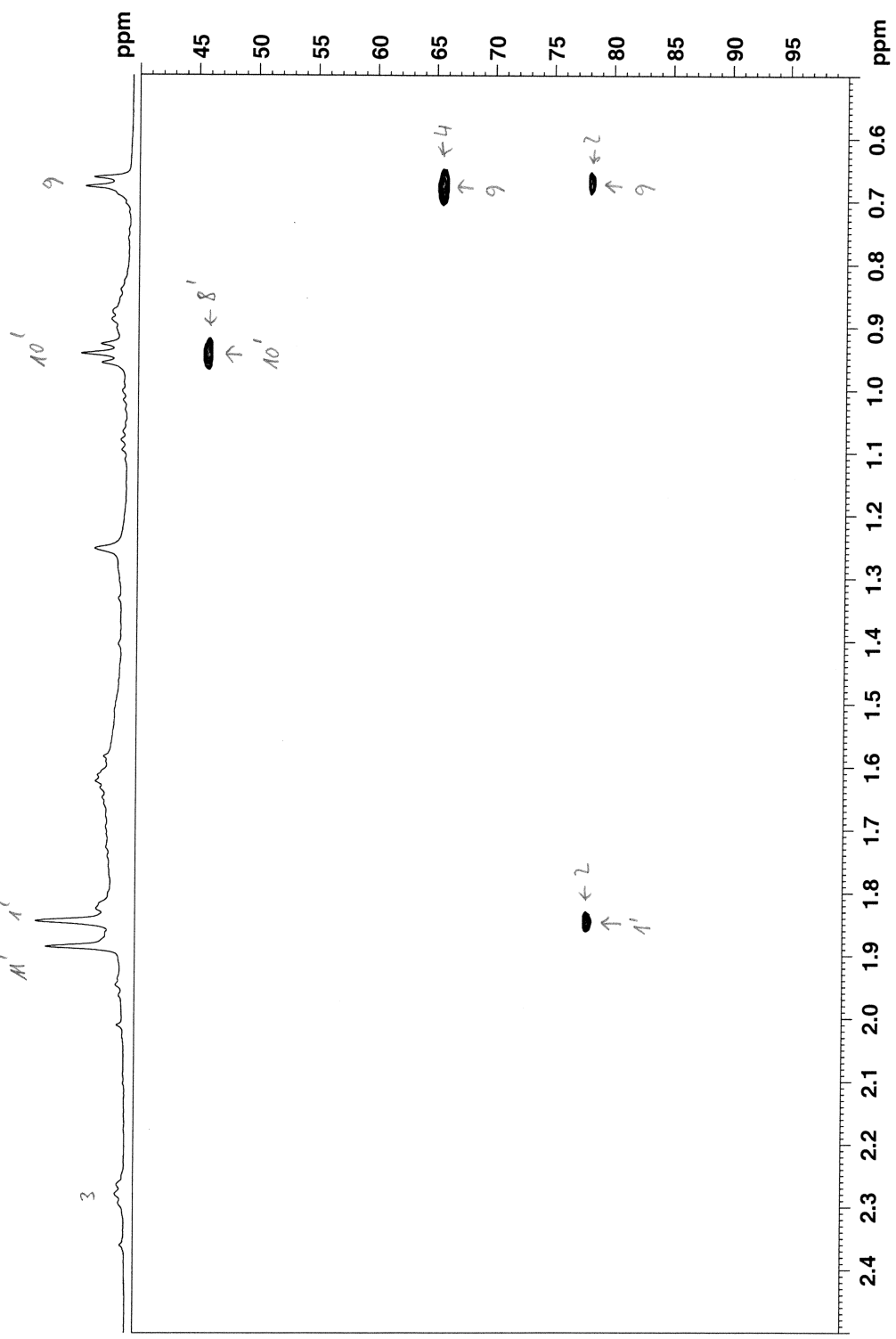
LN303\_VP4\_P4 in cdcl<sub>3</sub> (HMBC) 27.1.2020



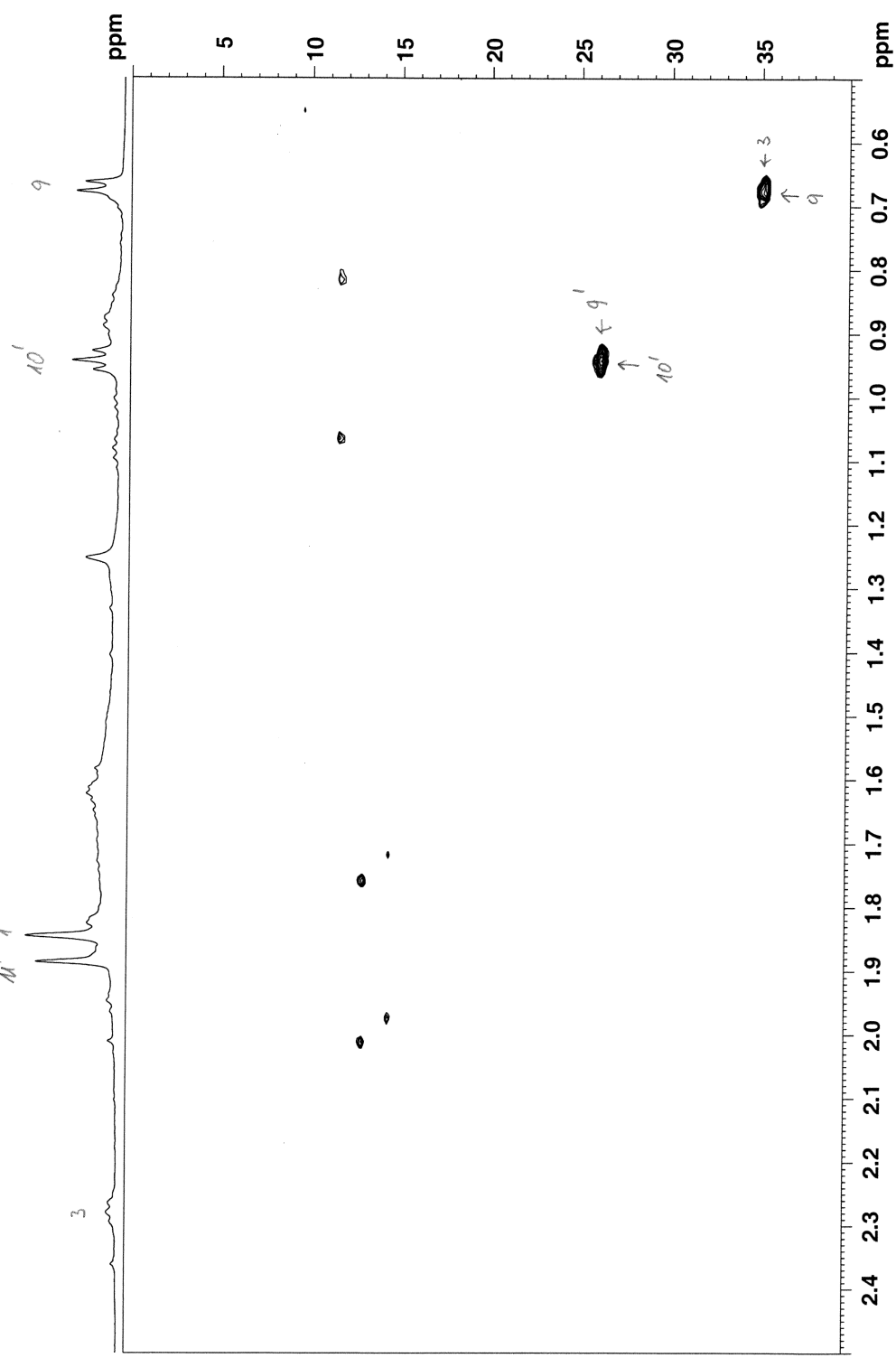
LNN303\_VP4\_P4 in cdc13 (HMBC) 27.1.2020



LN303\_VP4\_P4 in cdc13 (HMBC) 27.1.2020



LN303\_VP4\_P4 in cdc13 (HMBC) 27.1.2020



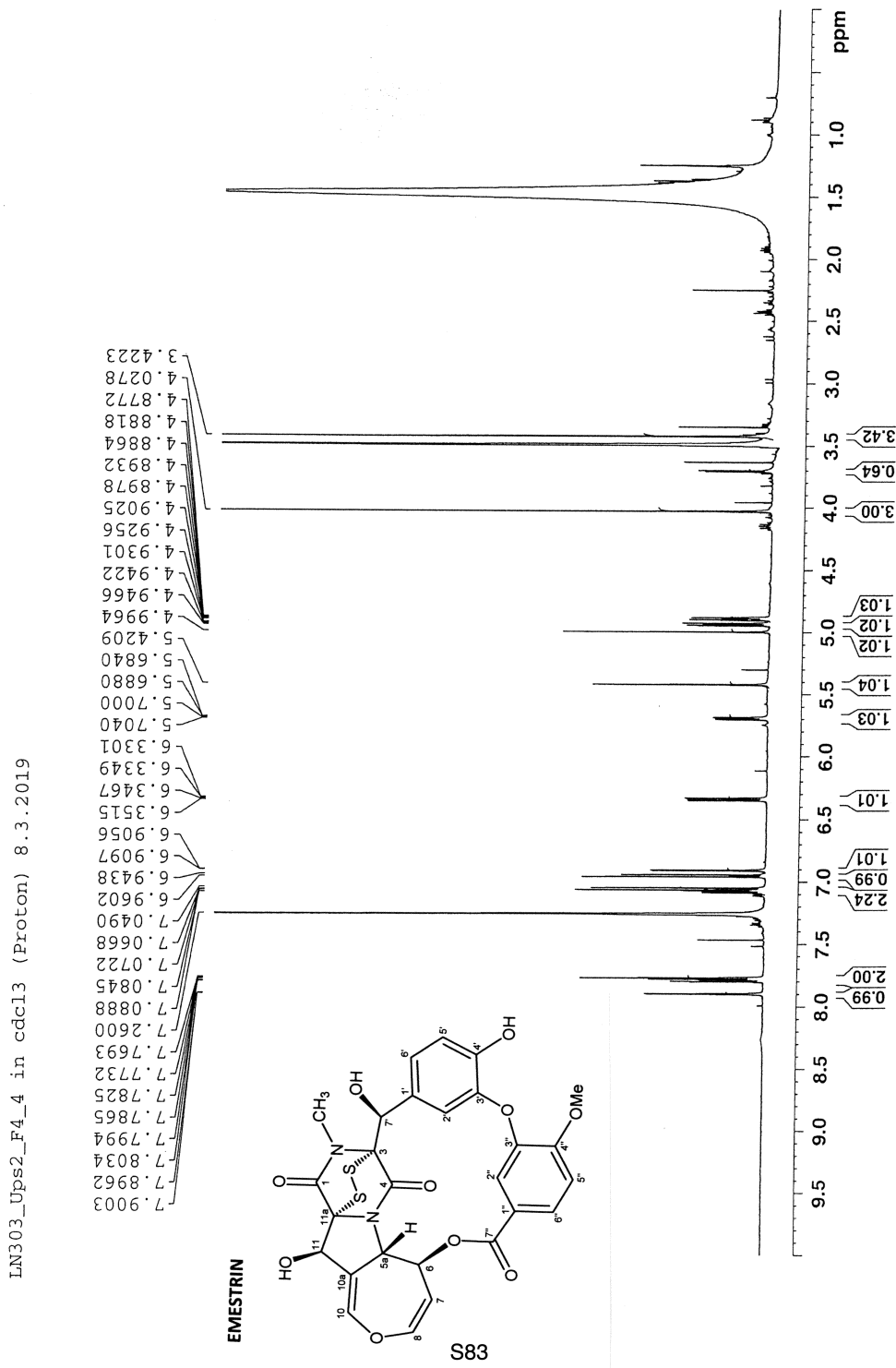
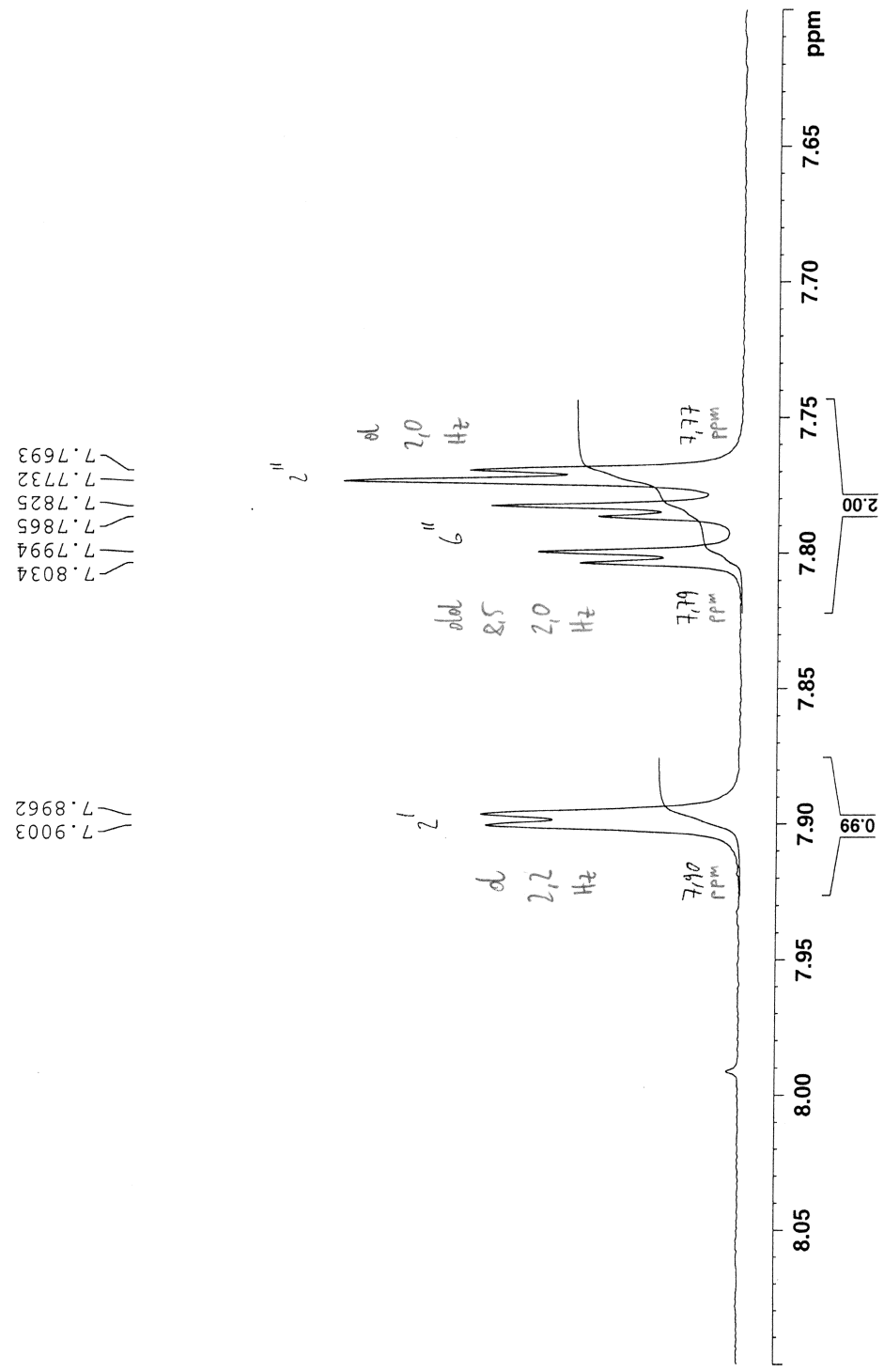
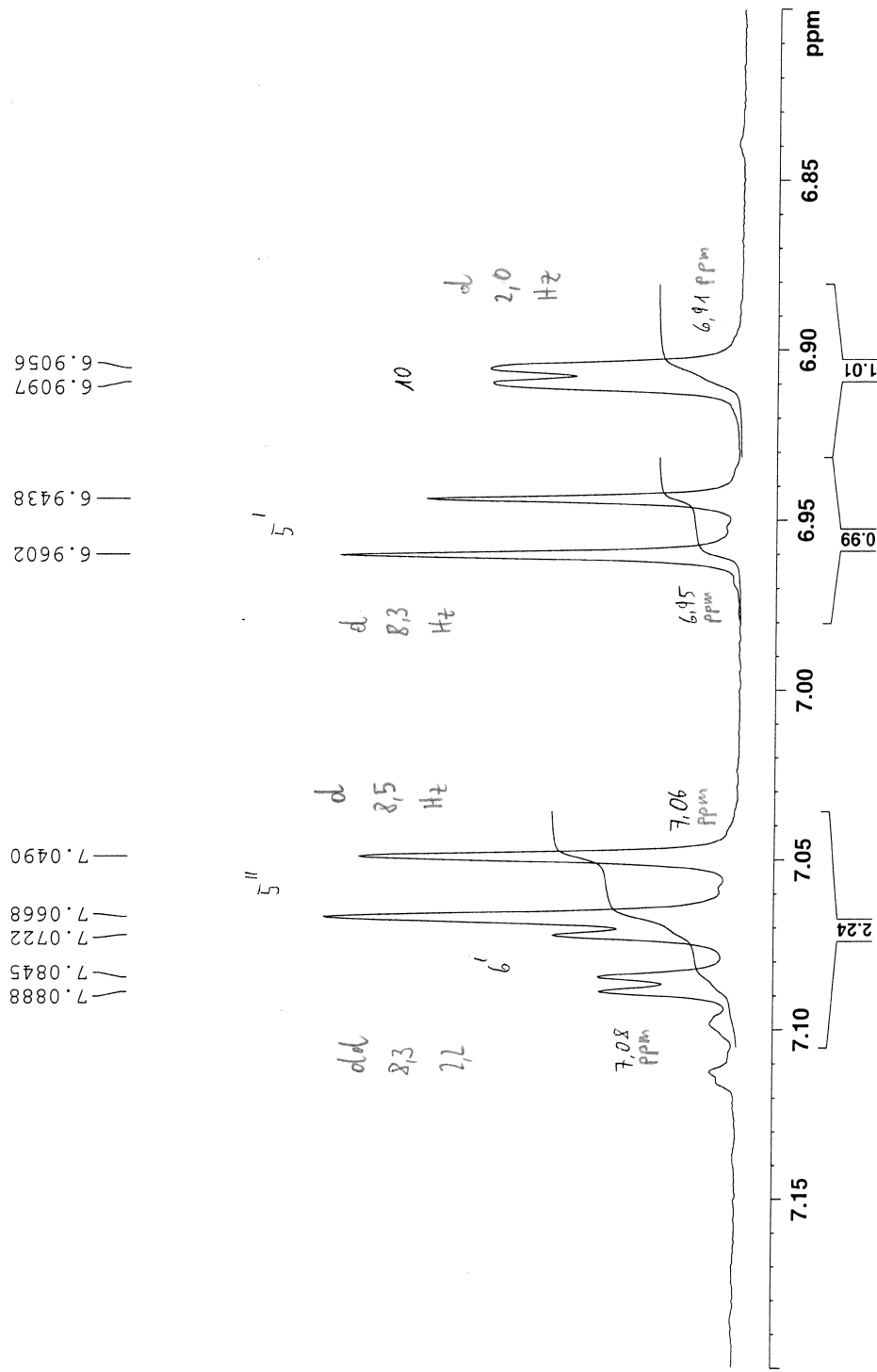
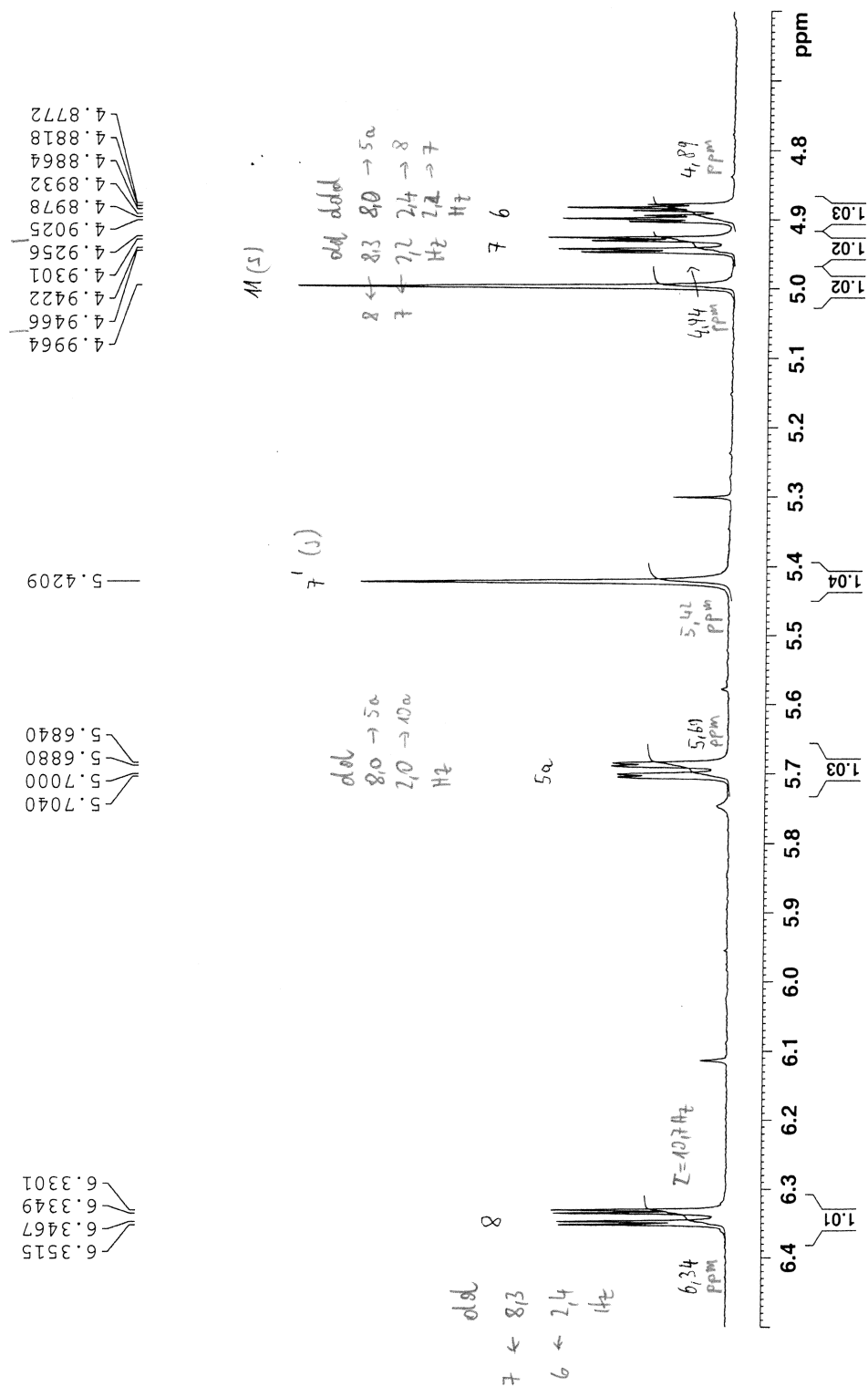
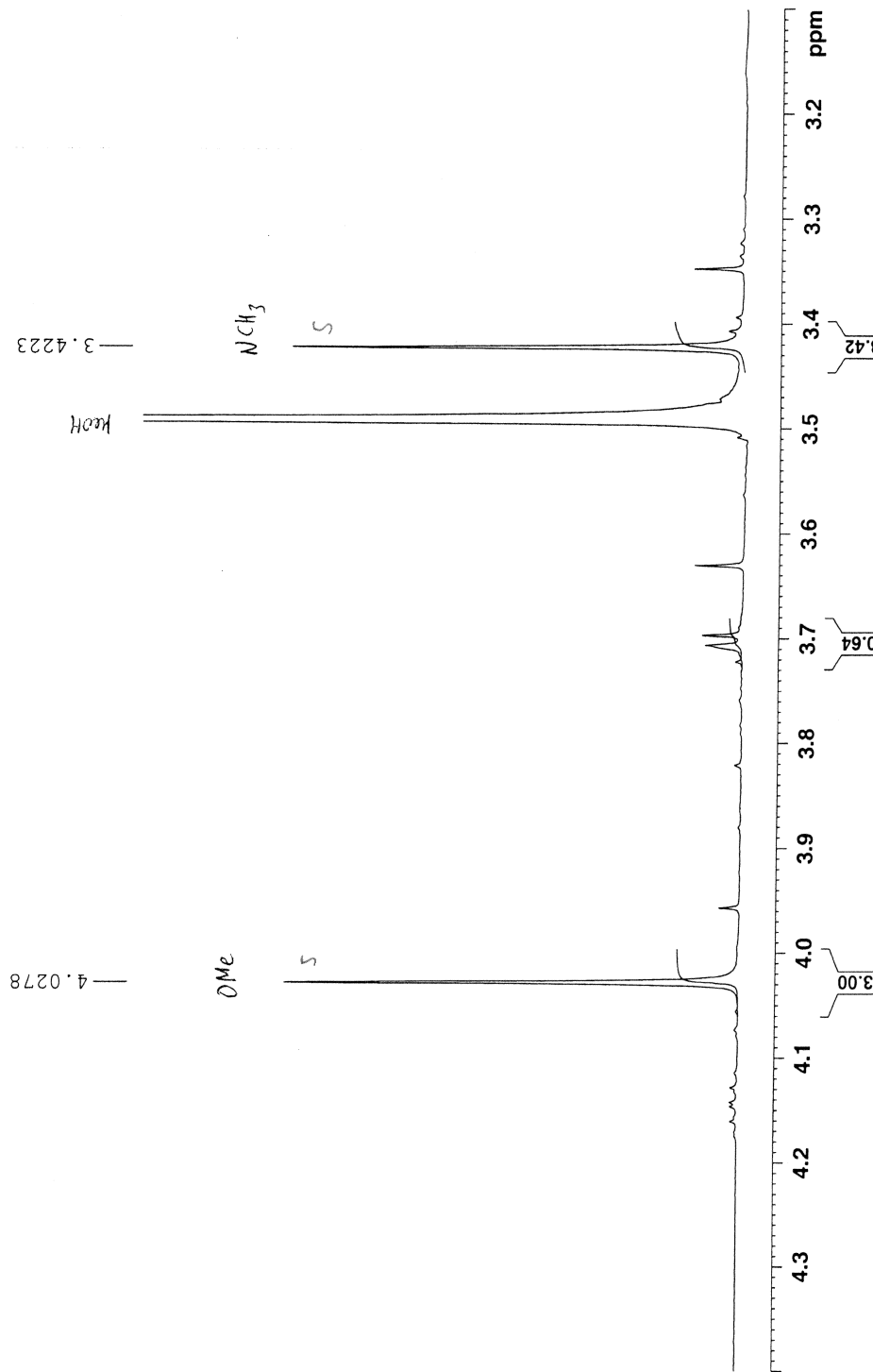


Figure S18. NMR data on compound 3.









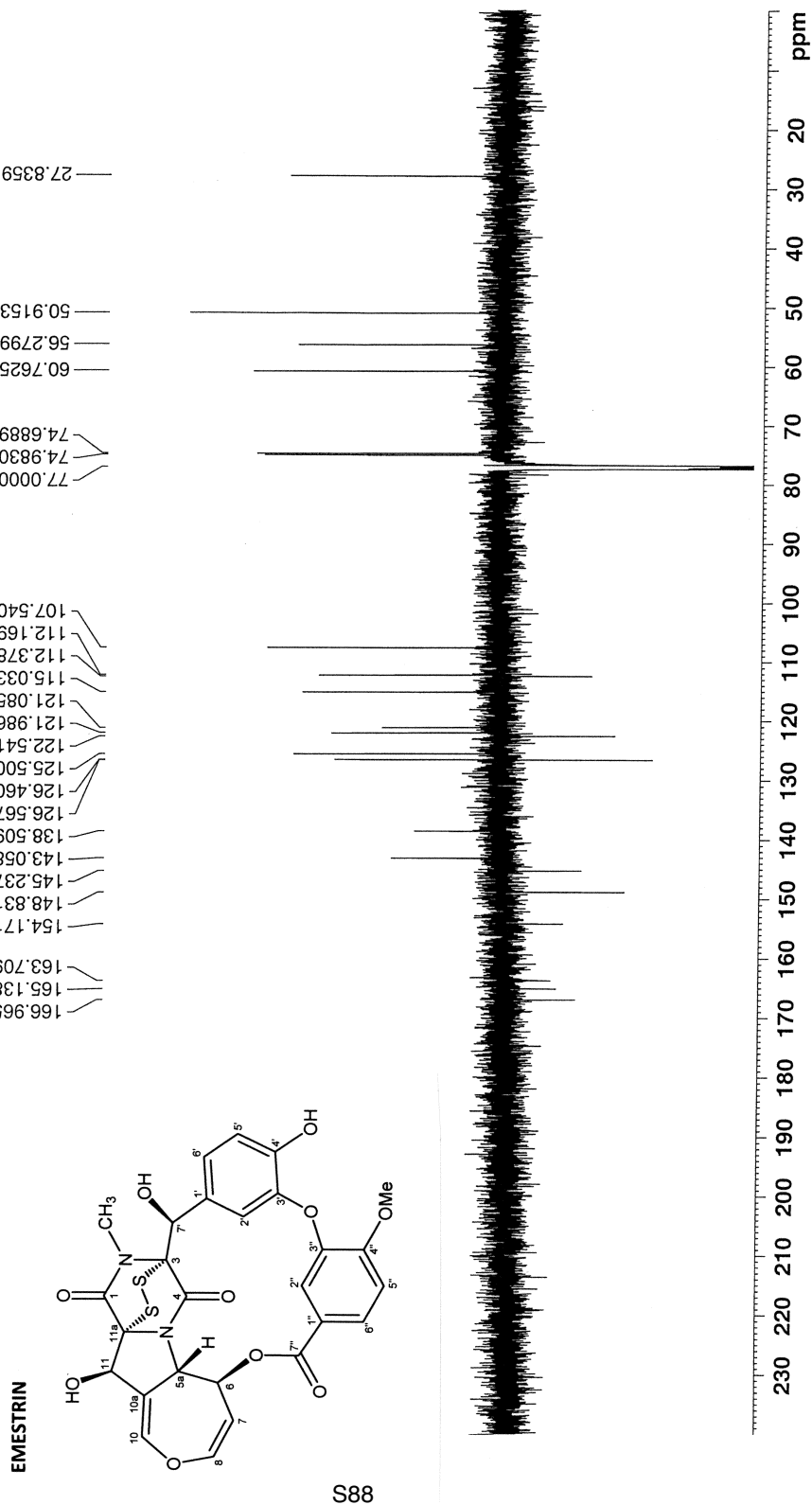
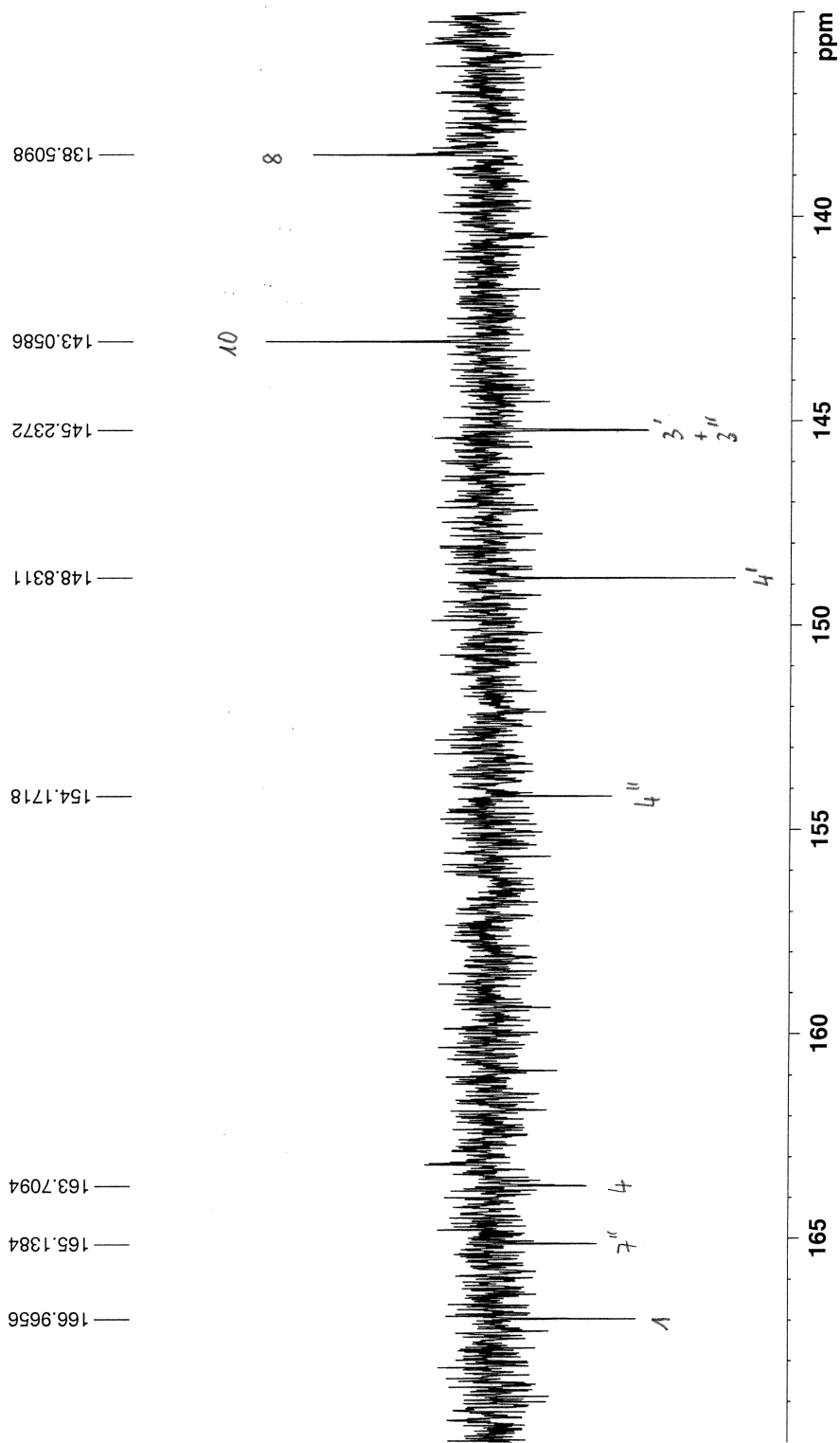
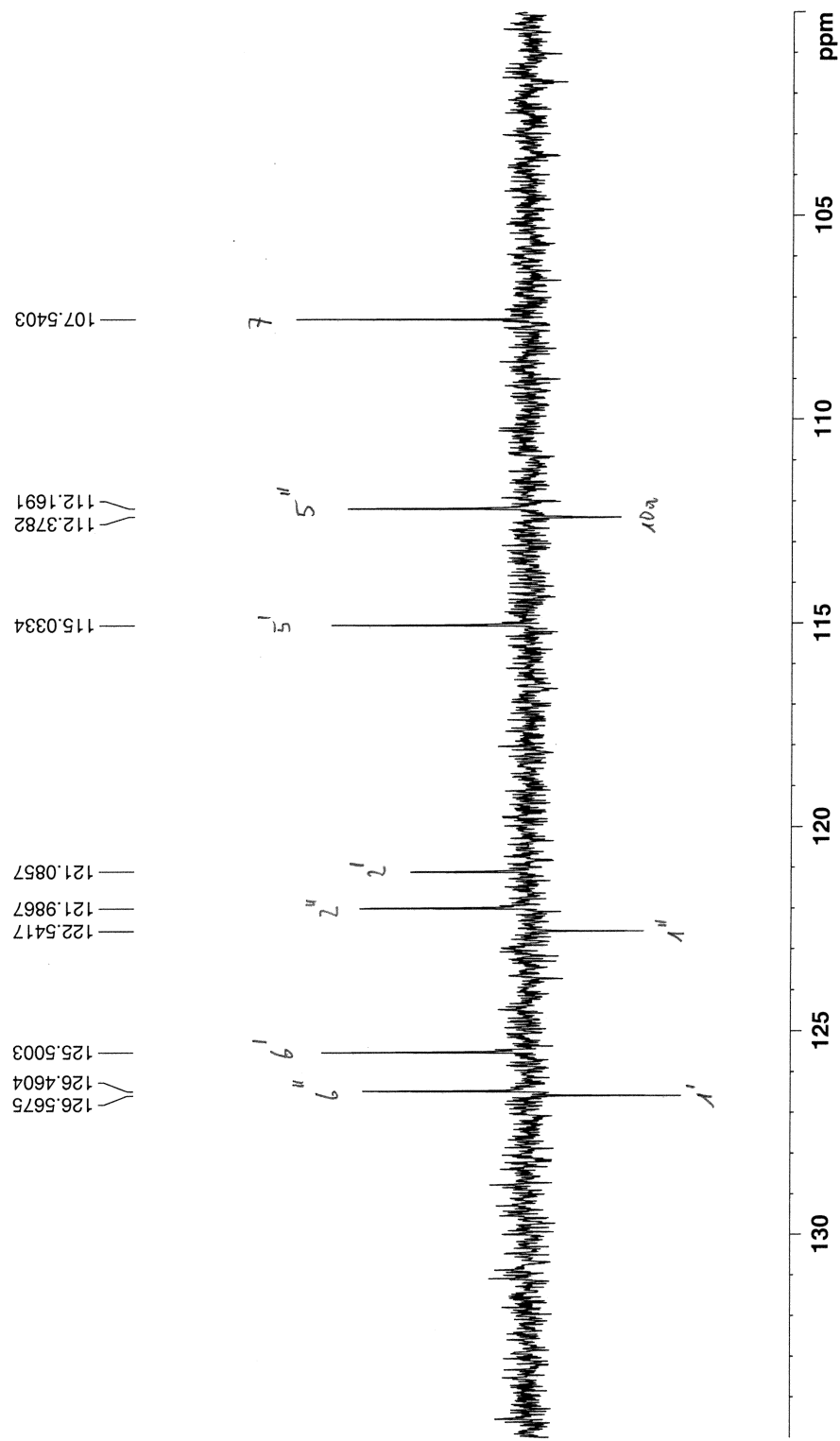
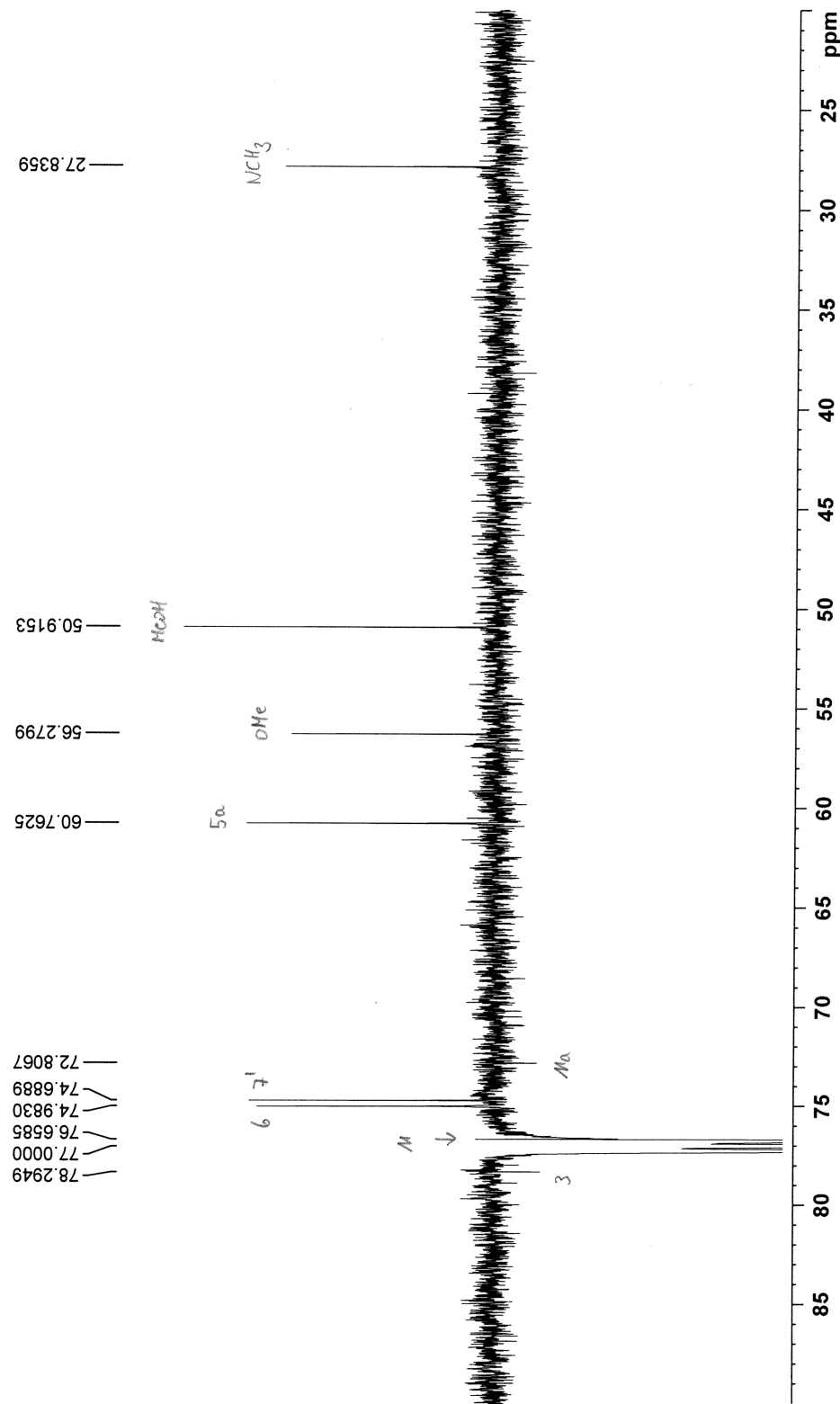


Figure S18 (pages S88-S91). <sup>1</sup>H NMR spectrum of **3** in CDCl<sub>3</sub> ( $\delta$  in ppm).







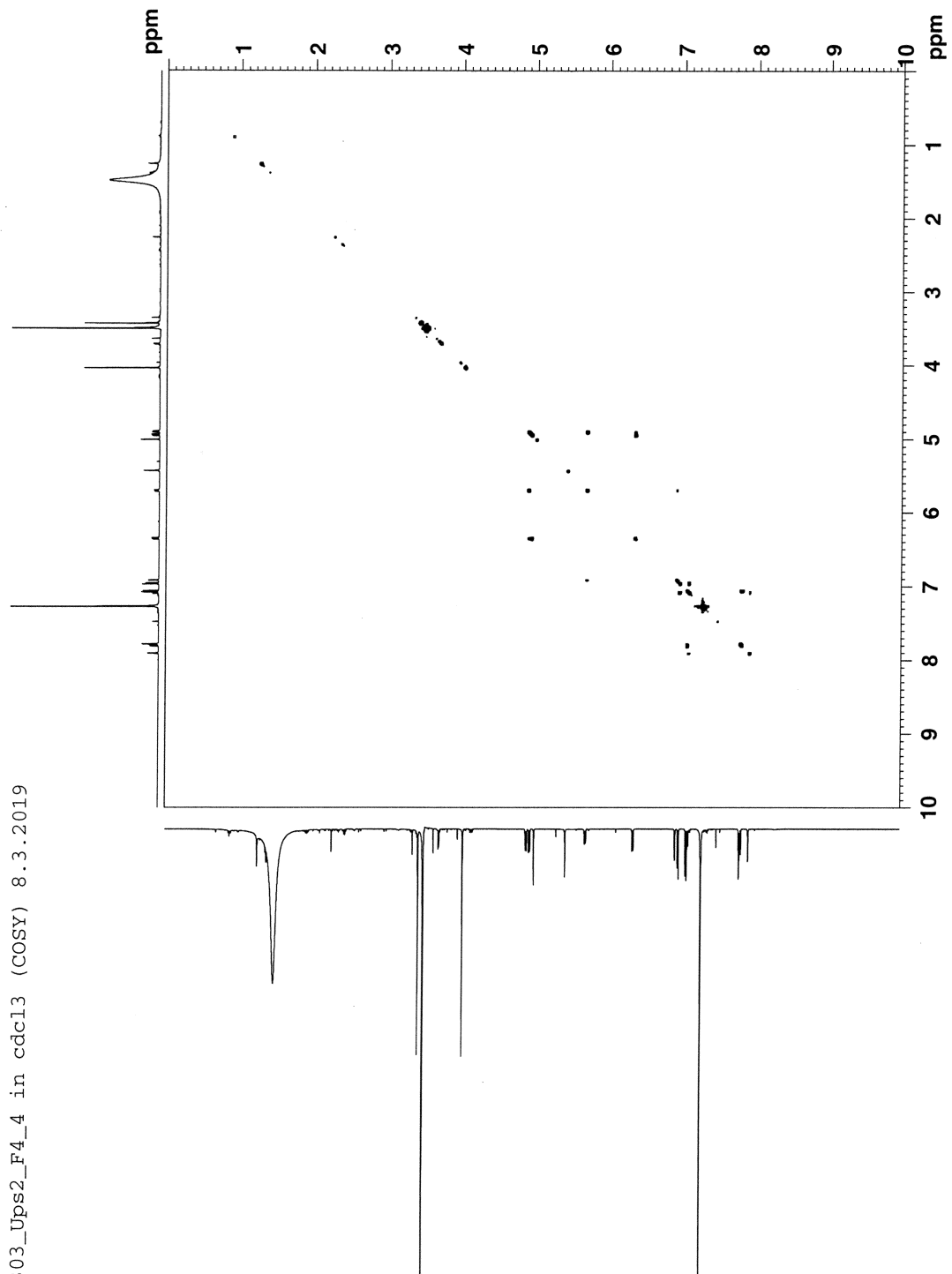
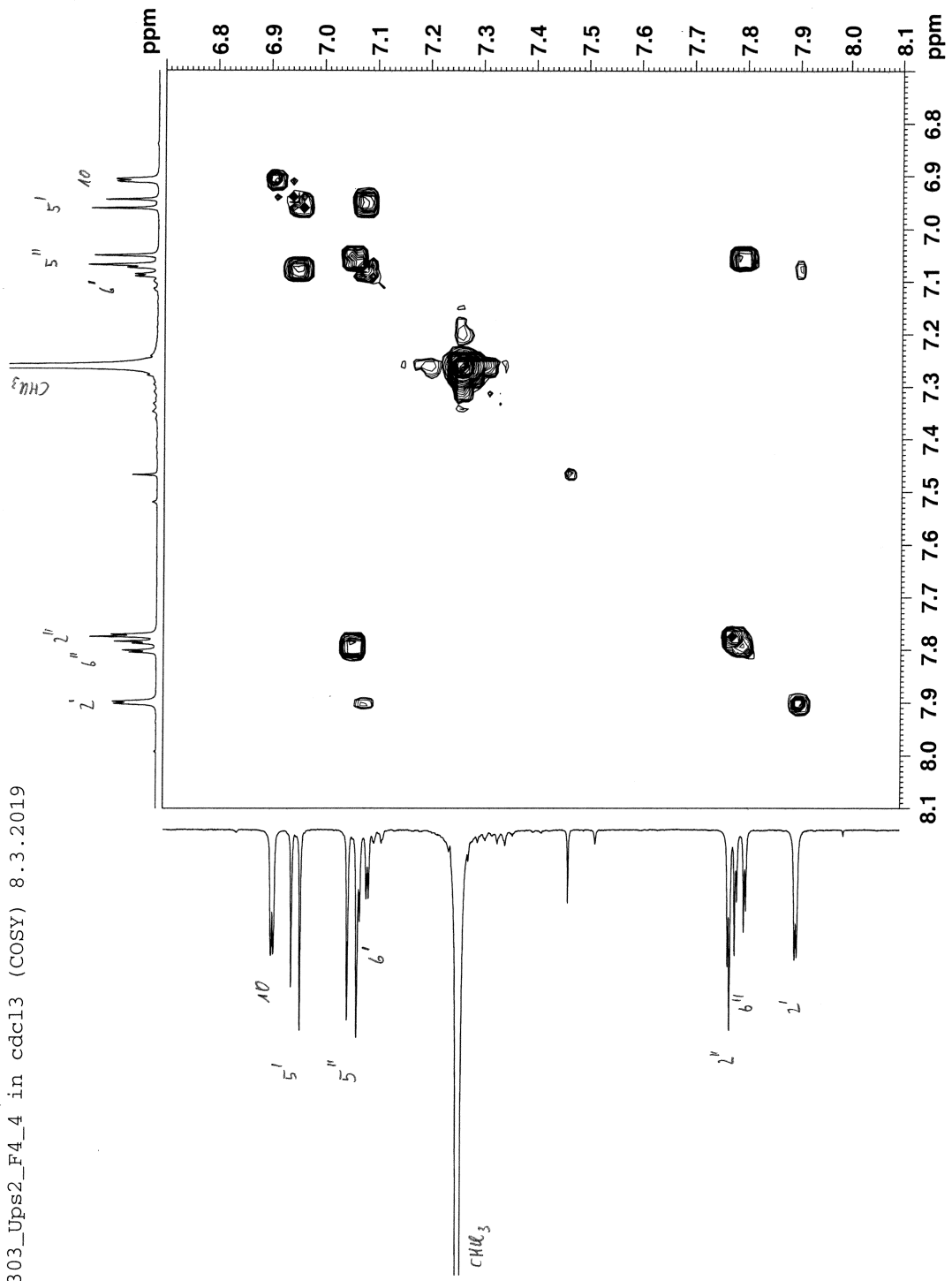
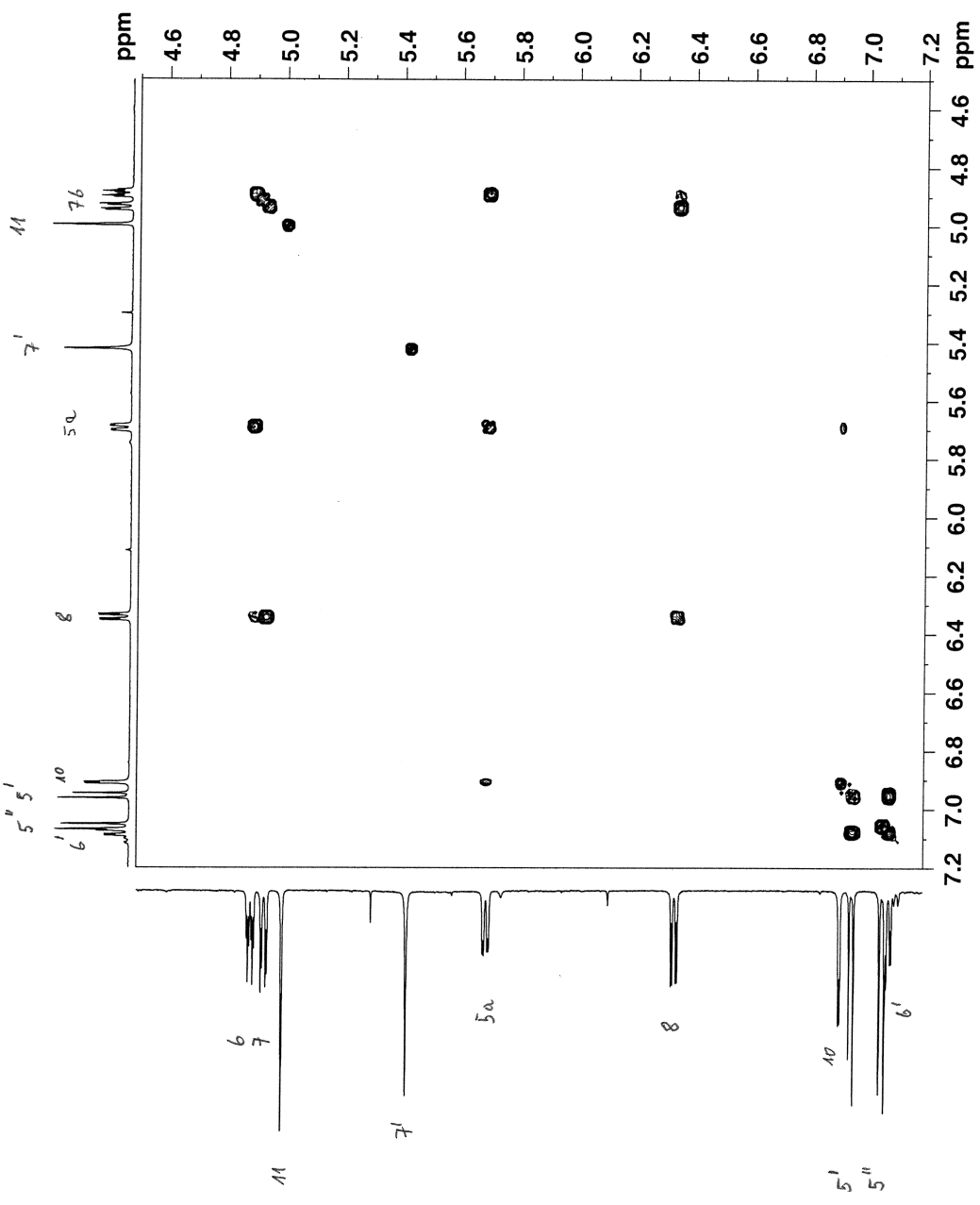


Figure S18 (pages S92-S94). COSY spectrum of **3** in CDCl<sub>3</sub> ( $\delta$  in ppm).

LN303\_Ups2\_F4\_4 in cdc13 (COSY) 8.3.2019



LNN303\_Ups2\_F4\_4 in cdcl3 (COSY) 8.3.2019



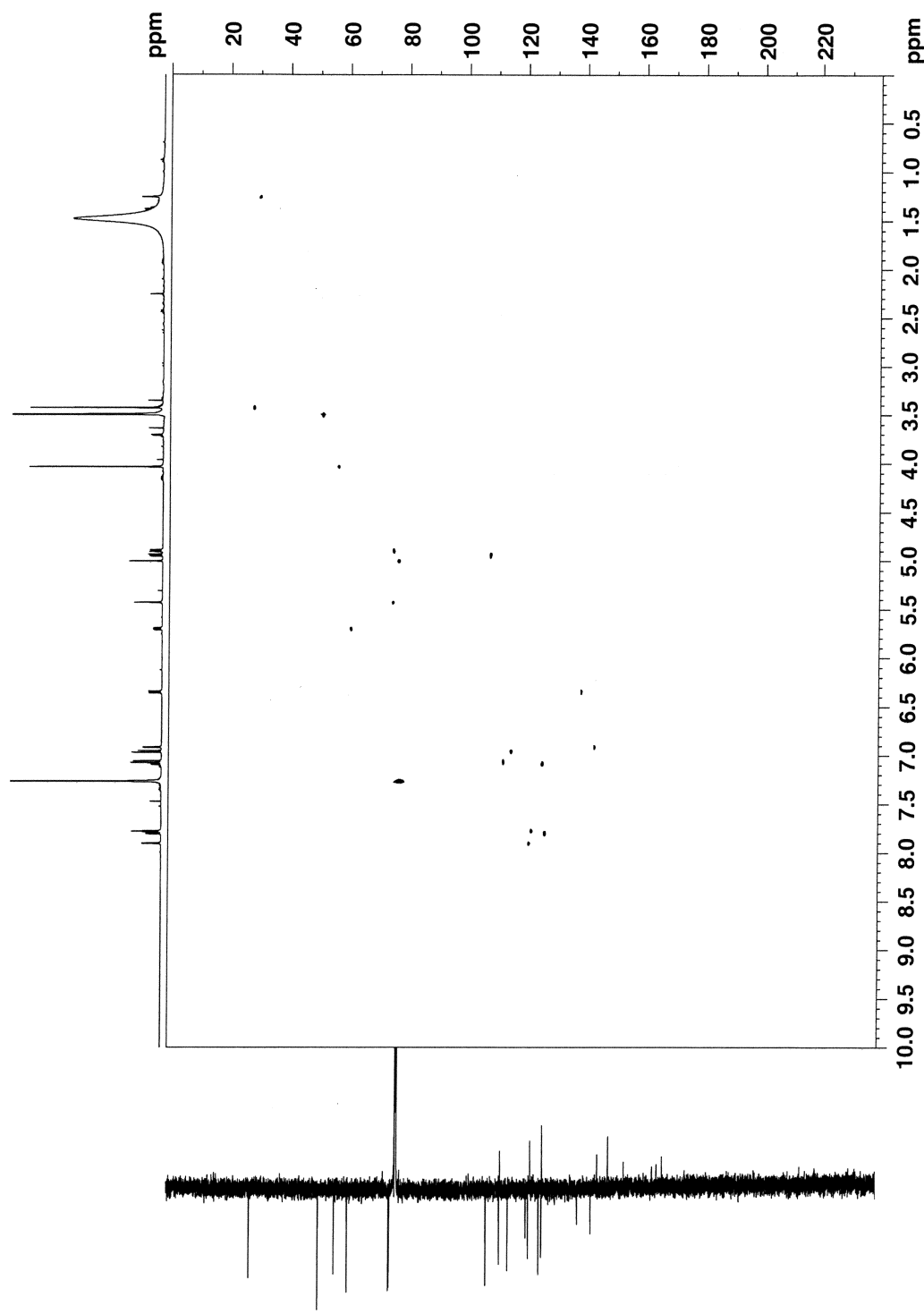
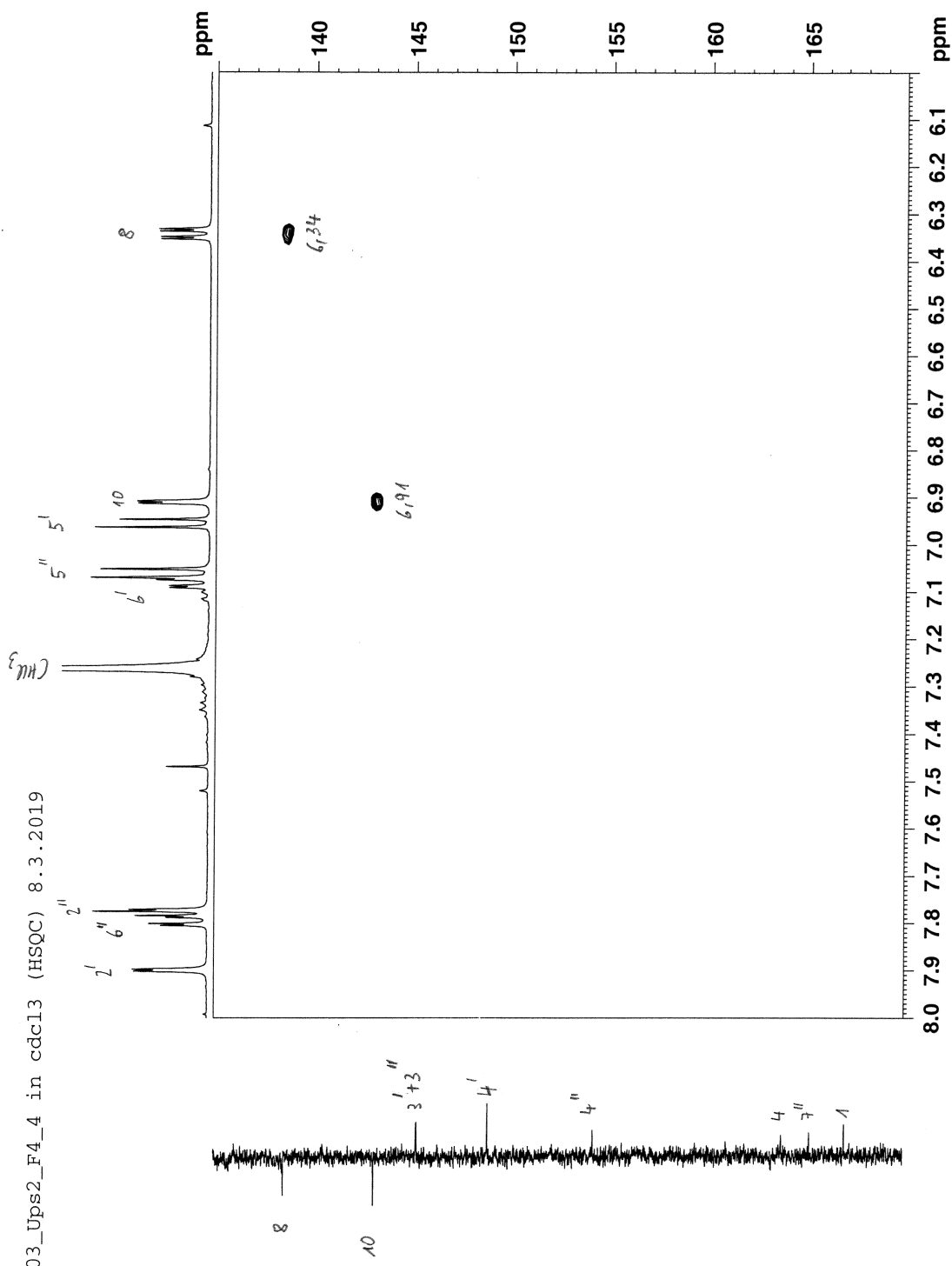
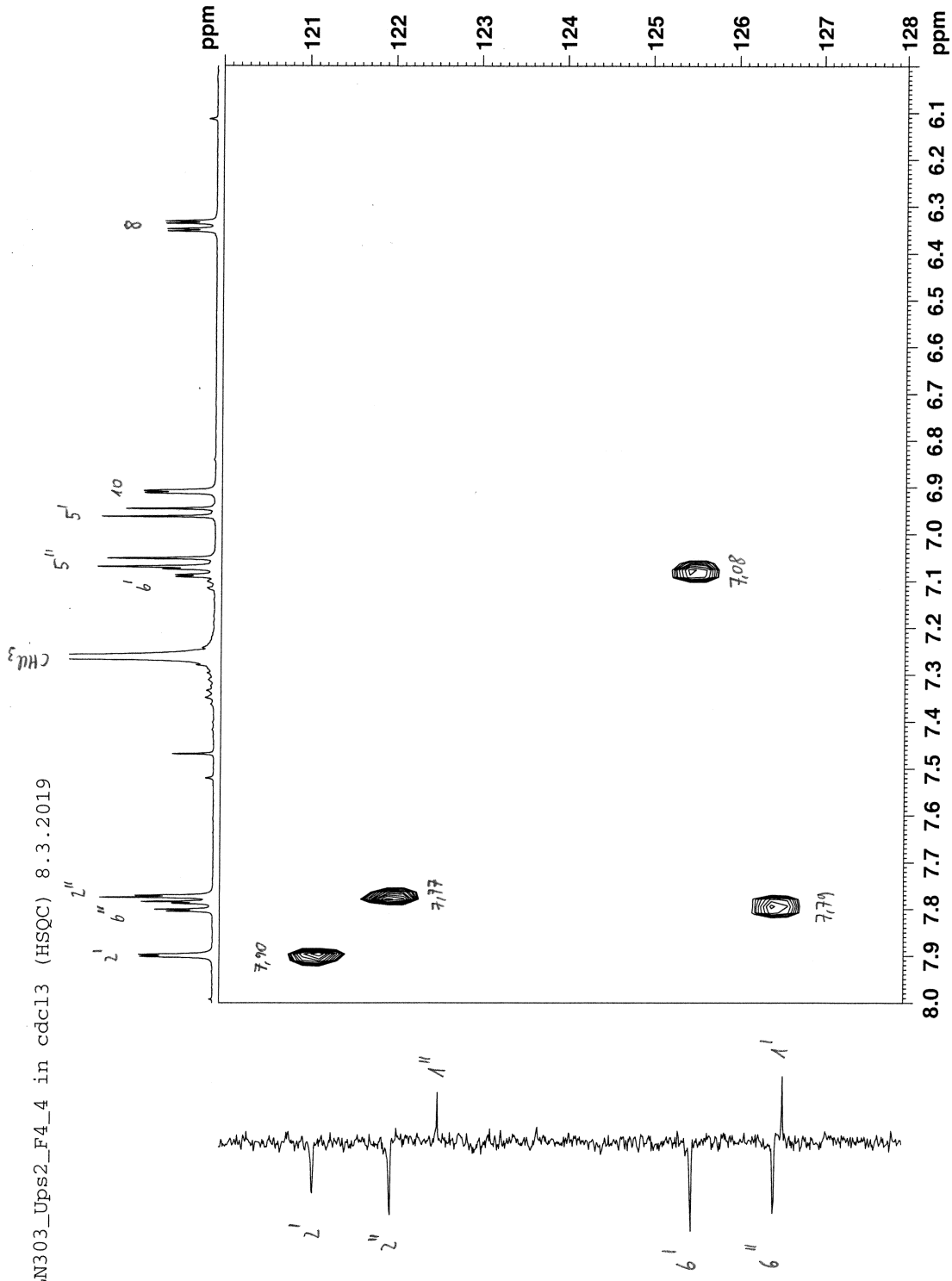


Figure S18 (pages S95-S101). HSQC spectrum of **3** in  $\text{CDCl}_3$  ( $\delta$  in ppm).

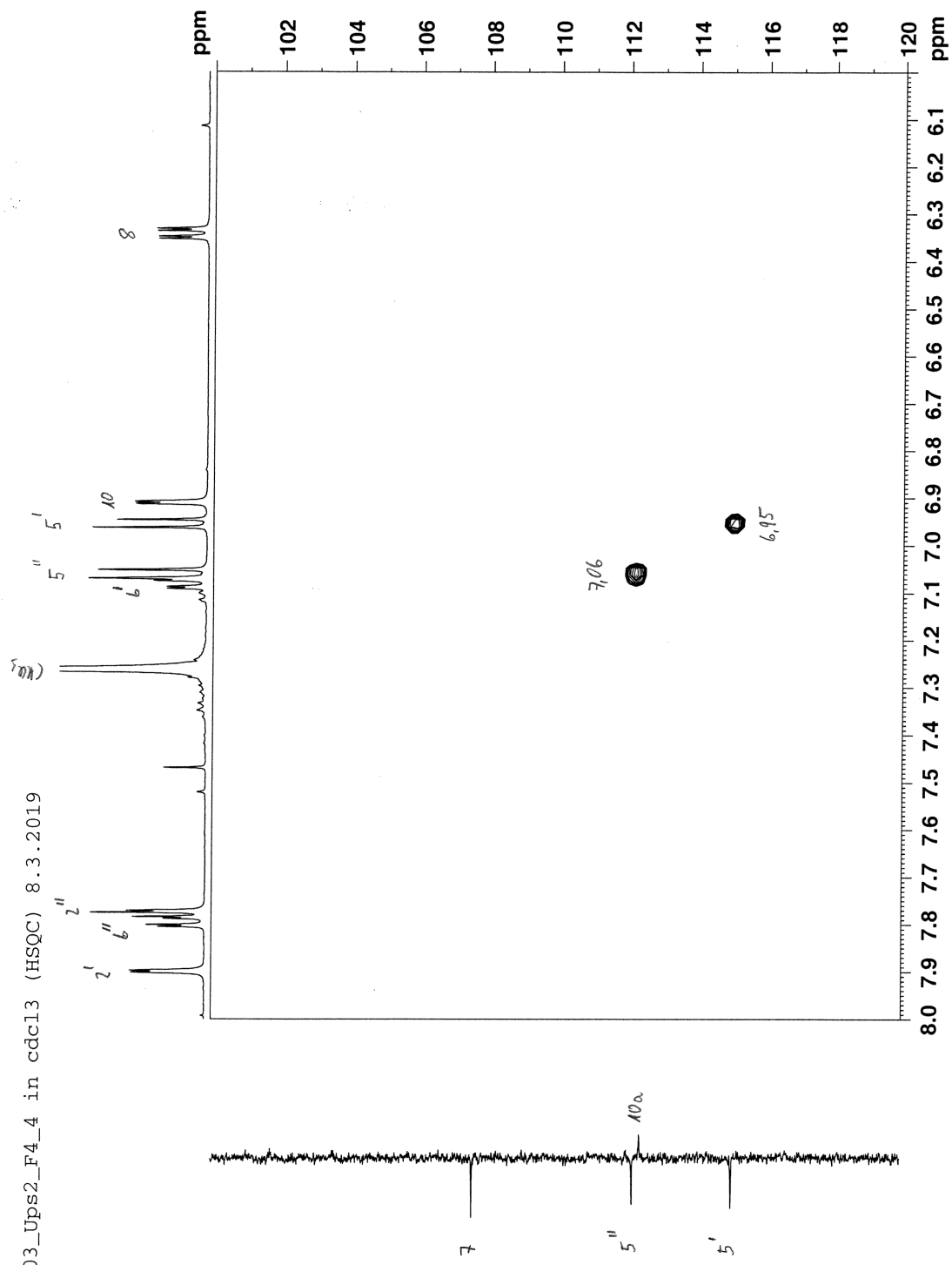
LN303\_Ups2\_F4\_4 in cdc13 (HSQC) 8.3.2019



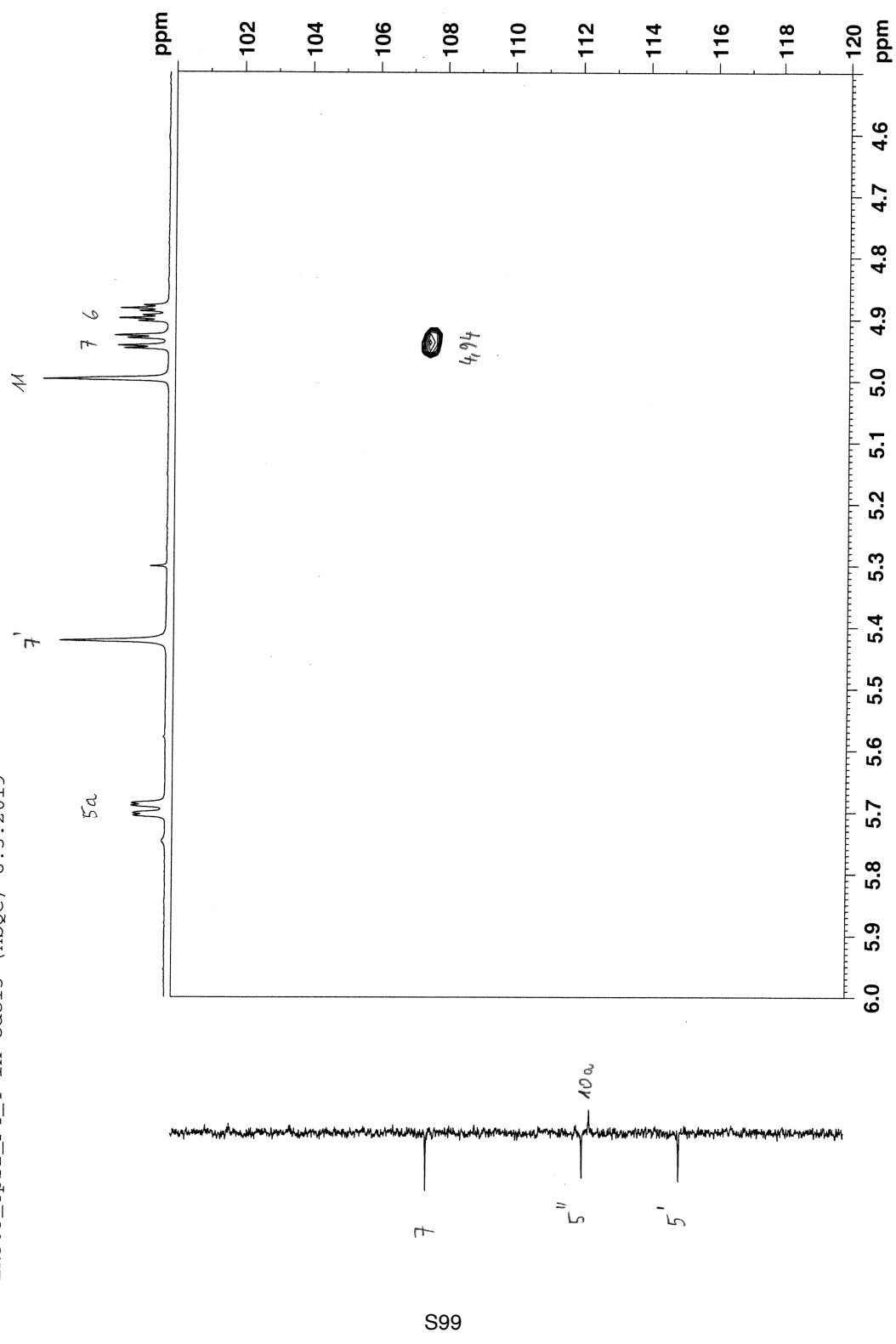
LN303\_Ups2\_F4\_4 in cdc13 (HSQC) 8.3.2019



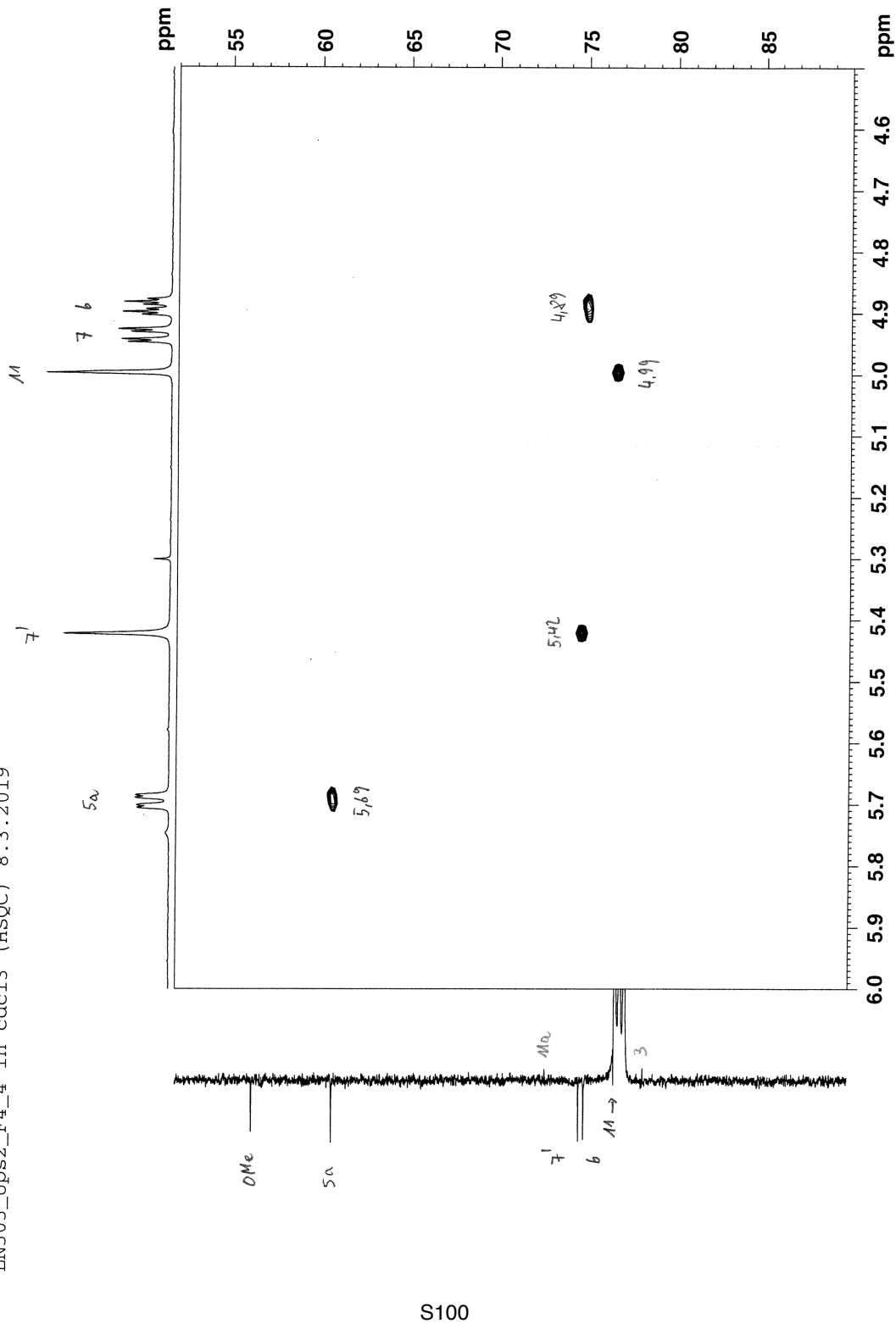
LN303\_Ups2\_F4\_4 in cdc13 (HSQC) 8.3.2019



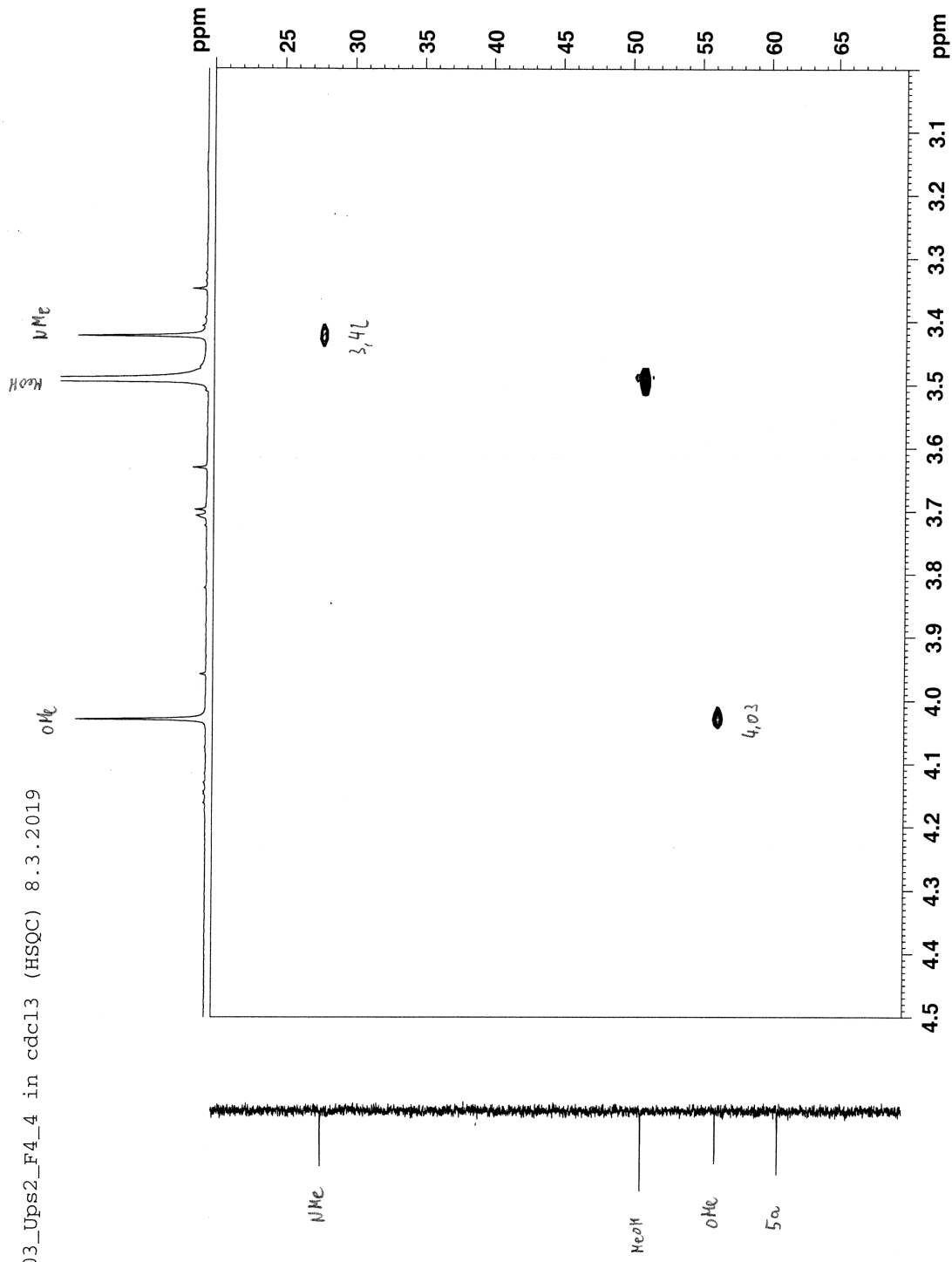
LN303\_Ups2\_F4\_4 in cdc13 (HSQC) 8.3.2019



LN303\_Ups2\_F4\_4 in cdcl3 (HSQC) 8.3.2019



S100



LN303\_Ups2\_F4\_4 in cdc13 (HMBC) 8.3.2019

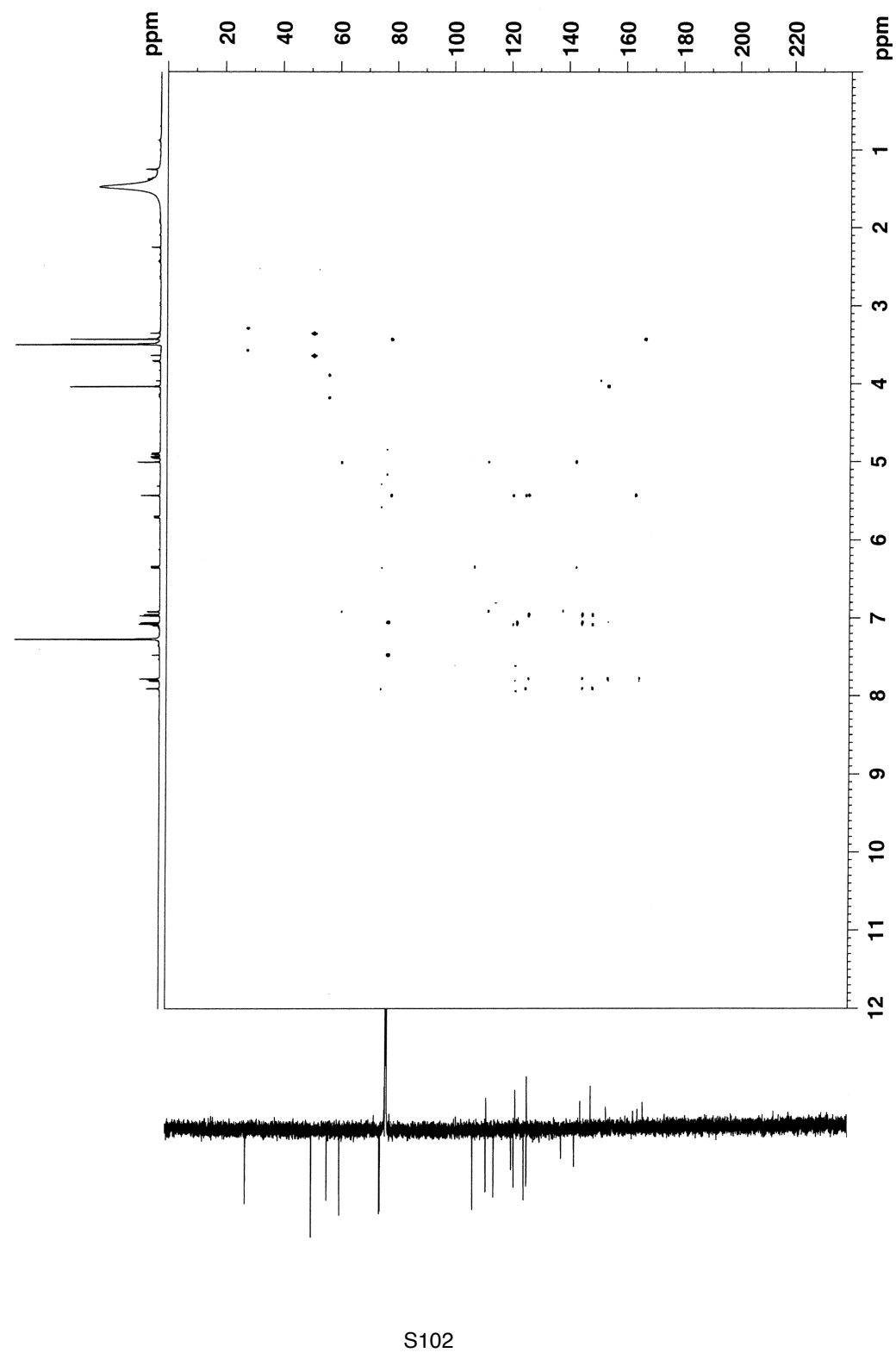
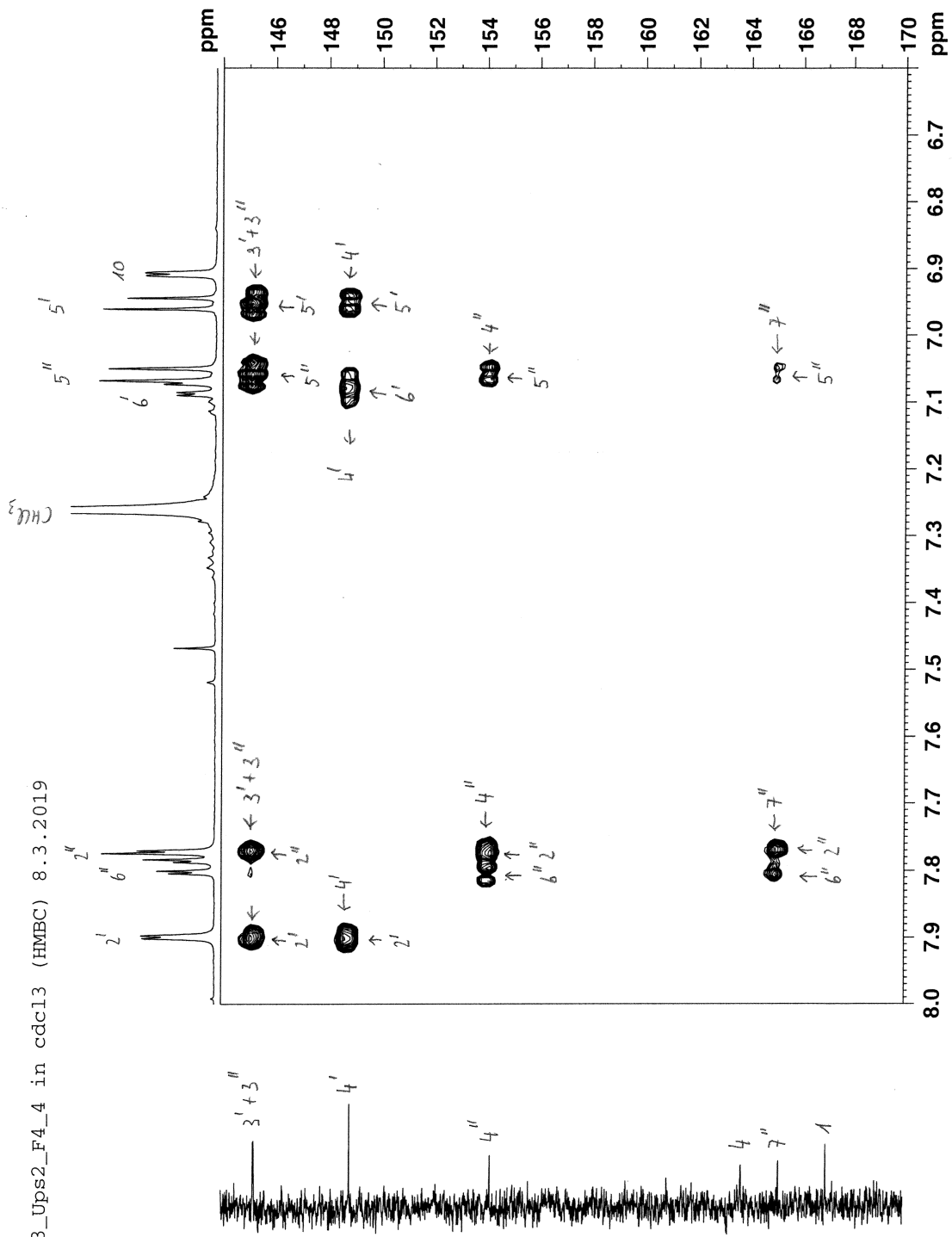
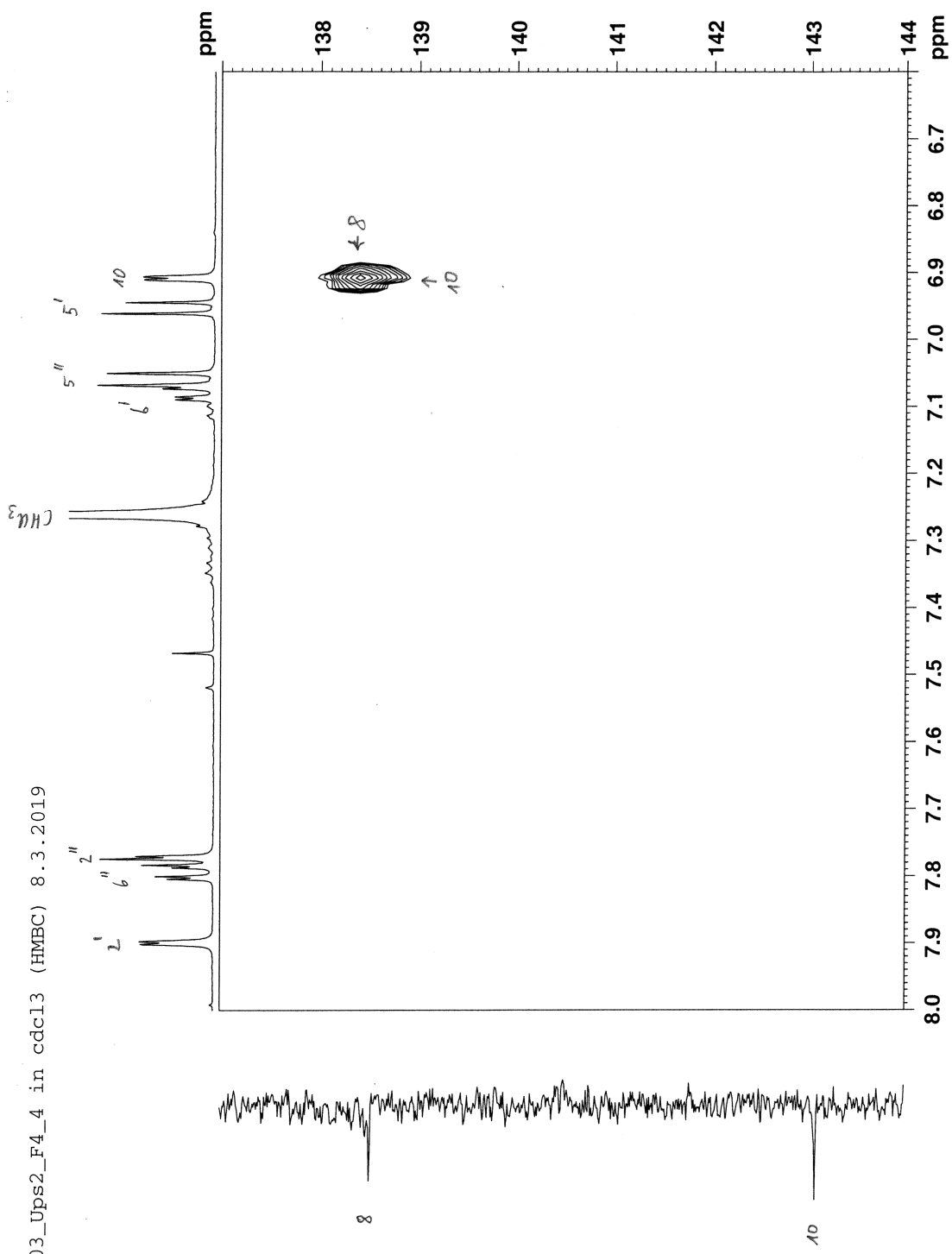


Figure S18 (pages S102-S112). HMBC spectrum of **3** in  $\text{CDCl}_3$  ( $\delta$  in ppm).

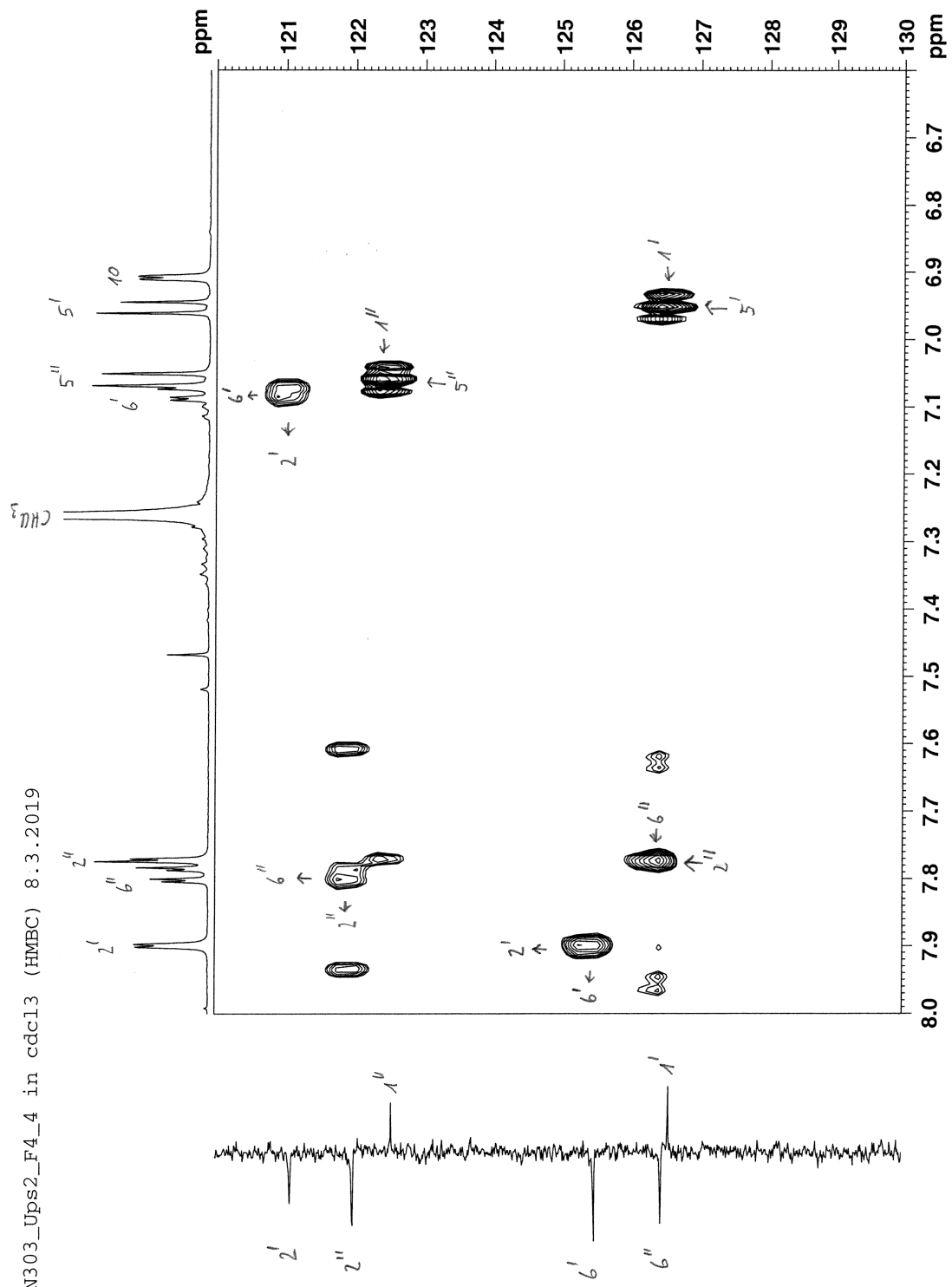
LNN303\_Ups2\_F4\_4 in cdc13 (HMBC) 8.3.2019



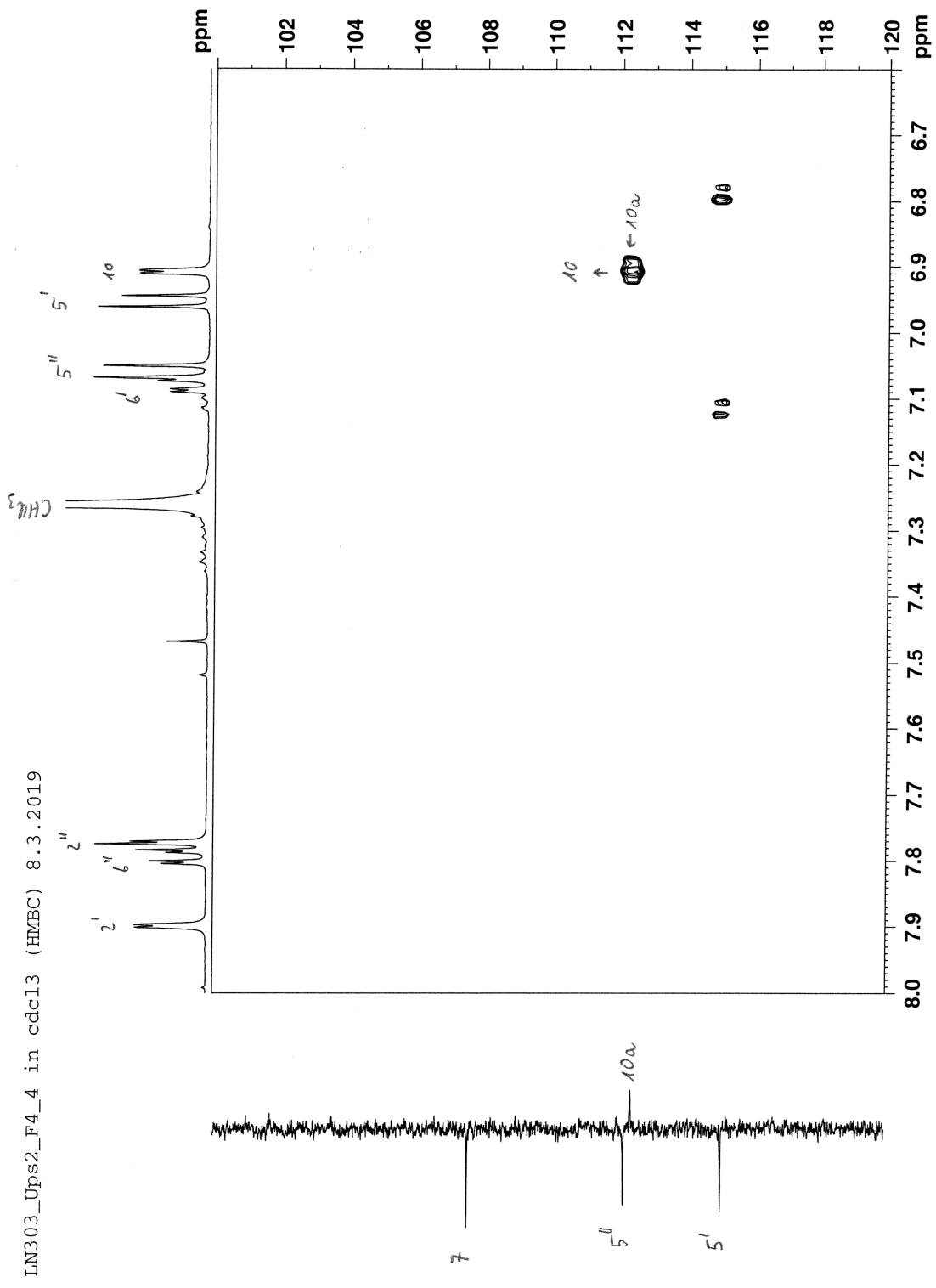
LN303\_Ups2\_F4\_4 in cdc13 (HMBC) 8.3.2019



S104

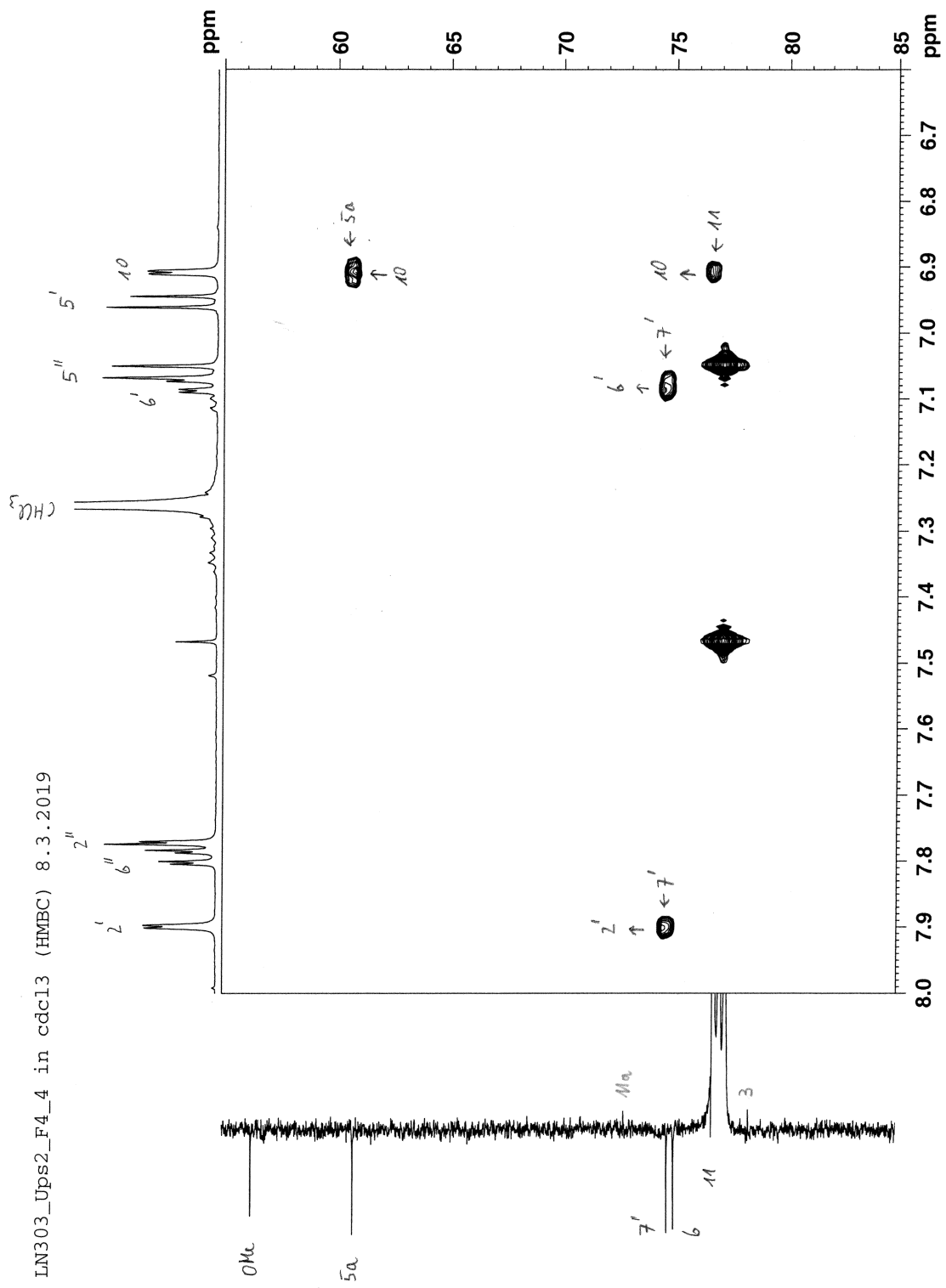


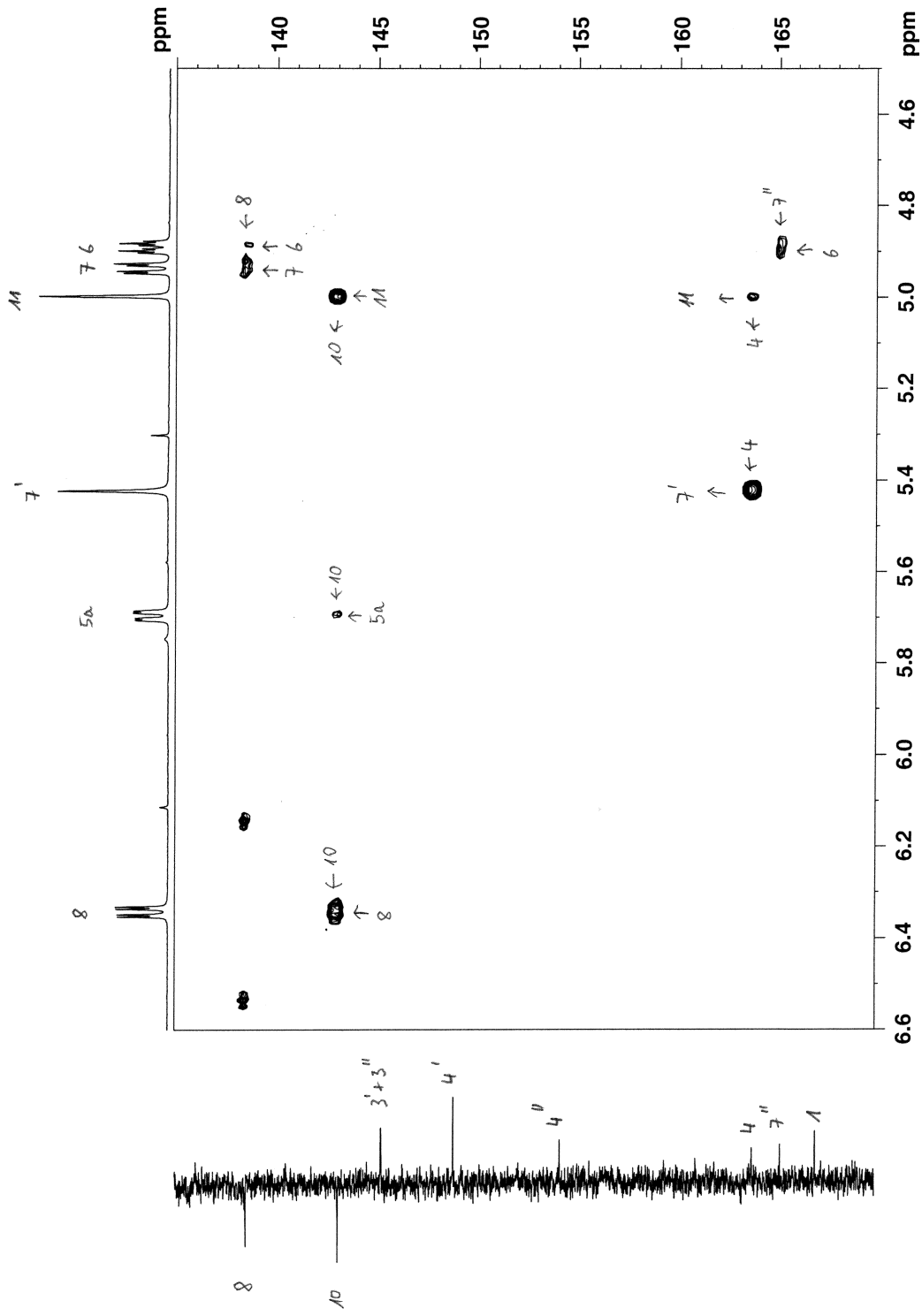
LN303\_Ups2\_F4\_4 in cdc13 (HMBC) 8.3.2019

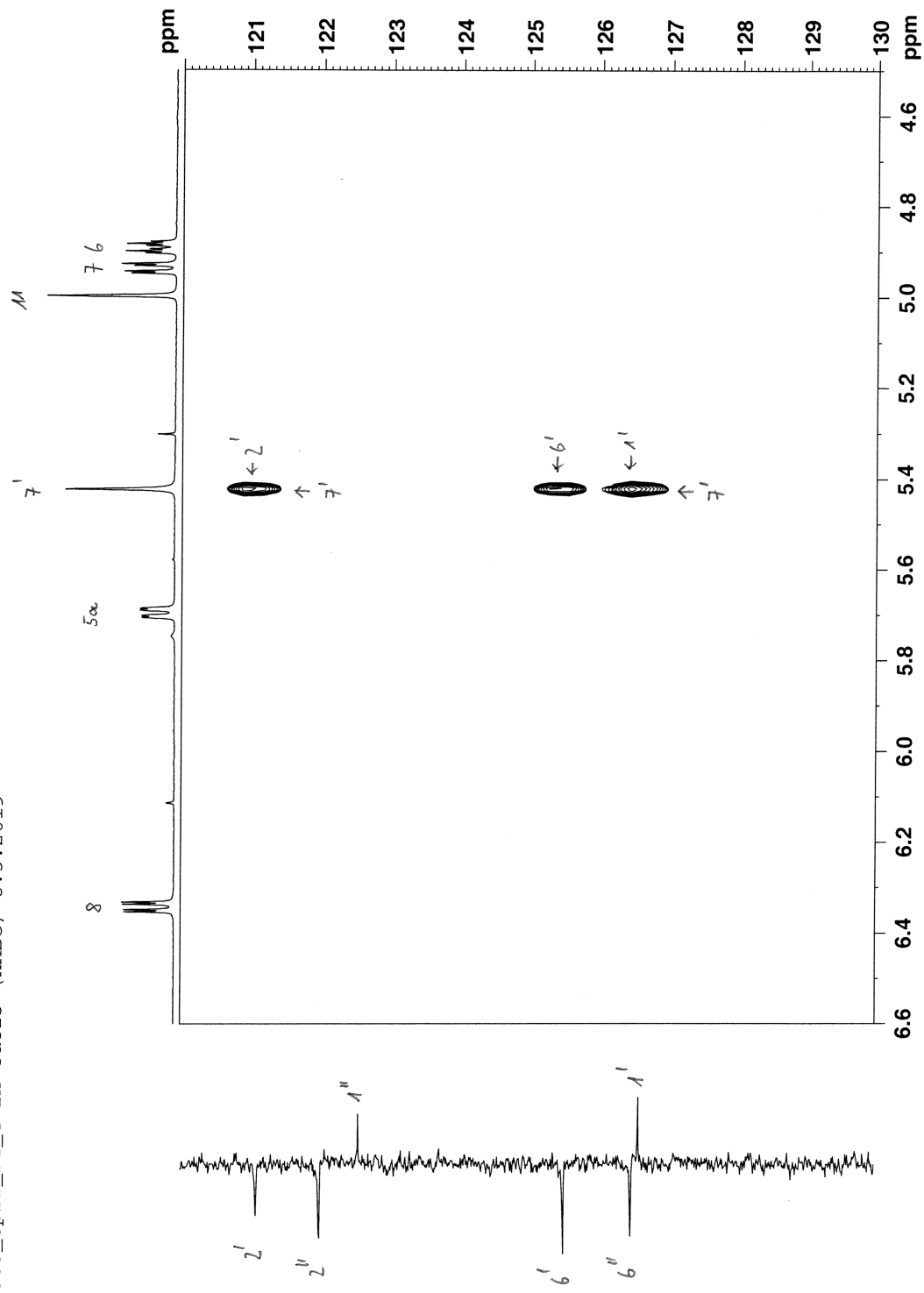


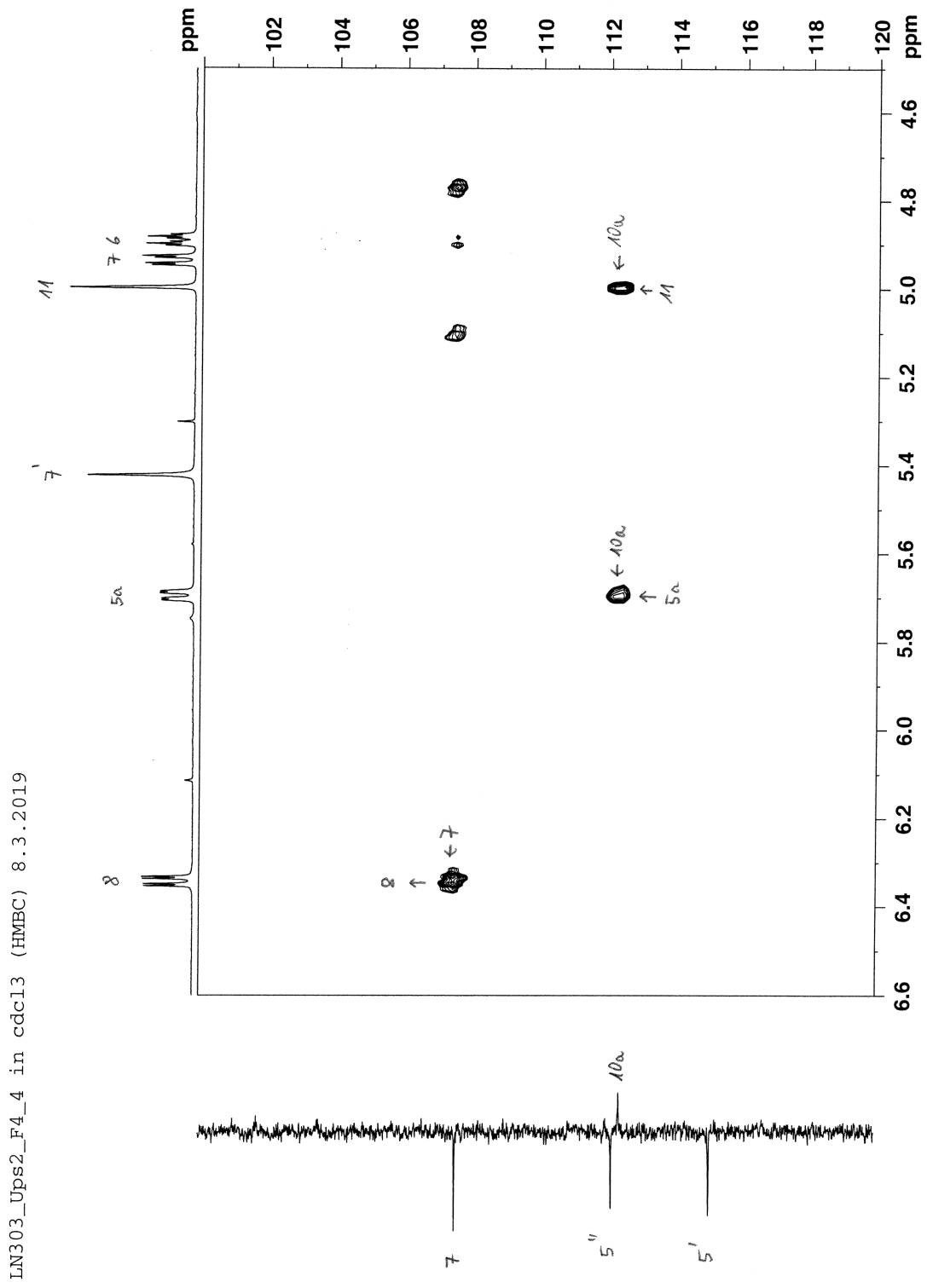
S106

LN303\_Ups2\_F4\_4 in cdc13 (HMBC) 8.3.2019

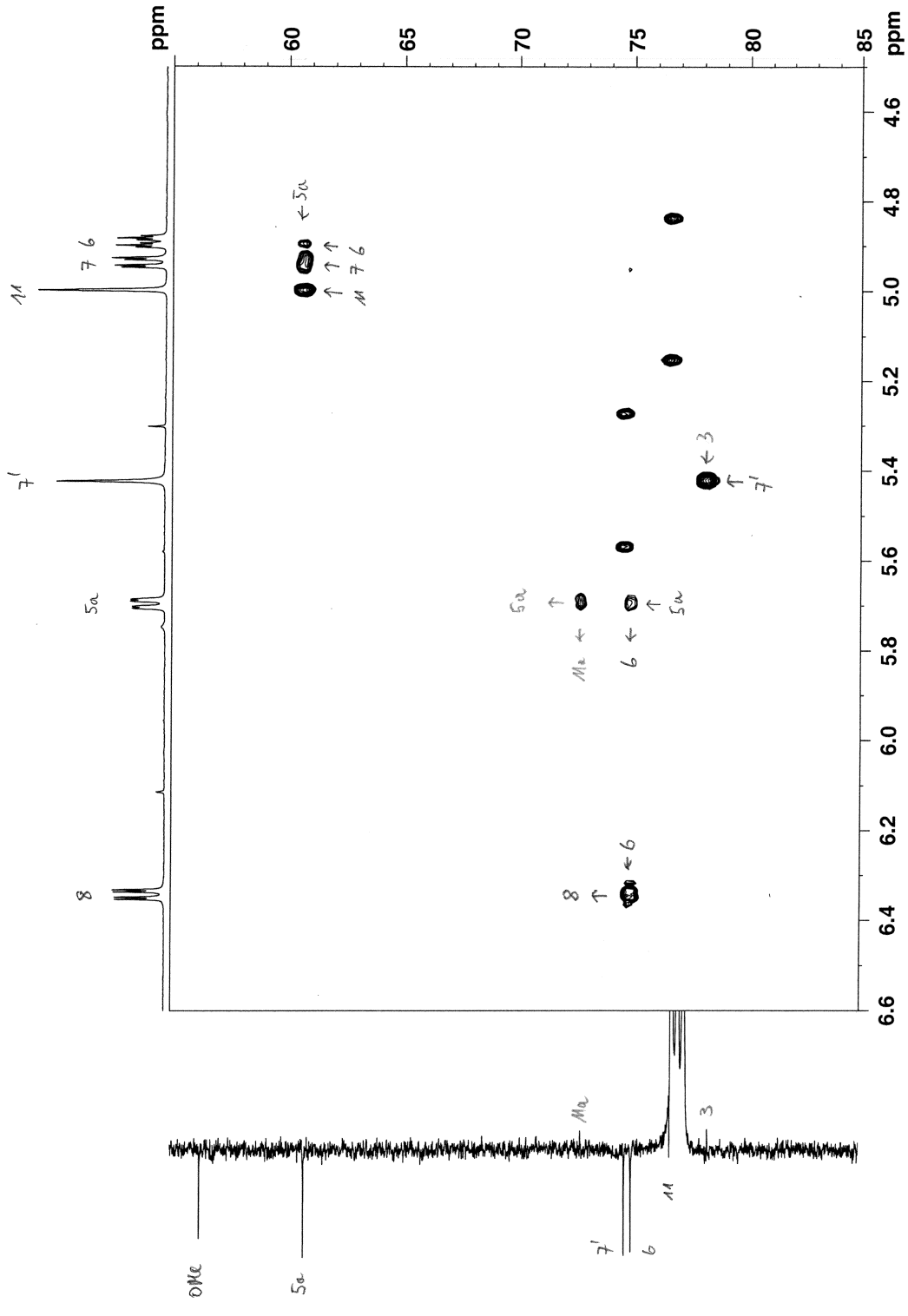








S110



LN303\_Ups2\_F4\_4 in cdc13 (HMBC) 8.3.2019

